Recent Advances in Iridium-Catalysed Transfer Hydrogenation Reactions

M. Pilar Lamata, Vincenzo Passarelli and Daniel Carmona

Abstract This review focuses on the contributions of the last five years to the application of iridium complexes as homogeneous catalysts in transfer hydrogenation (TH) reactions. The reduction of carbonyls, imines, alkenes and alkynes is considered. The TH of unsaturated alkene-carbonyl substrates and heterocycles is particularly studied. Recent results on the reduction of CO_2 are also included. Special attention is paid to THs performed in aqueous medium as well as to the development of TH in biological media. The employ of biomass-derived products as reagents or solvents in TH transformations is also reviewed. Finally, the proposed mechanisms for TH reactions are revised.

Keywords Aldehydes, Ketones, Alkenes, Alkynes, *N*-Heterocycles, α,β-Unsaturated substrates Half-sandwich complexes, Carbene complexes, Pincer complexes, Biological transfer hydrogenation, Sustainability, Mechanisms

M. P. Lamata, V. Passarelli and D. Carmona
Instituto de Síntesis Química y Catálisis Homogénea, CSIC-Universidad de Zaragoza, Pedro Cerbuna 12, 50009 Zaragoza, Spain
e-mail: plamata@unizar.es, dcarmona@unizar.es
V. Passarelli
Centro Universitario de la Defensa, Ctra. Huesca s/n, 50090 Zaragoza, Spain
e-mail: passarel@unizar.es

Contents

1 Introduction

Transfer hydrogenation (TH) reaction refers to the addition of hydrogen to an unsaturated molecule from a sacrificial hydrogen donor other than H_2 usually with the aid of a catalyst (Scheme 1).

Scheme 1 Catalysed transfer hydrogenation reaction

The use of readily available, inexpensive and easy to handle hydrogen donors avoids the risks associated with hazardous pressurized hydrogen, does not require special experimental setups and allows the selection of the most appropriate donor.

The first antecedent of this reaction is the Meerwein-Ponndorf-Verley reduction of alhehydes and ketones with alcohols. In 1925, Meerwein and Schmidt performed the reduction of aldehydes with ethanol in the presence of aluminium ethoxide [1]. In the same year, Verley reported the reduction of butyraldehyde by geraniol using the same catalyst [2]. One year later, Ponndorf published the reduction of ketones by secondary alcohols catalysed by aluminium isopropoxide [3].

An important step in the evolution of the TH reaction involved the incorporation in the 1960s of transition metal compounds as catalysts. As the first examples, Mitchell, Henbest and co-workers reported the reduction of cyclohexanones and *α*,*β*-unsaturated ketones by TH from 2-propanol by using iridium compounds as catalysts [4, 5]. Shortly after, Sasson and Blum showed that $[RuCl_2(PPh_3)_3]$ promotes the selective TH of C=C bonds in *α*,*β*-unsaturated carbonyl compounds by using primary and secondary alcohols as hydrogen donors [6, 7]. Aromatic aldehydes may also be used as hydrogen donors for this reaction which can be also catalysed by $[RhCl(PPh_3)_3]$ or $[IrCl(CO)(PPh_3)_2]$, although in lower yield [8].

An important breakthrough came some years later when Bäckwall and Chowdhury discovered that the TH of both aliphatic and aromatic ketones with 2-propano1 catalysed by $[RuCl_2(PPh_3)_3]$ was significantly accelerated upon adding a catalytic amount of NaOH [9]. Furthermore, in 1995, Noyori and co-workers reported that η^6-arene complexes of ruthenium containing the ligand (*1S*,*2S*)-(*N*-*p*-toluenesulfonyl)-1,2-diphenylethylenediamine [(*S*,*S*)-TsDPEN] efficiently catalysed the TH of aromatic ketones with 2-propanol affording high enantiomeric ratios (e. r.) [10]. The same group discovered that the TH reaction took place through a new bifunctional mechanism that involved cooperation between the metal and an NH moiety of the ligand [11].

These two important findings fuelled an extraordinary flourishing of the TH reaction which still continues nowadays. On the one hand, the scope of the substrates to be hydrogenated and that of the hydrogen donors to be used have been extended, asymmetric versions have been developed and water has been incorporated as one of the

solvents to be taken into account. On the other hand, metals and the class of compounds employed as catalysts have expanded notably. So, along with complexes of Ru, Rh and Ir, it has been shown that compounds of Ni [12, 13], Pd [14, 15], Re [16], Os [17, 18], Pt [19, 20], Au [21, 22], Mo [23, 24], Zn [25, 26], Zr [27, 28] and Bi [29] also efficiently catalyse the TH of a broad variety of unsaturated substrates. In particular, in recent years, more abundant, cheap and healthy transition metal such as Fe [12, 30-39], Co [12, 40, 41] and Mn [42-55] have attracted increasing attention.

Iridium compounds have played a key role in the development of TH, allowing for the achievement of important milestones. Among the most important advances propelled by iridium compounds it is worth mentioning the TH of linear imines. Back in 1996, Noyori's group reported that ruthenium complexes containing (*S*,*S*)-TsDPEN as a ligand could catalyse the asymmetric TH of cyclic imines with outstanding enantioselectivities [56]. However, it took until 2010 to have efficient catalysts for the TH of acyclic imines. In that year, Xiao and co-workers reported that the metallacycle complex resulting from the reaction of $[Cp^*IrCl_2]_2$ with the imine 4-methoxy-*N*-(1-phenylethylidene)aniline (complex **A**) was highly active for the TH of several acyclic imines using formic acid as a hydrogen source [57]. Since then a series of related iridacycles have been prepared and have shown excellent activity in reducing acyclic imines in a variety of reactions.

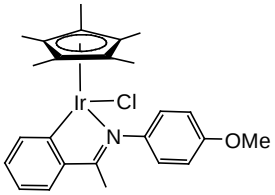

A

Another relevant example of the remarkable features of TH iridium catalysts comes from the employment of intracellular NADH as a hydrogen donor in order to promote anticancer activity. As we will see in what follows, half-sandwich iridium compounds are among the most efficient in catalysing NADH oxidation. In particular, compound **B** catalyses the reaction of dioxygen and NADH yielding H_2O_2, a reactive oxygen species that causes cellular oxidative stress and shows anticancer activity higher than cisplatin [58].

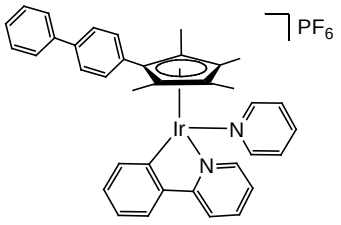

B

Although the first good results in the reduction of *N*-heterocyclic compounds were obtained with rhodium-based catalysts [59], the use of iridium compounds was gaining

more and more importance in the reduction of this type of substrates. As we will see below, pyridines, quinolines, isoquinolines, dehydroisoquinolines, quinoxalines, indoles and phenanthrolines are effectively reduced for a variety of iridium complexes bearing *N*-donor ligands.

In the present report we summarise the progress made thanks to complexes based on iridium in TH reactions. The chapter covers the work published in this area in the five year period from 2015 to January 2020. Previous contributions have been included in the excellent review by Astruc and Wang published in 2015 [60].

The work is structured in sections that classify the results obtained according to the type of ligand. Thus, in the first section we consider the pentamethylcyclopentadienyl ligand that under η^5 coordination originates semisandwich compounds. This ample section contains subsections specifically dedicated to TH of CO_2, TH in water or to the fascinating biological TH. Subsequent sections are devoted to the study of catalysts containing carbene or pincer ligands. In parallel, relevant topics such as TH of α,β-unsaturated alkene-carbonyl substrates, TH of *N*-heterocycles or TH and sustainability are treated in separate sections. To finish, in the last section, the mechanistic aspects of the process under study are discussed.

It is worth noting that Schemes 3-6 list the aldehydes (scheme 3), ketones (scheme 4), imines (scheme 5) and alkenes and alkynes (scheme 6) that have been successfully tested in TH reactions. Within each scheme, the substrates are grouped into families e. g. aliphatic aldehydes and aromatic aldehydes in scheme 3, 1,2-disubstituted alkynes and terminal alkynes in scheme 6 and so on.

2 Half-sandwich Iridium Complexes

After the application of η^6-arene ruthenium complexes containing the chiral (*S*,*S*)-TsDPEN ligand in TH reactions developed by Noyori, Tani, Mashima and Abe demonstrated that pentamethylcyclopentadienyl (Cp*) rhodium and iridium complexes bearing the same chiral ligand are also excellent catalyst precursors for the asymmetric reduction of ketonic substrates [61]. Since then, a number of Cp*-iridium complexes have been successfully applied as TH catalysts and the class of hydrogenated substrates has been widely extended.

2.1 Transfer Hydrogenation of C=O, C=N and C=C Bonds

Transfer hydrogenation of aldehydes, ketones and imines with molecular metallic catalysts is one of the most powerful and versatile tool to access alcohols and amines. Asymmetric versions complete the potential of this methodology. Although much less studied, alkenes can also be hydrogenated by TH. TH in water of the double bonds indicated in the subheading **2.1** will be treated in section **2.3** of this work.

Scheme 2 Half-sandwich iridium catalyst precursors (**1-18**)

Sarkar's group reported that mononuclear **1** [62, 63], dinuclear **2**, **3** [64, 65] and trinuclear **4**, **5** [65, 66] Cp*Ir complexes containing multidentate mesoionic carbene ligands (Scheme 2) promoted the reduction of benzaldehyde (Scheme 3), acetophenone, benzophenone and cyclohexanone (Scheme 4). 2-Propanol was employed as both a hydrogen source and a solvent and KOH as a promoter. At 100 ºC, benzaldehyde was quantitatively reduced to benzylalcohol after 3 h of reaction, at 0.01 mol % of precatalyst loading. Under the same conditions, lower conversions to the corresponding alcohol (55–92%) were achieved for the tested ketones. Mononuclear iridium complexes **1** bearing electron-withdrawing groups at the carbene ligands are catalysts superior to the related complexes with electron-donating substituents. For the homologous ruthenium and osmium complexes, the influence of the substituents was opposite [62, 63].

Scheme 3 Aldehydes

Scheme 4 Ketones

Transfer hydrogenation of the olefins cyclooctene (**D30**), *trans*-*β*-methylstyrene (**D10**) and *trans*-stilbene (**D11**) (Scheme 6) and *N*-benzylideneaniline (Scheme 5) derivatives with 2-propanol was also tested with precatalysts **1a**, **1c** and **1e**. At 100º C,

olefins **D10**, **D11**, **D30** were reduced at 1.0 mol % of catalyst precursor loading. Conversions up to 80 % were achieved after 24 h of treatment. With 1.0 mol % precatalyst loading, the same compounds converted *N*-benzylideneaniline into *N*-benzylaniline (17–50 %) after 18 h of treatment at 100 ºC [63].

Scheme 5 Imines

Scheme 6 Alkenes and alkynes

The dinuclear half-sandwich iridium complexes **6** and **7** having a bridging bis-*N*-heterocyclic carbene ligand catalysed the TH of methyl aryl (**B1**, **B10**), diaryl (**B66**), dialkyl (**B102**, **B113**) and cyclic (**B117**, **B118**) ketones (Scheme 4). Reactions were carried out in refluxing 2-propanol, under basic conditions (*i*PrONa, 3 mol %) and at 0.5 mol % of catalyst loading. After several hours, conversions in the range 5–100 % were achieved, the cationic complex **6** being more active than the neutral *ortho*-metallated complex **7** [67].

Half-sandwich iridium complexes **8a-c** bearing di and tridentate bis(2-pyridylimino)isoindolato ligands are catalytically active in the TH of ketones and imines. In refluxing 2-propanol, with 0.5 equiv of KOH and at 1 or 5 mol % of precatalyst loading, ketones **B1**, **B18**, **B27**, **B37**, **B66**, and **B118** (Scheme 4) were converted to the corresponding hydrogenated species in good yield. Under similar conditions, TH of the imines **C1** and **C14** (Scheme 5) afforded the corresponding amines in 53 and 16 % yield, respectively, after 4 h of reaction [68].

Reduction of acetophenone was carried out at 95 ºC in 2-propanol and KOH as a base. At 2 mol % loading of the precatalysts **9a** and **9b** conversions of 96 and 98 %, respectively, were achieved after 24 h of reaction [69].

The half-sandwich complexes **10**-**12** (Scheme 2) with monodentate, bidentate chelating or bidentate bridging ditriazolylidine ligands containing alkyl or ether linkers of different lengths between the triazolium heterocycles were investigated as catalyst precursors for the TH of benzophenone. At a substrate:base:catalyst molar ratio of 100:10:1, in refluxing 2-propanol, yields in the range 30–98 % were obtained after 4 h of reaction. Activity generally increases with the length of the linker. Bimetallic complex **12** is among the least active species [70].

The catalytic activity of complexes **13**-**16** was evaluated in TH under standard conditions, *i. e.*, refluxing 2-propanol as the sacrificial hydrogen source and KOH (10 mol %) and at 2 mol % of catalyst loading. Benzophenone was taken as the model substrate. In general, good conversions (35–97 %) were obtained after 8 h of treatment [71]. The presence of the hydroxyl functionality enhances the reactivity of **13** and **14** with respect to that of the unfunctionalised triazolylidene ligand in **15**. It has been

suggested [71] that, in basic medium, a metal-bound alkoxide could be formed. Such alkoxide would increase the electron density at the iridium centre and enhance the activity in TH. Alternatively, the alkoxy group may facilitate the dihydrogen abstraction from 2-propanol through an outer sphere mechanism.

A set of aryl-substituted pyridylideneamide (PYA) compounds has been used as ligands in combination with the Cp*Ir moiety affording complexes **17** and **18** [72]. Up to three methoxy substituents have been incorporated to the phenyl ring of the *C*,*N*-bidentate chelating PYA (complexes **17b-e**, Scheme 2). Under optimised conditions, these complexes catalyse the TH of benzophenone using 2-propanol as a hydrogen source. Incorporation of one methoxy substituent to the phenyl ring of the PYA ligand markedly improved the catalytic activity from 27 % conversion for **17a** to 99 and 96 % for **17b** and **17c**, respectively, at 4 h of reaction. Incorporation of a second methoxy group further enhances the catalytic rate (93 % conversion for complex **17d**, after 2 h) probably due to the increase of the electron density at the iridium centre. However, in the presence of a third methoxy group, complex **17e**, the conversion drops even below that of the unsubstituted complex **17a** (30 % conversion, at 24 h of reaction). The relative low activity of **17e** has been tentatively attributed to steric reasons [72].

Complex **17d** has been tested as the catalyst precursor in the TH of ketones **B1**, **B18**, **B20**, **B38-B40**, **B118** (Scheme 4). Under standard conditions good conversions were achieved in all cases. Electron-withdrawing substituents on the aromatic ring (**B20**, **B38-B40**) increased the reduction rate and electro-donating substituents (**B18)** had the opposite effect.

Imines were also investigated as substrates for TH under the standard conditions. Complexes **17a-17e** catalysed the hydrogenation of *N*-benzylideneaniline to the corresponding amine in 80–94 % conversion after 4 h of treatment. With these substrates, the different degree of substitution at the phenyl ring of the PYA ligand does not affect significantly the catalytic activity. Complex **17b** hydrogenates aldimines **C4**, **C8**, **C9**, **C12** and **C14** (Scheme 5) in yields up to 90 %, after 24 h of reaction. Notably, ketimine **C15** was not converted at all and it was suggested that substitution at the α carbon may hamper or even prevent substrate binding due to steric constraints.

The iridium complex **17e** was investigated in the TH of aldehydes. Under standard conditions *i. e.* refluxing 2-propanol, 1 mol % catalyst loading and 10 mol % KOH, essentially full conversion of benzaldehyde was achieved within 5 min; however the yield of benzyl alcohol was only 50 % and benzoic acid and benzoate were also obtained. When this reaction was carried out without a base, aldehyde conversion was slower (85 %, 24 h) but it was completely selective to benzyl alcohol. In the absence of a base, other aryl aldehydes such as **A24**, **A29** and **A35** were also selectively converted to the corresponding alcohol. Both electron donating and withdrawing substituents at the phenyl group of the PYA ligand slow down the catalysis. In contrast to the

behaviour of ketones, 2-pyridinecarboxaldehyde and the aliphatic aldehyde **A54** (Scheme 3) were not hydrogenated in the absence of a base. Probably, under base-free conditions coordination of the pyridine nitrogen to the iridium centre is favoured thus preventing the catalytic TH [72].

Scheme 7 Half-sandwich iridium catalyst precursors (**19-36)**

Chiral amidoiridium complexes **19**-**21** (Scheme 7) catalyse the asymmetric TH of acetophenone in 2-propanol, in the absence of a base, with a substrate/catalyst (S/C) ratio of 200 at 30º C [73]. The mononuclear amido complexes **20** and **21** reached almost complete conversion within 30 min. The catalytic activity of the dinuclear complex **19** is remarkably lower. Catalytic rates can be related to the relative ability of complexes **19**-**21** to dehydrogenate 2-propanol. The bridging complex **19** is inert in 2-propanol but the mononuclear complexes **20** and **21** were completely converted into diastereomeric mixtures of the amino complexes **A** and **B**, respectively, by addition of excess of 2-propanol (Scheme 8). The (*S*)-product was obtained in all cases with an e. r. of about 80/20.

Scheme 8 Dehydrogenation of 2-propanol by the amido complexes **20** and **21**

The $C_{carborane}$-cyclometallated complex **22** and the $B_{carborane}$-cyclometallated complexes **23** and **24** reduce acetophenone to 2-phenylethanol, in the presence of *t*BuOH, with 2-propanol as a hydrogen source and at a catalyst loading of 0.5–1.0 mol %. Conversions greater than 90 % were achieved after 1 h of reaction. Cyclometallation of the carborane moiety enhances catalysis greatly compared to the non-cyclometallated counterparts. The B-cyclometallated complex **23** is more active than the corresponding C-cyclometallated **22** [74].

Cp*Ir(III) complexes (**25**-**27**) bearing imidazolium ion tethered TsDPEN ligands (Scheme 7) are efficient catalysts for asymmetric TH of α-ketophosphonates **B137**-**B148** (Scheme 4) in water. At RT, moderate yields (44–78 %, 4-8 h of reaction) and good to excellent e. r.'s (up to > 99.5/0.5) were obtained by using 1 mol % of $[Cp^*IrCl_2]_2$, 2 mol % of the ligand and HCOONa as hydrogen donor [75].

Half-sandwich iridium complexes bearing pyridinesulfonamide ligands (**28**-**34**, Scheme 7) were assessed as precatalysts for TH of methyl aryl (**B1**, **B3**, **B10**, **B15**, **B18**, **B22**, **B27**) diaryl (**B66**), methyl alkyl (**B96**, **B103**) and cyclic (**B117**-**B119**) ketones (Scheme 4) [76]. In general, good conversions are obtained after 3 h of reaction, in refluxing 2-propanol, at 1 mol % of catalyst loading and in the absence of a base. With electro-donating groups, on the 4-substituted acetophenone substrate, the observed conversion after 6 h drops in comparison with substrates with electron withdrawing

substituents. On the other hand, precatalysts bearing electron-rich substituents on the pyridinesulfonamide ligand (complexes **28**, **31** and **33**) exhibited the highest conversion of 4-nitroacetophenone to the corresponding alcohol, while precatalysts **29**, **32** and **34**, which possess electron withdrawing substituents on the ligand, afforded only moderate conversions. Under the same conditions, trials conducted using precatalyst **28** reduced benzophenone (82 % conversion, 24 h reaction), dialkyl ketones **B96** (52 %, 24 h) and **B103** (65 %, 3 h), and cycloaliphatic ketones **B117** (85 %, 3 h), **B118** (99 %, 3 h) and **B119** (63 %, 3 h) [76].

The same iridium pyridinesulfonamide complexes **28-34** are active for the TH of a variety of aryl (**A1**, **A3**, **A4**, **A12**, **A13**, **A22-A24**, **A27**, **A30**, **A32**, **A38**, **A43**), alkyl (**A56**) and heterocyclic (**A64**, **A65**) aldehydes (Scheme 3) [77]. Reductions occur with moderate to high conversions (39–100 %), under base free conditions and at high rates. Thus, for example, benzaldehyde derivatives are hydrogenated within 30 min in 2-propanol at 85º C, at 1 mol % of catalyst loading. As observed for substituted acetophenones, the combination of electron-donating groups on the ligand of the precatalysts with substrates possessing electron-withdrawing moieties entailed the highest rate of conversion to the alcohol. Decylaldehyde was quantitatively reduced in the presence of complex **30** in 12 h, under the above mentioned conditions. The heterocyclic substrates 2-furfural **A64** and 5-hydroxymethylfurfural **A65** were selectively reduced to the corresponding alcohol in 95 and 100 % conversion, respectively, in 30 min. A metal-ligand cooperative mechanism has been proposed for the catalytic TH reaction, the trihydride bridged dimer $[Cp^*Ir(\mu\text{-}H)_3IrCp^*]^+$ being the resting state [77].

Methyl aryl (**B1**, **B3**, **B18**, **B20-B22**, **B27**, **B36**), methyl alkyl (**B94**, **B96-B98**, **B101**, **B107**) and alkyl aryl (**B51**) ketones (Scheme 4) are reduced using chiral Cp*Ir compounds **35** and **36** (Scheme 7) containing C_2-symmetric ferrocenyl bis(phosphinite) ligands [78-81]. At 82 ºC, using 2-propanol as hydrogen source and solvent, with KOH (5 mol %) as a base and at 1 mol % of catalyst loading, almost quantitative conversions and moderate-to-good e. r.'s (from 68/32 to 99.5/0.5) were obtained, after 0.25-8 h of reaction.

Scheme 9 Half-sandwich iridium catalyst precursors (**37**-**52**)

Chiral cyclometallated 1-naphthylethaneamine iridium complexes featuring up to three stereogenic centres displayed excellent activity for asymmetric TH, albeit with modest enantioselectivities [82]. Complex **37** (Scheme 9), at 2 mol % catalyst loading, with acetophenone as the substrate, 2-propanol as the reducing agent and in the presence of *t*BuOK (5 mol %) afforded 2-phenylethanol in 99 % conversion, after 15 min of

treatment at 20 ºC, with an e. r. of 76/24. Working at -30 ºC, a conversion of 97 %, with 84.5/15.5 of e. r., was achieved after 1 h of reaction.

Cp*Ir(III) complexes with chalcogenated Schiff bases of anthracene-9-carbaldehyde **38**-**41** (Scheme 9) were tested for the TH of aldehydes **A1**, **A23**, **A24**, **A30**, **A31**, **A38** and **A61** (Scheme 3) and ketones **B1**, **B15**, **B21**, **B47 B101** and **B117** (Scheme 4) under base-free conditions [83]. At 80 ºC, in 2-propanol, at catalyst loading of 0.1–0.5 mol %, conversions in the 66–98 % range were obtained, after 1-6 h of reaction. For iridacycles **38** and **39**, a mechanism involving the loss of the Cp* ring was proposed [83].

The iridium dimer $[Cp^*IrCl_2]_2$ reacts with methyl (*S*)-2-phenyl-4,5-dihydrooxazole-4-carboxylate selectively giving a *N*,*C*- (**42**) or a *N*,*O*-chelated (**43**) complex (Scheme 9) depending on the reaction conditions [84]. Interestingly, the *N*,*O*-chelated complex **43** is much more active and selective in the asymmetric TH of ketones than its *N*,*C*-chelated isomer **42**, using mixtures of formic acid/amine as a hydrogen source, in CH_2Cl_2. Furthermore, the sense of asymmetric induction is different for each isomer. The favoured configuration of the alcohol is *S* for the *N*,*O*-chelated complex **43** and *R* for *N*,*C*-chelated analogue **42**. Thus, for example, in the presence of 1 mol % of complexes **42** or **43**, 4-nitroacetophenone could be reduced by using an azeotropic mixture of formic acid/triethylamine, in CH_2Cl_2 at RT. However, while with precatalyst **43** 100 % of the corresponding alcohol was obtained after 2 h of reaction, with an 86.5/13.5 of e. r. in favour of the *S* enantiomer, with the analogous precatalyst **42** only 75 % of conversion was measured after 15 h of treatment with a 48/52 e. r. in favour of the *R* enantiomer. Regarding the formic acid/amine mixture, besides NEt_3 also Et_2NH, Cy_2NH, *i*$PrNH_2$ and *t*$BuNH_2$ have been tested. Using the catalyst precursor **43**, the highest e. r. (99/1) for the TH of ketone **B27** was obtained with a formic acid/*i*$PrNH_2$, 2/1 mixture. No reasons have been proposed for this behaviour.

The *N*,*O*-chelated complex **43** catalyses the TH of a variety of methyl aryl (**B1**-**B6**, **B14**, **B15**, **B17**, **B18**, **B22**, **B27**, **B30**-**B33**, **B35)** and alkyl aryl ketones (**B47**, **B49**, **B55**, Scheme 4) using a formic acid/*i*$PrNH_2$, 2/1 mixture. Excellent e. r.'s, between 95/5 and 99.5/0.5, were obtained with yields ranging from 7 to 98 %, when the reactions were carried out overnight, at RT in CH_2Cl_2. The lowest activity corresponds to acetophenones that bear highly electro-donating substituents (e. g. **B17**, 7 % yield) or 2-substituted acetophenones (e. g. **B2**, 18 % yield) [84].

Half-sandwich iridium complexes **44**-**47** (Scheme 9) containing a triazenide group as a ligand have been tested as precatalysts in the TH of acetophenone, in 2-propanol as both hydrogen donor and solvent, at 70 ºC [85]. Reactions were performed in the presence of KOH as a base with a catalyst loading of 2 mol %. The chloride compounds **44** and **45** need 42 and 62 h of reaction, respectively, to achieve, in both cases, 95 % yield. However, if the hydride complex **46**, derived from **45**, is used as catalyst a yield

of 83 % was obtained just after 4 h and in the absence of a base. Complex **47**, without imidazole substituents on the triazenido moiety, also reduced acetophenone without a base (98 % yield in 86 h) [85].

Scheme 10 Chiral phosphoric acid used as additive in the TH of imines

The chiral iridium complex **48** (Scheme 9) in cooperation with the chiral phosphoric acid depicted in Scheme 10 efficiently catalyse the asymmetric TH of *N*-benzyl **C15-C25**, *N*-*p*-methoxybenzyl **C16**, *N*-*p*-methoxyphenyl **C26-C31** and **C33**, dialkyl substituted **C34**, **C35** and aryl ethyl **C32** imines [86]. Unexpectedly, the efficiency and enantioselectivity of the TH can be tuned by the use of different alcohols as the hydrogen donor. In general, benzylic alcohols provided high efficiency and 1,2-diphenylethane-1,2-diol gave the highest enantioselectivitity (Scheme 11). Treatment of the imines in toluene, at 80 ºC, over 24 h, with 3 equivalents of this alcohol, in the presence of 5 mol % of complex **48** and 5 mol % of phosphoric acid afforded the corresponding amines with yields from 60 to 90 % and e. r.'s from 87/13 to 98/2. Based on experimental studies and DFT calculations, a mechanism involving an iridium alkoxide as the reducing agent was proposed [86].

Scheme 11 Screening of hydrogen donors for the TH of imines

2.2 Transfer Hydrogenation of CO_2

With the aim of reducing the concentration of CO_2 in the atmosphere, methods to convert it into valuable chemicals have been the subject of intense investigation in recent years [87]. Among them, catalytic methods for CO_2 direct hydrogenation to one-carbon molecules such as formic acid or methanol using homogeneous metallic catalysts are, probably, the most intensively studied ones (for recent reviews, see refs. [88-91]). However, the protocols reported so far require, in general, harsh conditions of temperature and pressure. TH approaches could try to avoid this problem and allow for the use of renewable hydrogen sources with inherent advantages from a perspective of sustainability. However, reports on TH of CO_2 are scarce. Most of them involve half-sandwich ruthenium or iridium complexes bearing strongly electron-donating *N*-heterocyclic carbene ligands. In 2010, the group of Peris reported the formation of formic acid from CO_2 in the presence of 2-propanol as the hydrogen donor. With the iridium catalyst precursor **49** under 50 bar of CO_2, in a 0.5 M KOH solution, a TON of 150 was obtained after 72 h at 110 ºC [92]. The same group showed that the sulfonate

substituted bis-abnormal carbene complex **50** afforded a TON of 2700 under 50 bar of CO_2, in a 0.5 M KOH solution, after 75 h at 200 ºC [93].

More recently, Choudhury's group studied the application of the half-sandwich iridium complexes **51** and **52** in the catalytic conversion of CO_2 to formates via TH using glycerol, a renewable biomass derivative, as a hydrogen source [94]. Complex **51** performs better than complex **52** under all the tested conditions. Notably, the catalytic system works at ambient-pressure of CO_2, in water as the solvent. Glycerol showed to be superior to methanol or 2-propanol as the hydrogen donor. Under optimised reaction conditions (0.15 μmol of complex **51**, 1.0 M aqueous K_2CO_3 as a base, at 150 ºC) a TON of 149 was achieved after 1 h of reaction. Control experiments showed: i) formate was not formed from the carbonate used as the base; ii) under standard conditions, formation of hydrogenocarbonate was observed in the reaction mixture; iii) hydrogenocarbonate also renders formate at lower rate than CO_2, in parallel and simultaneously; iv) hydride **II** (Scheme 12) was stoichiometrically prepared by treating complex **51** with glycerol in acetonitrile or with 2-propanol in water, in both cases, in the presence of K_2CO_3; v) this hydride reacts with aqueous hydrogenocarbonate affording formate.

Scheme 12 Proposed catalytic cycle for the TH of CO_2

All these data suggest the mechanism depicted in Scheme 12. Complex **51** forms the alkoxy intermediate **I** from the alcohol in basic medium. Subsequently, hydride **II** is generated through β-hydrogen elimination. This compound delivers its hydride to the substrates, CO_2 or $HCOO^-$, to produce the formato species **III**. Complex **III** releases formate and, upon reaction with an alcohol and a base, regenerates the alkoxy complex **I** that restarts the catalytic cycle [94].

2.3 Transfer Hydrogenation in Water

The development of aqueous TH reactions offers economic and environmental benefits because water is cheap and non-toxic. Research into TH reactions in water started in the 1980's. Sasson, Blum and co-workers reported on the aqueous-organic biphasic reduction of C=C and C=O bonds with phosphine ruthenium and rhodium complexes in the presence of formate salts as hydrogen donor [95-97]. Joó's group reported on the hydrogenation of unsaturated bonds by using water soluble rhodium and ruthenium complexes bearing sulfonated phosphine ligands [98-100]. Thereafter, great progress was made in the TH of C=C and C=O and also C=N bonds. The most widely employed catalysts are half-sandwich compounds, Cp*Ir complexes playing a remarkable role

[101-108]. We collect here new contributions in this area that have appeared in the last 5 years.

Iridium complexes containing imidazolium ion tethered TsDPEN ligands (Scheme 13) catalyse the TH of a range of α-ketophosphonates (**B137-B148**, Scheme 4) in water, employing HCOONa as the hydrogen donor. The products were obtained in moderate to good isolated yield (44–78 %) with good to excellent e. r.'s (up to > 99.5/0.5) after 4-8 h of treatment at RT [75].

Scheme 13 TsDPEN and imidazolium ion tethered TsDPEN ligands and phosphonate reduction

Cationic half-sandwich iridium complexes bearing pyridine-2-yl-methyl aniline ligands (**53**, Scheme 14) were investigated for catalytic TH of acetophenone in water as a solvent. A HCOOH/HCOONa mixture was used as a hydrogen source. The best results were obtained with a HCOOH/HCOONa, 7.5/3.5 molar ratio, in 2 mL of H_2O (pH = 2.60). At 60 ºC, with a catalyst loading of 0.5 mol %, 95–96 % of conversion was achieved after 4-6 h of reaction [109].

Scheme 14 Half-sandwich iridium catalyst precursors (**53-57)**

When complex **53d** with a protected amine group (N–Me) was tested for the TH of acetophenone, moderate catalytic activity was observed (52 % conv, 24 h). This result indicates that for complexes **53** the preferred mechanism is the Noyori's bifunctional mechanism.

The catalytic activity of the related imine compound **54** (Scheme 14) is lower than that of the corresponding amine compound **53a**. To achieve 96 % conversion, 24 h of reaction were necessary, under the optimised conditions [109].

In 2017, the Tang's group reported on the reduction of a range of aldehydes in water in the presence of formic acid as the hydrogen source using half-sandwich iridium complexes **55** containing imidazolyl-pyridine ligands (Scheme 14). It is remarkable the good tolerance for a wide variety of functional groups such as alkene (**A25**) and alkyloxy (**A26**), halogens (**A16**, **A30**, **A31**, **A44**, **A45**), phenols (**A2**, **A41**, **A42**), ketones (**A34**), carboxylic acids (**A20**, **A36**), cyano (**A19**) or nitro (**A38**, **A44**).

Under the optimal conditions (0.02 mol % of catalyst loading, 4 equiv of HCOOH, 2 mL of water, 80 ºC) high conversion (91–99 %) was obtained for most of the substrates tried, in about 15 min [110].

The catalytic process is chemoselective. Thus, for example, only the aldehyde group of the ketonic substrate **A34** was reduced. The system also works at a catalyst loading as low as 0.005 mmol % and, notably, a TOF value of 73,800 h^{-1}, at 49 % of conversion, was achieved for 4-methoxybenzaldehyde [110].

However, the group of Tang and Xu demonstrated that, properly adjusting the reaction conditions, ketones can be efficiently reduced employing the same type of imidazolyl-pyridine iridium complexes. The most important changes in the reaction conditions were that the amount of formic acid was increased up to 12 equiv and that the catalytic reactions were carried out under inert atmosphere [111]. Under these conditions, aryl alkyl (**B1**, **B3**-**B5**, **B9**, **B10**, **B12**-**B15**, **B20**-**B26**, **B27**, **B37**, **B47**), methyl alkyl (**B100**, **B104**, **B107**), methyl heterocyclic (**B38**, **B41**) and cyclic (**B118**, **B119**, **B121**) ketones were hydrogenated. Yields between 57 and > 99 % were obtained after 4-12 h of reaction. The reduction rates are dependent on the pH values of the reaction media, conversions dramatically decreasing when pH increases. The standard S/C ratio employed was 10,000 but catalysis also occurs at an S/C ratio of 100,000. A TOF of 26,000 h^{-1}, at 52 % of conversion, was achieved in the reduction of acetophenone, employing catalyst **55a** [111]. Furthermore, a wide range of ketones containing a variety of functional groups such as aryloxy (**B106**), halogens (**B57**, **B64**), cyano (**B63**-**65**) or ester (**B54**, **B61**, **B108**) were also reduced. Typically, conversions higher than 90 % were obtained, at 80 ºC, within 3-12 h [111].

The Fu's and Zhou's group reported on the asymmetric TH of non-*ortho*-substituted-2-pyridylketone *N*-oxides (Scheme 4) using chiral diamine-derived iridium complexes (**56**) (Scheme 14). A H_2O/*i*PrOH mixture and sodium formate were employed as the solvent and the hydrogen source, respectively. The *N*-oxide function was removed by treating the resulting alcohols with Zn/NH_4Cl [112].

After screening, by examining the reduction of 2-(4-chlorobenzoyl)pyridine *N*-oxide (**B80**), complex **56a** was selected as the best catalyst, in terms of yield and enantioselectivity. Under the optimised conditions (5 mol % of catalyst loading, 10 equiv of HCOONa, H_2O/*i*PrOH, v/v:1/1, RT, 24 h) a wide variety of 2-pyridyl ketone *N*-oxides with different functionalities and electronic properties (**B74**-**B90**) were reduced. Yields from 56 to 90 % and e. r. from 78.7/26.3 to 99.1/0.9 were obtained [112].

Structurally diverse aldehydes and ketones were reduced, in water, with formic acid as a hydrogen source, by using half-sandwich iridium complexes **57** as catalyst precursors (Scheme 14). Under aerobic conditions, the reduction of benzaldehyde was completed with catalyst **57a** within 9 min using an S/C ratio of 2,000. At 5,000 and 10,000 S/C ratios reduction of benzaldehyde was not observed. However, under nitrogen atmosphere, in degassed water, good results were obtained at S/C ratios as high as 20,000 and 10,000 for aldehydes (including benzaldehyde) and ketones, respectively.

Catalyst **57a** proved to be more active than its congeners **57b** and **57c**. With complex **57a** as the catalyst and at the standard conditions of a S/C ratio of 20,000, 5 equiv of HCOOH, at 90 ºC and under N_2 atmosphere, a series of diverse aldehydes (**A1**, **A2**, **A16**, **A19**, **A23**, **A24**, **A28**, **A30**-**A32**, **A34**, **A36**-**A38**, **A42**, **A44**, **A46**, **A47**, **A50**,

A55, **A59**, **A63**, **A64**, **A67**, Scheme 3) were reduced in excellent isolated yield (90–99 %), after 2 h of reaction [113].

Catalysts **57** also actively reduce ketones. Like for Tang's imidazolyl-pyridine iridium catalysts, to obtain good results an excess of formic acid (15 equiv) greater than that for TH of aldehydes (5 equiv) has to be used. Higher excess of formic acid provides more acidic conditions to activate carbonyl groups and dissolves ketones. In fact, ketones that were not reduced in the presence of 5 equiv of formic acid were easily reduced by using 15 equiv of this acid.

A variety of substituted acetophenones with electron-donating or withdrawing group was reduced to the corresponding alcohols. Halogen (**B20-B22**), nitro (**B27**) and cyano (**B24**) groups were compatible as well as heterocyclic substituents (**B38**, **B41**). Methyl alkyl ketones (**B100**, **B107**), cyclohexanone, cycloheptanone, or ketones containing acidic functional groups (**B25**) were also reduced.

Again, complex **57a** was the catalyst of choice. With this complex, yields from 78 to 99 % were obtained after 12 h of reaction, with an S/C ratio of 10,000, at 90 ºC and under N_2 atmosphere [113].

2.4 Biological Transfer Hydrogenation

Artificial metalloenzymes (ArMs) are hybrid catalysts that result from combining an abiotic metal cofactor with a protein with the aim of taking advantage of the features of both metal-based and enzymatic catalysis [114, 115]. In the field of artificial transfer hydrogenases, many efforts have been devoted to the development of imine reductases. Since 2005, the Ward's group has been using Noyori-type piano stool metallic cofactors combined with either wild type streptavidin (Sav WT) or streptavidin mutants as host proteins to develop artificial asymmetric transfer hydrogenases. The metallic cofactor was completed by bonding the Noyori's diamine ligand to biotine which acts as a anchor to the protein [116-118] (Scheme 15). The intricate network of interactions in the biological scaffold creates a chiral second coordination sphere environment around the catalytic metal site responsible for enantioselection. Given the prevalence of the chiral 1,2,3,4-tetrahydroquinoline in natural alkaloids and synthetic drugs [119] the salsolidine precursor imine 1-methyl-6,7-dimethoxy-3,4-dihydroquinoline was usually employed as a model substrate (Scheme 15). 3-(*N*-morpholino)propanesulfonic acid (MOPS) buffer and sodium formate were usually employed as the reaction medium and the hydrogen source, respectively, [120-122] (Scheme 15).

Scheme 15 Transfer hydrogenation of imines catalysed by artificial metalloenzymes

Based on the biotine-streptavidin technology developed by the Ward's group, Rimoldi et al. have investigated the catalytic activity of the iridium complexes depicted in Scheme 16 employing wild-type Sav and the Sav mutants indicated in the same Scheme.

Scheme 16 Artificial metalloenzymes for the TH of the salsolidine precursor developed by Rimoldi et al. [123]

Reactions were carried out at 30-40 ºC, by using 1 mol % of iridium complex, 0.33 mol % of tetrameric wild-type Sav or Sav mutants, in 1 mL of MOPS buffer at pH 6.5-7.0 and in the presence of HCOONa (3M) as the hydride source. When the transition metal compound is embedded in the host protein, a decrease in activity was observed accompanied by an improvement of stereoselectivity. The best results (60 % conversion, 82.5/17.5 e. r., 24 h) were achieved with the S112C mutant in combination with the complex bearing the biotine anchored to the para position in the ligand (Scheme 16) [123].

Rimoldi's group has also investigated half-sandwich iridium complexes with the biotine moiety anchored to the Cp* ring for the TH of the imine precursor of salsolidine. Sav WT as well as different Sav mutants at position S112 or K121 and a double mutation at positions S112 and K121 or L124 were investigated as the host proteins (Scheme 17).

Scheme 17 Artificial metalloenzymes for the TH of imines [124]

Reactions were carried out at 30 ºC, in 0.6 M MOPS buffer with 1 mol % catalyst loading and 3 M HCOONa as a hydrogen source. Poor conversion and e. r. were obtained, the best results being achieved for the chiral amino hydroquinoline ligand **IV** (5–77 % conversion, 46/54–16/84 e. r., 18 h). In all cases, both conversion and e. r. decrease in the presence of host protein with respect to the values obtained by using metallic cofactors alone. The *S*-enantiomer of the hydroquinoline ligand **IV** always gives preferentially *S*-salsolidine and the *R*-enantiomer of the ligand always gives preferentially *R*-salsolidine indicating that the chiral environment of the host protein affected the chirality of the product to a lesser extent [124].

Ward, Maréchal and co-workers have applied directed evolution to an artificial transfer hydrogenase to improve its catalytic activity and selectivity for the reduction of cyclic imines. The introduction of the cofactor depicted in Scheme 18 within Sav isoforms affords asymmetric transfer hydrogenases that can be optimised by directed evolution protocols [125, 126]. Two mutants were identified (see Scheme 18) that increased the reaction rate for the reduction of the cyclic imine shown in Scheme 18

and, under the indicated conditions, enantiomeric rates of 97.5/2.5 (*R*) and 7.5/92.5 (*S*) were achieved [119].

Scheme 18 Observed enantiodivergence with two selected Sav-mutants obtained by directed evolution

A biotinylated iridium half-sandwich complex was incorporated into streptavidin-mutant S112A to generate an ArM (Scheme 19). Selective deuteration of nicotinamide adenine dinucleotide (NAD^+) mediated by this ArM, employing deuterated sodium formate as a deuterium source, generate deuterated NAD^2H in high diastereomeric excess [127].

Scheme 19 Diastereoselective reduction of NAD^+

ArM based on Sav variants and biotinylated iridium cofactor enable the regeneration of various synthetic NADH mimics (mNADH) from NAD^+, with formic acid as a hydrogen source. The involved TH can be coupled with ene reductase-catalysed reduction of α,β-unsaturated compounds. Scheme 20 shows the iridium cofactor and NAD^+ mimics as well as the α,β-unsaturated substrates which are hydrogenated. Sav 112A and Sav 112K mutants were used as the host protein and the ene reductase of the Old Enzyme family from *Thermus scotuductus* was selected as an mNADH-accepting enzyme. Scheme 20 also shows a particular case of the two coupled processes [128].

Scheme 20 Reduction of a NAD^+ mimics by the Sav 112K mutant combined with the iridium shown cofactor (top). Reduction is coupled with the enzymatic hydrogenation of an α,β-unsaturated substrate (bottom)

Biological reducing agent nicotinamide adenine dinucleotide phosphate (NAD(P)H) serves as an efficient hydrogen source for the reduction of cyclic imines. An ArM formed by combining a biotinylated Cp*Ir compound with either wild-type Sav or Sav mutants was used as the catalyst. To regenerate the consumed NAD(P)H, glucose dehydrogenase was incorporated into the process and, to increase the enantiomeric excess, a monoamine oxidase and a catalase were also integrated into the system. The resulting four-enzyme system catalyses the reduction of 1-methyl-3,4-dihydroisoquinoline with NAD(P)H as a hydrogen source. Quantitative conversion and perfect enantioselectivity, in favour of the (*R*)-enantiomer were achieved by combining the iridium cofactor, shown in Scheme 21, with the Sav K121R mutant after 24 h of treatment at 37 ºC [129].

Scheme 21 Transfer hydrogenation employing NAD(P)H as a hydrogen source

Human carbonic anhydrase II (hCA II) offers an attractive scaffold for the assembly of ArMs using arylsulfonamide as a high affinity anchor [130]. An X-ray structure determination shows that arylsulfonamide can interact with the Zn ion which lies at the bottom of a deep hydrophibic funnel-shaped cavity of the protein [131]. To anchor to hCA II, the arylsulfonamide bearing iridium complexes [(η^5-Cp*)Ir(picolylamine)Cl] and [(η^5-Cp^{propyl})Ir(picolylamine)Cl] (Cp^{propyl}= penta-*n*-propylcyclopentadienyl) depicted in Scheme 22 were prepared. Application of the computational design software Rosetta [132] to the combination [(η^5-Cp*)Ir(pico)Cl]/hCA II WT afforded four hCA II variants that significantly increased affinity for the catalysts. The combination of designed hCA II mutations with the η^5-Cp^{propyl} complex renders productive (TON up to 100) and highly selective (up to 98/2 e. r.) ArMs for the reduction of cyclic imines, under the conditions indicated in Scheme 22 [133].

Scheme 22 TH of isoquinolines mediated by ArMs. The Ir-cofactors are shown at the top and the host proteins employed are hCAII WT or mutants computationally designed

A half-sandwich iridium complex was assembled to a periplasmic binding protein such as CeuE, an iron siderophore of *Campylobacter jejuni*, by using an azotochelin siderophore as binding anchor. The remaining two coordination sites around the iron centre were occupied by solvent molecules in the free cofactor. Nonetheless, it was hypothesised that those sites are used to bind Y288 and H227 of CeuE. The resulting ArM slowly reduces salsolidine precursor (TON 400, 24 h) with an e. r. of 67.7/32.3. CeuE mutant H227A increases TON (400, 2 h) but at the expense of a substantially lowered e. r. (51.7/48.4) [134] (Scheme 23).

Scheme 23 TH of 1-methyl-6,7-dihydroxy-3,4-dihydroisoquinoline by the ArM formed by combination of the Ir-cofactor wiyh the host protein shown at the top

NADH and NAD(P)H play important roles as cofactors in numerous biocatalysed processes [135]. In 2012, the groups of Sadler [136] and Fukuzumi [137] independently showed that half-sandwich iridium complexes can utilise NADH as a hydride donor to generate an iridium-hydride complex. The hydrido complex is able to transfer the hydride moiety to organic substrates. Regeneration of the iridium-hydride from NADH completes the TH catalytic cycle. In particular, the hydride can be transferred to molecular oxygen increasing the levels of hydrogen peroxide and reactive oxygen species (ROS). Oxidative stress caused by generation of ROS is an effective method of killing cancer cells [138].

The half-sandwich iridium complex depicted in Scheme 24 bearing an *N*-phenyl-2-pyridinecarboxamidate ligand catalyse the reduction of aldehydes to the corresponding

alcohols in *t*-BuOH/phosphate-buffered saline 2/8 at 37 ºC, employing NADH as a hydrogen donor. After 24 h of treatment, conversions of 30 to 90 % were obtained, at a catalyst loading of 2 mol %. Neither acetophenone nor 4-heptanone were reduced and the electron deficient 4-nitroacetophenone was converted to the corresponding alcohol but in only 11 % yield [139].

Scheme 24 Iridium catalyst and aldehydes that are hydrogenated. NADH was employed as a hydrogen donor

Aldehydes derived from lipid peroxidation, such as 4-hydroxynon-2-enal, are implicated in various diseases and, therefore, reduction of these aldehydes to the corresponding alcohol may lead to detoxification. The same pyridinecarboxamidate iridium complex reduced 4-hydroxynon-2-enal with NADH acting as a hydrogen source. Under the conditions shown in Scheme 25, 88 % of 4-hydroxynon-2-en-1-ol and 6 % of 4-hydroxynonan-1-ol were obtained. Increasing the reaction time led to higher ratios of the saturated dialcohol suggesting that the C=O group is first hydrogenated. The putative hydride intermediate [Cp*IrH(pyridinecarboxamidate)] was detected and characterised by NMR spectroscopy [139].

Scheme 25 TH of 4-hydroxynon-2-enal pyridine catalysed by the carboxamidate iridium complex shown. NADH was the H-donor

The Do's group showed that the reduction of aldehydes catalysed by the pyridinecarboxamidate iridium complex above mentioned can take place inside living cells [140]. This complex catalyses the reduction of BODIPY-CHO to BODIPY-OH (Scheme 26) inside of NIH-3T3 mouse embryo fibroblast cells, using NADH as the hydrogen donor. The fluorescence that the BODIPY-OH compound develops within the cytoplasm of the cell was employed to monitor the TH reaction. When the generation of NADH was artificially reduced, the cells did not show an increase in fluorescence indicating that NADH acts as an endogenous hydride source [140].

Scheme 26 Reduction of Bodipy-CHO

Chemosensitiser agents are compounds that added to drug cocktails make cells more susceptible to the effects of the active drug [141]. The Do's group has shown that the biocompatible bipyridine Cp*Ir complex presented in Scheme 27 is an excellent metallochemosensitiser in combination with carboplatin. Treatment of Y79 eye/retina cancer cells with this complex and carboplatin led to a NAD^+/NADH ratio 2.2 times greater than that in untreated cells. In contrast, after a similar treatment, the non-cancerous ARPE-19 eye/retina cells did not show significant differences in the

NAD^+/NADH ratio, relative to untreated cells. Most probably, NADH acts as a hydrogen donor to the iridium complex. The plausible iridium hydride [Cp*IrH(2,2'-bipyridine]$^+$ was independently synthesised and isolated as a hexafluorophosphate salt. Notably, this hydrido complex dissolved in a mixture of methanol/phosphate-buffered saline, 1/1 and when exposed to the air yields H_2O_2 in up to 40 % yield [142].

Scheme 27 Bipyridine iridium complex and carboplatin

The half-sandwich iridium complexes shown in Scheme 28 catalyse the oxidation of NADH to NAD^+ and lead to the generation of ROS [143-147]. These iridium complexes display promising anticancer activities toward Hela human cervical [143-146] and A549 [144-146] cancer cells. The increase of ROS appears to contribute to the anticancer activity.

Scheme 28 Iridium complexes with anticancer activity

The cationic Cp*Ir complex depicted in Scheme 29 catalyses the TH of a set of linear and cyclic imines in water. NADH or a *N*-benzyl-1,4-dihydronicotinamide (an NADH mimic) can be used as the hydrogen source. NAD(P)H and HCOONa can also be used as the hydrogen donors. Moderate to excellent yield (58–99 %) was obtained under the conditions indicated in Scheme 29 [148].

Scheme 29 Reduction of imines with a half-sandwich iridium catalyst with NADH and an NADH mimic as a hydrogen donor

The iridium complex presented in Scheme 30 facilitates the formation of NADH from NAD^+ in the presence of formate. Intracellular co-administration of the iridium complex with sodium formate enhances the antiplasmodial activity in the chloroquine-resistant strain of *Plasmodium falciparum*. This result indicates that TH reactions could be studied in terms of application to infectious diseases such as malaria [149].

Scheme 30 Quinoline-based half-sandwich organoiridium complex

Rimoldi's group has shown that antibiotic vancomycin is able to coordinate Cp*Ir(III) moieties, although its coordination mode remains uncertain. The resulting system was applied to the asymmetric TH of cyclic imines. Different cyclic imines were reduced in aqueous media, under mild reaction conditions, affording the corresponding amine, with moderate to appreciable e. r.'s. In particular, for imine **II** (Scheme 31) a conversion of 35 % with 80.5/19.5 e. r. was achieved, after 18 h of treatment at 25 ºC, in 2-(*N*-morpholino)ethanesulfonic acid (MES) buffer 1.2 M pH 5, with 4 mol % of

vancomycin and 1 mol % of $[(\eta^5\text{-Cp*})IrCl_2]_2$, in the presence of HCOONa 3 M as hydrogen source [150].

Scheme 31 Structure of vancomycin and application of the $[(\eta^5\text{-Cp*})IrCl_2]_2$/Vancomycin system to the TH of cyclic imines

3 Carbene Iridium Complexes

The use of *N*-heterocyclic carbenes as ancillary ligands in catalysis and, in particular, in TH has experienced a remarkable increase in the last years. In this section we will discuss the contributions of the last five years in iridium complexes containing carbene ligands that have been applied as TH catalysts. Note that the half-sandwich iridium complexes bearing carbene ligands have been considered in Section 2.

Crabtree's group explored the application of the iridium bis(*N*-heterocyclic carbene) complexes **58** and **59** (Scheme 32) to the TH of ketones and imines using MeOH as a hydrogen source.

Scheme 32 Carbene iridium catalysts (**58**-**64**)

The best results were achieved with catalyst **59a**. Several aromatic ketones were reduced using 5 mol % of **59a** and 1-5 equiv of KOH versus substrate. Reactions were carried out under microwave irradiation (120 ºC) because this mode of heating greatly improved yields compared to conventional heating at the same temperature. Acetophenones (**B1**, **B18**, **B23**) gave generally poorer yields (28–70 %, 5 h reaction) than benzophenones (**B66**, **B71**, **B72**, 61 – >95 %, 5 h) due to competing methylation of the α-CH_3 group [151].

Under the same reaction conditions, several imines were reduced using complex **59a** as the catalyst precursor. *N*-benzylideneaniline was reduced to the corresponding amine (> 95% yield); however, imines with $R^2 \neq$ Ph (Scheme 33) underwent both reduction and *N*-methylation. When R^1 = H a double methylation at nitrogen was also observed [151].

Scheme 33 Reduction of imines by catalyst **59a**

Cationic iridium complexes containing two N- or O-functionalised *N*-heterocyclic carbene ligands (**60**, Scheme 32) reduce cyclohexanone using 2-propanol as a hydrogen source and KOH as a base. Under the optimised reaction conditions (0.1 mol % catalyst, 5 equiv of KOH, 80 ºC) good conversions were obtained after 6-8 h of reaction. Neither

the wingtip fragment of the carbenes nor the anion (Br^- or PF_6^-) have significant influence on the catalytic activity [152].

Iridium(III) complexes featuring methylene bridged bis-*N*-heterocyclic carbene ligands **61** catalyse the reduction of a variety of ketones and imines in 2-propanol as a hydrogen donor, *t*BuOK as a base (5 equiv versus substrate) and at catalyst loading of 1 mol %. Cyclohexanone and methyl aryl ketones **B1**, **B3**, **B15**, **B18** and **B20** were efficiently reduced. Conversions from 77 to 99 % were obtained in 0.33-23 h of reaction with TOF of up to 615 h^{-1} at 50 % conversion. A remarkable enhancement of the activity in the reduction of both ketones and imines, was observed for carbenes with *N*-substituents where an oxygen atom is present [153]. ***N***-benzylideneanilines **C1-C4** were also efficiently hydrogenated. Conversions from 38 to 96 % were obtained after 2-24 h of treatment [153].

Iridium complexes containing *N*-heterocyclic carbene ligands derived from a chiral fused bicyclic scaffold (**62**, Scheme 32) have been explored in asymmetric TH of ketones. Under the optimised reaction conditions (0.5 mol % of catalyst **62c**, *i*PrOH, 8 equiv of *t*BuOK, 75 ºC) a variety of aryl ketones (**B1**, **B2**, **B15**, **B16**, **B19**, **B20-B22**, **B27**, **B28**, **B49**, **B50**, **B52**, Scheme 4) were reduced. Moderate to high yields (18–95 %) and low e. r.'s, from 51.5/48.5 to 62/38, were obtained. Iridium complex **62c** performs better than its rhodium counterpart in terms of both yield and enantioselectivity for most of the tried ketones [154].

An iridium(I) compound with a triazolylidene ligand that contains a pendant methyl group (**63**, Scheme 32) efficiently catalyses the TH of ketones, aldehydes, imines, allylic alcohol and olefins [155].

After screening it was established that the optimized reaction conditions are: 0.5 mol % of catalyst and 5 mol % of *i*PrONa, in refluxing 2-propanol. Under these conditions, ketones with different steric and electronic properties (**B1**, **B3**, **B10**, **B13**, **B15**, **B18**, **B23**, **B47**, **B52**, **B66**, **B118**) including heterocyclic ketones (**B38-B42**, **B45**) were reduced in high yield (81-99 %) with TOFs in the 260-1800 h^{-1} range, measured after 5 min of reaction. As usually, conversion increases both when the steric demand decreases and when the electro-withdrawing character of ketone substituents increases.

Several aldehydes (**A1**, **A3**, **A12**, **A17**, **A24**, **A32**, **A64**, **A68**) were also reduced by catalyst **63** under the same reaction conditions. The activity follows the same trend as that observed for the reduction of ketones, although, in general, when using complex **63** aldehydes are reduced significantly faster than ketones.

Complex **63** was also applied to the TH of the imines *N*-benzylideneaniline and ***N***-2-methyl benzylideneaniline, under the optimised reaction conditions above indicated. The TOF (770 h^{-1}) measured for the aldimine was significantly greater than that observed for the ketimine (30 h^{-1}), which was rationalised in terms of the higher steric demand of the ketimine.

Full reduction of the allylic alcohols depicted in Scheme 34 to the corresponding saturated alcohols was observed within 1 hour. Deuterium labelling experiments showed that the formed alcohol contained deuterium not only at the double bond but also at the allylic position, which indicates a competing isomerisation pathway.

Scheme 34 Deuterium labelling experiments in the reduction of allylic alcohols by complex **63**

Complex **63** induces the efficient reduction of a range of olefins (**D1**, **D10**-**D12**, **D15**, **D19**, **D21**, **D22**, **D29**, **D30**, **D32**, **D33**, Scheme 6) under mild reaction conditions (0.5 mol % catalyst, 5 mol % *i*PrONa, 4-6 h, refluxing 2-propanol, quantitative conversion). In general, the catalytic activity was insensitive to the olefin substitution pattern as well as to the geometry of the double bond and activities were similar for linear mono- and di-substituted olefins.

To assess the relative rate of olefin hydrogenation versus alkene double bond isomerisation, deuteration labelling experiments were performed using *trans*-*β*-methylstyrene and allyl benzene as the substrates (Scheme 35). Deuterium incorporates at both olefinic and allylic positions with almost equal ratios for both substrates. This result suggests that the reductions proceed via a tandem isomerisation/TH reaction and that isomerisation is faster than reduction [155].

Scheme 35 Deuterium labelling experiments in the reduction of olefins by complex **63**

A cyclometalating *N*-heterocyclic carbene iridium complex featuring metal-centred chirality (**64**, Scheme 32) is an efficient catalyst for the asymmetric TH of a wide variety of cyclic *N*-sulfonylimines (**C36-C51**) and benzofused *N*-sulfonylimines (**C52-C59**) (Scheme 5). Enantioselective reduction of *N*-sulfonylimines yields chiral sultams, which are present in a range of biologically active compounds [156]. Yields in the range 82–99 % and e. r.'s greater than 97/3 were obtained after 3-9 h of treatment, using HCO_2NH_4 (9 equiv) as a hydrogen source, at a catalyst loading of 0.05 or 0.2 mol %, in DMF/H_2O (2/1 mixture) at 60 ºC. Other common hydrogen donors that do not contain ammonium such as HCO_2Na or HCO_2H/NEt_3, 5/2, led to poorer results. A tentative mechanism including NH_3 containing intermediates was proposed [157].

A half-gram-scale synthesis of bioactive sultam **I** (Scheme 36) with anti-HIV activity was developed based on asymmetric TH of *N*-sulfonylimine **C58** followed by an *N*-methylation step [157].

Scheme 36 Enantioselective synthesis of sultam **I**

4 Pincer Iridium Complexes

The term “pincer” refers to ligands that generally coordinate in a *mer* tridentate configuration [158]. This tridentate coordination mode results in strong binding to the metal centre and high stability for the metal-tridentate ligand unit. Additionally, pincer ligands have a modular nature that allows for a high tunability of their electronic and steric properties. Within the last two decades, the use of pincer compounds for chemical transformations has increased greatly [158-161]. A number of reviews focusing on the catalytic applications of this type of complexes have been published in the recent years [162-170]. In particular, some pincer iridium complexes have been found to be effective for the TH of unsaturated substrates [171-175]. Here, we summarise the progress in this area since 2015.

With only 0.1 mol % of the chiral *P*,*N*,*N*’-pincer catalyst **65a** (Scheme 37), at 40 ºC, several aromatic ketones with electron-donating or eletron-withdrawing substituents in 2- 3- and 4-positions (**B1-B3**, **B5**, **B6**, **B8**, **B10-B12**, **B15**, **B18**, **B21**, **B22**, **B34**, **B37**, **B47**) as well as selected methyl alkyl (**B99**, **B104**) and the methyl pyridinyl ketone **B39** were reduced. Potassium *t*-butoxide (4 equiv versus substrate) was employed as a base but also in the presence of other bases such as *t*BuONa, KOH, and K_2CO_3 acetophenone was hydrogenated to 2-phenylethanol with comparable activity and selectivity. Isolated yields from 87 to 99 % and e. r.’s from 90/10 to 99/1 were obtained within 10 h. Ethanol was used as a hydrogen source. Using 2-propanol, instead, gave rise to significantly lower e. r.’s (99/1, EtOH versus 92/8, *i*PrOH) [176].

Scheme 37 Pincer iridium TH catalysts

A practical and sustainable method for the preparation of optically active propargyl alcohols was developed by the Zhou’s group [177]. The tridentate spiro-pyridine-aminophosphine iridium complexes **65** depicted in Scheme 37 catalyse the chemoselective reduction of a series of alkynyl ketones to the corresponding propargyl alcohols. Both the unsubstituted complex **65a** and the methyl-substituted derivatives **65b**,**c** were more active and enantioselective than compound **65d** having a *t*Bu substituent. The optimised reaction conditions were 1 mol % of catalyst **65b**, HCO_2Na (2 equiv), 60 ºC and ethanol as solvent. Under these conditions, high yield (86–99%) and high e. r.’s (93/7–98.5/1.5) were obtained within 4-48 h. Alkynyl ketones containing electron-withdrawing (**B130**, **B132**, **B135**, **B136**) and electron-donating (**B123-B125**, **B129**, **B131**, **B133**, **B134**) or additional ester (**B127**, **B128**) groups as well as the trifluoromethyl ketone **B126** were efficiently and chemoselectively reduced [177].

Some remarkable features of the process are:

i) No base is required. Indeed, in the presence of *t*BuOK, 4-phenylbut-3-yn-2-one (**B123**) only gave the Michael addition byproduct formed by the ethoxide addition to the carbon-carbon triple bond of **B123**

ii) The TH of **B123** did not occur using HCO_2H/NEt_3 instead of HCO_2Na as a hydrogen donor

iii) Other alkali metal formates such as HCO_2Li, HCO_2K and HCO_2Cs can also be used as hydrogen sources although HCO_2Li gave lower reaction rate and conversion

iv) Ethanol is the best solvent, indeed, the reaction in MeOH or *i*PrOH gave low conversion and low enantioselectivity

v) Under the optimised conditions but using HCO_2Cs as a hydrogen donor, the TH of the trifluoro alkynyl ketone **B126** mediated by **65b** was monitored by in situ IR spectroscopy.

These results indicate that the formate salt and EtOH served as the hydride and proton sources, respectively, in the TH reaction (Scheme 38) [177].

Scheme 38 Transfer hydrogenation of ketone **B126** with HCO_2Cs in ethanol

The iridium complex **66** (Scheme 37) containing a functionalised *N*-heterocyclic olefin (Scheme 39) acting as a tridentate ligand has been applied as a catalyst for the reduction of ketones, benzaldehyde and imines [178].

Scheme 39 Resonance structures of *N*-heterocyclic olefins

The reaction conditions entailed the use of 0.1 mol % of catalyst, *i*PrOH as a solvent and a hydrogen donor, *t*BuOK (5 equiv) as a base and working at 80 ºC. Under these conditions, cyclohexanone, substituted acetophenones (**B1**, **B3**, **B15**, **B18**, **B20**), dialkyl (**B114**) and diphenyl (**B66**) ketones were efficiently reduced. For example, the TH of cyclohexanone to cyclohexanol was completed in 7 min with a TOF value of 2222 h^{-1}, at 10 % conversion [178]. No relationship was observed between the substitution of the acetophenones and the catalytic activity. The reduction rate of aliphatic ketones is higher than that of their aromatic counterparts. Remarkably, the TH of benzaldehyde to benzyl alcohol was completed in 40 seconds.

Catalyst **66** showed good activity in the TH of imines. *N*-benzylideneaniline was transformed into *N*-benzylaniline, using 1 mol% of catalyst, in 45 min with a TOF value of 1118 h^{-1} at 10 % conversion. Substituted imines 3-methoxy-*N*-benzylideneaniline and 4-methoxy-*N*-benzylideneaniline were also converted into their corresponding amines, under the same reaction conditions, featuring TOFs of 548 h^{-1} and 110 h^{-1}, respectively [178].

Polypyridyl iridium(III) compounds **67** and **68** (Scheme 37) were tested as catalysts for the TH of a range of aromatic aldehydes, in aqueous ethanol, with HCO_2Na as a hydride source and using microwave assisted heating. The best results were obtained with catalyst **67a**. Catalytic reactions were performed at 100 ºC, at a catalyst loading of 0.2 mol %, with 4.5 equiv of HCO_2Na, in an EtOH/H_2O mixture, 70/30 (v/v). Under these reaction conditions, yields from 68 to 99 % were obtained within 5-90 min. Reaction tolerates a wide range of substituents including halogens (**A5**-**A7**, **A14**-**A16**, **A29**-**A31**), phenols (**A11**, **A22**, **A49**), alkoxy (**A3**, **A12**, **A24**, **A40**, **A48**, **A49**), ketones (**A18**, **A34**), carboxylic acids (**A9**, **A20**, **A36**), cyano (**A19**, **A35**) and nitro (**A21**) groups, as well as heteroarenes (**A66**, **A68**-**A71**). Under the same conditions, catalysts **67a** and **67b** (Scheme 37) also reduced alkyl aldehydes **A54**, **A56**, **A58**-**A60** in 82–97 % yield within 25-90 min [179].

Pincer compounds **69** (Scheme 37), equipped with different functional groups in the secondary coordination sphere, were employed as the catalysts in the chemoselective TH of nitroarenes (Scheme 43) to anilines. Reactions were carried out in dimethoxyethane, at 60-80 ºC with a catalyst loading of 1 mol %, with 2 equiv of HCOOH/NEt_3 azeotrope as a hydrogen source. Although reduction of nitroarenes to amines is often accompanied by incomplete reduction to hydroxylamines or azocompounds, almost complete conversion of nitrobenzene into aniline (99 %) with excellent selectivity (99 %) was achieved with catalyst **69a**. The OMe modified catalyst **69b** gave a more modest conversion but with the same selectivity [180].

Methyl- (**E4**), amino- (**E9**) and chloro- (**E10**-**E12**) substituted nitrobenzenes were fully converted into the corresponding anilines. Cyano- (**E18**), amido- (**E16**), ester- (**E17**) and keto- (**E15**) substituted nitrobenzenes as well as 2-nitrostyrene displayed moderate chemoselectivity owing to partial reduction of the functional group present in the substrates [180].

In contrast with the well-established TH of aldehydes, ketones and imines, TH reactions of non-activated C-C multiple bonds have been much less studied. Huang's group has recently demonstrated that a series of *N*,*C*,*P*-pincer iridium(III) complexes (**70**-**72**, Scheme 37) efficiently reduced a wide variety of alkenes and alkynes [181, 182] (Scheme 6). Notably, ethanol was employed as a solvent and as a hydrogen donor. Ethanol is an abundant, sustainable and environmentally benign source of hydrogen. However, it has been seldom applied to TH reactions [38, 176, 177, 179, 183-184] because acetaldehyde, its dehydrogenation product, readily undergoes metal-mediated decarbonylation leading to catalytically inactive metal carbonyl species. In Huang's system EtOAc was the only detectable byproduct. Probably, the acetaldehyde resulting from EtOH dehydrogenation reacts with another molecule of EtOH to yield hemiacetal, which is further dehydrogenated to EtOAc thus eliminating the possibility of catalyst poisoning by the acetaldehyde [181].

Complex **72** gave the best results. Thus, for example, upon activation with *t*BuONa, this complex (1 mol %) completely reduced both cyclooctene and 1-octene at 60 ºC within 20 min. Under these conditions, other non-activated (**D17**, **D25**, **D31**, **D33**, **D36**, **D37**, **D39**-**D48**, **D52**-**D56**), aryl (**D1**, **D5**-**D7**, **D11**, **D13**, **D18**, **D23**, **D24**) and electron-rich (**D28**, **D38**) alkenes were efficiently reduced. Yields from 65 to > 99 % were obtained, within 0.5-12 h [181].

Complex **72** was also active for the full reduction of alkynes. Non-activated aliphatic alkynes, 6-dodecyne and alkynes bearing Cl (**D128**) or OH (**D127**) functionalities were reduced (94–97% yield, 1.5 h) to the corresponding alkanes using 1 mol % of **72**, at 80 ºC. Ethyl 2-octynoate and internal alkynes (**D57**, **D58**, **D88**, **D90**) gave the reduction products in > 95 % isolated yield, at 2 mol % of catalyst loading. Reduction was always complete due the good activity of catalyst **72** for alkene TH [181].

However, complex **72** can be used for the semi-hydrogenation of a range of internal alkynes [182]. Ethanol was also employed as a solvent and *E*-alkenes were streoselectivily obtained. Transformations can be stopped at the alkene step because the catalyst itself was used as a colour indicator for endpoint detection. Catalysis proceeds through the sequence alkyne → *Z*-alkene → *E*-alkene, the second step being faster than the first. The green iridium(I) π-alkyne complex **I** and the yellow iridium(III) hydride **II** act as the resting states for the first and second step, respectively (Scheme 40).

Scheme 40 Selective TH of alkynes to *E*-alkenes with EtOH

The full consumption of alkyne produces a sharp colour change of the solution from green to yellow due to the shift of the resting state from **I** to **II**. Quenching the reaction at this point allows for a high *E*-selectivity and minimizes over-reduction.

A broad variety of internal alkynes, including diaryl (**D57**-**D60**, **D62**-**D68**, **D71**, **D73**-**D77**, **D91**, **D92**, **D122**), aryl alkyl (**D88**, **D90**, **D95**-**D98**) and dialkyl (**D124**, **D126**-**D128**) alkynes were transformed in the corresponding *E*-alkenes. Functional groups such as amine (**D64**, **D83**), aryl halides (**D67**, **D68**, **D71**, **D73**), amide (**D75**), ester (**D76**) and ferrocenyl (**D86**) were tolerated. Alkynes containing various *O*- or *N*-heteroaromatic rings including furane (**D84**), benzofurane (**D85**), *N*-ethylcarbazole (**D83**), *N*-tosylindole (**D82**) and quinoline (**D81**) were also reduced. Generally, yields greater than 95 % were achieved within 2.5-292 min.

Several alkynes containing biologically relevant skeletons can also be semi-hydrogenated to the corresponding *E*-alkene using catalyst **72** in EtOH. Scheme 41 shows some of the *E*-alkenes obtained [182].

Scheme 41 Alkenes containing biologically active skeletons

5 Other Iridium Complexes

Mixtures of $[IrCl(COD)]_2$ (COD = 1,5-cyclooctadiene) and a variety of ligands (Scheme 42) have been tested as catalysts for the TH of a range of nitroarenes (Scheme 43).

Scheme 42 Phosphorus and nitrogen donor ligands employed in combination with $[IrCl(COD)]_2$ in the TH of ketones

Reactions were carried out under nitrogen atmosphere, in *i*PrOH, at 83 ºC, with 1 mol % iridium dimer and 2 mol % of the corresponding ligand. Monodentate phosphines displayed low catalytic activity. Bidentate phosphines and nitrogen donor ligands gave full conversion of nitroarenes but variable aniline yields (53–98%). The bidentate nitrogen ligand 1,10-phenanthroline (**L11**) showed the highest yield in aniline [185].

A monitoring experiment and a series of controlled experiments employing nitrobenzene as the substrate showed that the transformation proceeds via phenylhydroxylamine and azobenzene intermediates. However, after 15 h of treatment under the reaction conditions above indicated, using $[IrCl(COD)]_2$/**L11** as the catalyst, a series of nitroarenes (**E1-E3**, **E5-E14**, **E19-E24**, **E26-E30**, Scheme 43) were completely reduced to the corresponding anilines in 70–98 % yield.

Scheme 43 Nitroarenes

A phosphine bisbenzothienyl iridium(III) complex (**73**, Scheme 44) was applied to the TH of ketones. Under the best conditions found, namely, 2 mol % of **73**, 1.5 equiv of *t*BuOH, toluene as the reaction solvent, at 110 ºC, several methyl aryl ketones (**B1**, **B2**, **B10**, **B156**, **B20**, **B27**, Scheme 4) were hydrogenated. Yields of the corresponding alcohol up to 68 % were obtained [186].

Scheme 44 Other iridium complexes employed as TH catalysts (**73**-**78)**

A range of ketones was reduced to the corresponding alcohols by $[IrCl(COD)]_2$/chiral amine ligand mixtures. The amino ligands employed are collected in Scheme 45.

Scheme 45 Chiral amino ligands employed in combination with $[IrCl(COD)]_2$ in the TH of ketones

The best reaction conditions were as follows: a 1/2 metal/ligand ratio, a 1/1 mixture of formic acid and sodium formate (pH 3.5 at the beginning of the reaction) and water/methanol (1/1) as a solvent. After 1 hour of treatment at RT under argon atmosphere, the reducing agent was added and the solution heated at 70 ºC. Under these conditions, moderate to high isolated yields (41–87 %) and e. r.'s (57.5/42.5–99.5/0.5) were obtained for the reduction of a range of methyl aryl ketones (**B1**, **B2**, **B8**, **B12**, **B18**, **B21**-**B25**, **B27**, **B34**) [187].

A bis-cyclometallated iridium(III) complex (**74**, Scheme 44) with metal-centred chirality catalyses the enantioselective TH of ketones in the presence of an additional pyrazole ligand. Reactions were carried out in THF/H_2O 1/1 (v/v) mixtures, at 40 or 60 ºC, with $HCOONH_4$ (9 equiv) as the hydrogen source. The best results were obtained by adding to the catalyst precursor **74** (0.2 mol %) 10 equiv of 5-(4-methoxyphenyl)-3-methyl-1*H*-pyrazole. Under these reaction conditions, a wide range of ketones were hydrogenated. Generally, yields greater than 90 % with e. r.'s > 98/2 were achieved, within 8-36 h [188].

Acetophenones with electro-donating or withdrawing groups (**B1**, **B2**, **B15**, **B18**, **B21**, **B29**, **B34**, Scheme 4), aromatic ketones containing a naphthyl moiety (**B37**) heteroaromatic ring (**B41**-**B46**), larger aliphatic groups (**B47**-**B49**) or an additional ester functionality (**B62**) as well as a cyclic ketone **B121** provided both high yield and good e. r. Diaryl ketones **B68** and **B69** also afforded satisfactory results. Dialkyl ketones **B107** and **B110** gave the corresponding alcohol in high yield (> 90 %) but with low e. r. (< 30 %). However, ketone **B111** with a bulky alkyl substituent gave the desired alcohol with 93 % yield and 97/3 e. r. The catalytic system also works at a lower catalyst loading. Thus, 2-acetyl benzothiophene was completely reduced to the corresponding alcohol within 108 h at a catalyst loading as low as 0.005 mol %. The reaction was proposed to proceed through the bifunctional Noyori's mechanism [189, 190]. In the proposed transition state, an iridium-hydride and the N–H funcionality of a coordinated pyrazole molecule interact with the C=O bond of the ketone (Scheme 46) [188].

Scheme 46 Proposed transition state for the TH of ketones catalysed by complex 74

The iridium phosphine complexes **75** and **76** (Scheme 44) are active in the TH of ketones. The best results in conversion to the alcohol were obtained using catalyst **75c**.

Reactions were carried out in *i*PrOH, at 80 ºC, with a catalyst loading of 0.5 mol % and KOH (5 mol %) as a base. A series of methyl ketones (**B1**, **B18**, **B27**), one example of an ethyl ketone (**B47**), cyclic ketones (**B118**, **B122**) or the bulky ketones **B112** and **B122** were tested in the reaction. Generally, moderate to high yields were obtained (69 – > 99 %) but the ethyl ketone **B47** and the bulky ketones **B112** and **B122** were converted to the corresponding alcohol in low yield (< 36 %) [191].

Mixtures of the dimer $[IrCl(COD)]_2$ and chiral ferrocenyl alcohols (Scheme 47) have been applied to the TH of alkyl aryl (**B1**, **B47**) and phenyl heteroaryl **B91** and **B92** ketones.

Scheme 47 Chiral ferrocenyl amino alcohols employed in combination with $[IrCl(COD)]_2$ in the TH of ketones

The reactions conditions were as follows: a 1/1 $[IrCl(COD)]_2$/ligand ratio in *i*PrOH as a solvent and a hydrogen source, at 25 or 50 ºC and in the presence of KOH (2 equiv) as a base. Moderate yield (35–89 %) and e. r. (52/48–91/9) were obtained [192].

The iridium complexes **77** and **78** (Scheme 44) reduced ketones under TH conditions. Tipically, reactions were performed at 0.25 mol % of catalyst loading, in the presence of KOH (40 equiv) as a base and at 82 ºC. Alkyl aryl ketones **B1**, **B5**, **B6**, **B18**, **B21**, **B22**, **B28**, **B47**, methyl alkyl ketones **B93-B95**, **B97**, **B109** and naphthyl aldehyde were reduced. It was found that bimetallic complexes **77** were more active than monometallic complex **78**. Yields higher than 90 % within 15-30 min were obtained [193].

Sawamura's group reported on the reduction of C=C bonds of alkenes with 1,4-dioxane as a solvent and a two-hydrogen donor, in the presence of $[IrCl(COD)]_2$ and a diphosphine ligand (Scheme 48). Reactions were performed at 120-130 ºC at a catalyst loading of 1-4 mol%.

Scheme 48 Diphosphines employed in combination with $[IrCl(COD)]_2$ in the TH of alkenes and alkynes

The reactivity of the TH was enhanced by using bulky and electron-donating diphosphines such as 1,2-bis(dicyclohexylphosphino)ethane **VI**. Styrene derivatives **D2-D4**, **D8**, **D9**, **D13**, **D20**, **D23** and **D26** (Scheme 6), exocyclic (**D26**) and cyclic (**D13**) olefinic bonds as well as aliphatic alkenes (**D16**, **D32**, **D35**) including 1,1-disubstituted terminal (**D35**) and disubstituted (**D27**, **D34**) or trisubstituted (**D30**) internal alkenes were efficiently hydrogenated by $[IrCl(COD)]_2$/diphosphine **VI** mixtures. Tetrasubstituted alkenes such as 2,3-dimethyl-1*H*-indene and tetraphenylethylene were not hydrogenated even at higher reaction temperature (140 °C).

Alkynes also underwent TH reaction with the $[IrCl(COD)]_2$/diphosphine **VI** catalyst using 1,4-dioxane as a hydrogen donor. Thus, diphenylacetilene was converted into 1,2-diphenylethane through double TH with 4 mol % of catalyst loading, at 140 ºC after 20 h of treatment [194].

Transfer hydrogenation of internal and terminal alkynes to alkenes can be achieved with the $[IrCl(COD)]_2$/DPPE (DPPE = 1,2-bis(diphenylphosphino)ethane) using EtOH as a hydrogen donor [195, 196].

Internal alkynes were reduced to *E*-alkenes in THF, at 120 ºC using 2.5 mol % of $[IrCl(COD)]_2$, 20 mol % of DPPE and 20 equiv of EtOH. Under these conditions, a variety of diaryl alkynes (**D57**, **D61**, **D70-D74**, **D78**, **D100-D102**, **D104-D117**, **D121**, Scheme 6) were converted into *E*-alkenes in 73–92 % yield, with *E*/*Z* molar ratios from 4/1 to > 99/1, within 22 h under N_2 atmosphere. Notably, the *E*/*Z* ratio can be inverted in favour of the *Z* isomer working under the conditions above indicated but adding to the reaction medium 2 equiv of COD. Thus, yields between 71 and 95 % with *Z*/*E* molar ratios from 4/1 to > 99/1 were achieved in the TH of the diaryl alkynes **D57**, **D61**, **D67**, **D69**, **D78**, **D100**, **D101 D103-D105**, **D107**, **D109**, **D118** (Scheme 6). The observed change in the alkene selectivity was attributed to the increase of the steric hindrance at the metal centre generated by the addition of the diolefin [195].

Under comparable conditions (THF, 70 ºC, 2.5 mol% of $[IrCl(COD)]_2$, 20 mol % of DPPE, 2 equiv of EtOH) terminal alkynes were reduced to alkenes [196]. A series of activated (**D130-D155**) and unactivated (**D156-D159**) terminal alkynes were reduced in 67–94 % yield within 24 or 48 h, respectively. The reaction of the non-activated alkynes was carried out at 100 ºC.

6 Transfer Hydrogenation of α,β-Unsaturated (and Non-conjugated) Alkene-Carbonyl Substrates

Transfer hydrogenation protocols have also been applied to the reduction of α,β-unsaturated carbonyl compounds [197]. In principle, both partial hydrogenation to aliphatic ketones or allylic alcohols and complete reduction to saturated alcohols are possible (Scheme 49). The energy barriers for the reduction of C=O and C=C conjugated bonds are often similar. For this reason, mixtures of reduction products are sometimes obtained and one of the major goals in the reduction of unsaturated carbonyl compounds is to achieve high chemoselectivity. As it will be seen herein, the pH value of the catalytic medium plays a key role in the chemoselectivity in TH of unsaturated alkene-carbonyl substrates.

Scheme 49 Partial and complete reduction of α,β-unsaturated carbonyl compounds

Iridium compounds are among the most used for α,β-unsaturated carbonyl compounds reduction. In this section we present the new contributions made in this field during the last five years.

6.1 Transfer Hydrogenation of α,β-Unsaturated Aldehydes

A variety of α,β-unsaturated aldehydes (Scheme 50) have been reduced employing iridium compounds as the catalysts (Scheme 51).

Scheme 50 α,β-Unsaturated aldehydes

Scheme 51 Catalysts for the reduction of α,β-unsaturated aldehydes

Compound **57a** catalyses the chemoselective reduction of cinnamaldehyde to the corresponding alcohol in 90 % yield, in water, using HCOOH (5 equiv) as a hydrogen donor [113].

Under neutral conditions, complex **79** is an efficient catalyst for chemoselective TH of unsaturated aldehydes using *i*PrOH as a solvent and a hydrogen donor [198]. Cinnamaldehydes **F1**, **F2**, **F4**, **F11-F13**, **F22** and **F23**, 3-(9-anthryl)acrylaldehyde, 3-(2-furyl)acrylaldehyde and aliphatic α,β-unsaturated aldehydes **F29** and **F30** were reduced in 80–97 % yield. A metal-ligand bifunctional mechanism was proposed for the catalytic TH reaction [198].

The polypyridyl iridium(III) **67a** in EtOH/H_2O, at 100 ºC, at 0.2 mol % of catalyst loading, in the presence of 4.5 equiv of HCOONa, reduced cinnamaldehyde. A 1/1 mixture of the allylic and saturated alcohol was obtained. However, using 9 equiv of HCOONa (initial pH of the reaction, 9) full reduction to the saturated alcohol was achieved. Similar results were obtained for α-methyl cinnamaldehyde and 4-methoxy cinnamaldehyde. Alternatively, when HCOOH was used to maintain acidic the reaction medium, unsaturated alcohol was predominantly obtained [179].

The Luo's group investigated the TH of a wide variety of α,β-unsaturated aldehydes, including cinnamaldehydes **F1**, **F3**, **F6- F11** and **F13-F23**, furan substituted aldehyde **F27** and aliphatic aldehydes **F31-F35**, mediated by catalyst **55h**. All the reactions were carried out at 0.1 mol % of catalyst loading, in H_2O at 80 ºC. Nonetheless, a set of reactions was performed using HCOONa (5 equiv) as a hydrogen donor and another set was carried out with HCOOH (5 equiv). Full reduction to the saturated alcohol was achieved with HCOONa and semi-reduction to the unsaturated alcohol was obtained with the acid. Typically, yields higher than 90 % were achieved,

in both cases [199]. Control experiments showed that 3-phenylpropanal was reduced to the saturated alcohol under the same conditions whereas the C=C bond of cinnamyc alcohol was not reduced by complex **55h**, when using HCOONa as a hydrogen donor. These results indicated that the formation of the fully reduced product starts with the reduction of the C=C bond to give the saturated aldehyde intermediate and follows with the reduction of the C=O bond to give the final product [199].

6.2 Transfer Hydrogenation of α,β-Unsaturated Ketones

A range of *α,β*-unsaturated ketones (Scheme 52) have been reduced employing iridium catalysts (Scheme 53).

Scheme 52 *α,β*-Unsaturated ketones

Scheme 53 Catalysts for the reduction of *α,β*-unsaturated ketones

The dimer $[Cp^*IrCl_2]_2$ chemoselectively reduced *α,β*-unsaturated ketones such as (*E*)-chalcones **G1**-**G3**, **G6**, **G8**-**G17**, **G21**, **G28**, heterocyclic *α*-enones **G29** and **G31**, activated *α,β*-unsaturated ketones **G32** and **G40** and cyclic enones **G49** and **G50**. All the reactions were performed in *i*PrOH, at 85 ºC, using 1 mol % of catalyst loading. When K_2CO_3 (5 mol %) was employed as a base, the saturated ketone was obtained in high yield (85–98%). However, when in the reduction of the (*E*)-chalcones **G1**-**G3**, **G6**, **G8**-**G14** and **G28**, KOH (50 mol %) was employed as a base, the corresponding saturated alcohols were obtained in 83–91 % yield [200].

The iridium(I) complex with triazolylidene ligands **63** catalyse the reduction of *α,β*-unsaturated ketones **G1**, **G3** and **G50**. Full reduction to the corresponding saturated alcohol was observed within 1 hour when the substrates were treated with 0.5 mol % of the catalyst, in refluxing *i*PrOH with *i*PrONa (5 mol %) as a base. Yields higher than 94 % were achieved. From deuterium labelling experiments it was suggested that the reaction proceeds via a tandem isomerisation/TH reactions [155].

In *i*PrOH, at 80 ºC, using KOH (10 mol %) as a base, the bis(phosphine) complex **75c** (0.5 mol %) reduced 2-cyclohexenone to the saturated ketone cyclohexanone as the main product (63 % yield). The unsaturated alcohol and full reduced cyclohexanol were obtained in 6 % and 31 % yield, respectively. Under similar conditions, the TH of carvone gave the product of the hydrogenation of the conjugate olefin and that of the hydrogenation of both conjugated olefin and carbonyl group. Hydrogenation of the isolated C=C bond was not observed [191].

The outcome of the reduction of 2-cyclohexenone with catalyst **55a** (S/C = 10,000, HCOOH 12 equiv, water, 80 ºC, N_2 atmosphere) was the saturated alcohol

cyclohexanol. Further studies showed that under the reaction conditions cyclohexanone could be completely reduced to cyclohexanol while cyclo-2-en-1-ol could not. This result indicated that the TH of 2-cyclohexanone should first occur at the C=C bond and then at the C=O bond. Experiments on 4-methylpent-3-en-2-one gave similar results [111].

The combination of the dimer $[IrCl(COD)]_2$ (4 mol %) with the ligand 1,2-bis(dicyclohexylphosphino)ethane (4 mol %) promoted the chemoselective TH of α,β-unsaturated ketones such as chalcone, benzylideneacetone and its derivatives **G32-G45**, conjugated enoates **G46** and **G47**, enamide **G48** and cyclic enone **G51**. 1,4-dioxane was employed as a solvent. Chemoselectivity towards C=C hydrogenation was found for all these enones. Yields from 93 to 99 % were obtained after 10 h of reaction at 130 ºC [194].

The iridium complex **80** bearing a tricyclic bisoxazoline-fused imidazole-derived *N*-heterocyclic carbene ligand (Scheme 53) catalysed the asymmetric TH of (*E*)-chalcones **G1**, **G2**, **G4**, **G5**, **G7**, **G8**, **G10**, **G11**, **G18-G20**, as well as that of the heterocyclic α,β-unsaturated ketones **G27** and **G31**. In *i*PrOH, at 75 ºC, at a catalyst loading of 1 mol %, using NaOH (8 mol %) as a base, moderate to good yields (36–91 %) in the corresponding full hydrogenated alcohol, were obtained within 3 h. Probably, the existence of an equilibrium between conformational isomers in the iridium catalyst **80** at the temperature of the reaction, originates a poor enantioface discrimination during the reaction resulting in poor e. r.'s (52.5/47.5–62.5/37.5). From detailed mass spectrometric studies a mechanism consisting of two catalytic cycles working in tandem was proposed [201].

Hydrogenation of the (*E*)-chalcone mediated by the bis(carbene)catalyst **9a** (Scheme 2) was performed in *i*PrOH, at 95 ºC using KOH (10 mol %) as a base. The catalytic reaction was selective for the C=C bond and required only 30 min to give 97 % yield. After this time, maintaining the reaction conditions, hydrogenation of the C=O groups gave the saturated alcohol in 63 % yield within 4 h [69].

6.3 Transfer Hydrogenation of Non-conjugated Unsaturated Aldehydes and Ketones

A handful of non-conjugated unsaturated aldehydes and ketones (Scheme 54) has been subjected to TH protocols based on iridium catalysts (Scheme 55).

Scheme 54 Non-conjugated unsaturated aldehydes and ketones

Scheme 55 Catalysts for the reduction of non-conjugated unsaturated aldehydes and ketones

In *i*PrOH, under a N_2 atmosphere, non-conjugated unsaturated aldehydes 3-cyclohexene-1-carboxaldehyde and 5-norbornadiene-2-carboxaldehyde were chemoselectively converted into the corresponding unsaturated alcohols in 93 and 97 % yield using the half-sandwich bipyridonate complex **79** (2 mol %) [198].

The non-conjugated ketone 5-hexen-2-one was chemoselectively transformed into 5-hexen-2-ol in 6 h with the dinuclear di(*N*-heterocyclic carbene) iridium complex **6** (0.5 mol % of catalyst loading, *i*PrOH, *i*PrONa (3 mol %), 82 ºC) in 96 % yield. Under the same conditions, 86 % yield was obtained with catalyst **7** within 10 h [67].

The same ketone and the related non-conjugated ketone 6-methyl-5-hepten-2-one were hydrogenated to the corresponding unsaturated alcohol by the bis(*N*-heterocyclic carbene) complex **9a** (2 mol % of catalyst loading, *i*PrOH, KOH (10 mol %), 95 ºC). Yields of 83 and 96 % were obtained within 6 h. Notably, the same catalyst under similar conditions hydrogenated selectively the C=C bond of the conjugated α,β-unsaturated ketone (*E*)-chalcone [67].

The catalytic behaviour of the half-sandwich iridium triazenide complex **45** in the hydrogenation of non-conjugated 5-alken-2-ones depends on the presence of a base. If KOH is present then the carbonyl group will be selectively hydrogenated in the first place. However, in the absence of the base, the C=C bond is preferably hydrogenated [85].

The carbonyl group of the dihydrocarvone **G60** was chemoselectively reduced with the bis(phosphine) iridium(I) complex **75c**. At 0.5 mol % of catalyst loading, in *i*PrOH, using 10 equiv of KOH, at 80 ºC, 90% yield was obtained within 24 h. The isolated olefin moiety was not hydrogenated under these conditions [191].

However, the isolated C=C bond of both 11-dodecen-2-one **G59** and 4-acetylstyrene **G53** was chemoselectively hydrogenated to the corresponding unsaturated ketone using the pincer iridium complex **72**, containing a rigid benzoquinoline backbone, as a catalyst. At 1 mol % of catalyst loading, in EtOH, using *t*BuONa (2,2 mol %) as a base, 95 % yields for **G59** and **G53** were obtained after 18 and 30 min, respectively [181].

A mixture of the dimer $[IrCl(COD)]_2$ (1 mol %) and the diphosphine 1,2-bis(dicyclohexylphosphino)ethane (4 mol %) promoted the highly chemoselective TH of the isolated alkene group of unsaturated ketones [194]. In 1,4-dioxane, at 130 ºC, terminal alkene groups bearing an acetophenone (**G53**-**G56**) or cyclohexanone (**G61**) underwent selective reduction of the alkene moiety. The isolated C=C bond of the estrone derivative **G63** was also chemoselectively reduced [194].

7 Transfer Hydrogenation of *N*-Heterocycles

Reduced *N*-heterocycles are frequently found in drugs, agrochemicals and dyes [120, 202] and, therefore, having efficient methods for their synthesis is highly desirable. Hydrogenation of *N*-heterocycles is the most obvious route to that type of compounds and heterogeneous [203] and homogeneous [204, 205] catalytic hydrogenation has been the most widely used methodology. Despite the advantages of TH in terms of sustainability, simplicity of application and safety, this approach has been much less investigated for the reduction of *N*-heterocycles [206-211]. Here we present recent contributions in this area. An example of selective reduction of benzofurans by TH protocols is also included in this Section.

The iridacycle complex **81** (Scheme 56) reduced quinolines **H1**-**H20** and **H22**-**H28** (Scheme 57) to tetrahydroquinolines in an aqueous HCOOH/HCOONa solution, using 0.1 mol % of catalyst. The solution pH is critical for the catalytic activity pH 4.5 giving the best yield. Typically, isolated yields higher than 90 % were obtained within 14 h [212].

Scheme 56 Iridium complexes for the reduction of *N*-heterocycles

Scheme 57 Quinolines

Complex **81** also catalyses the reduction of activated isoquinolines and pyridines by quaternisation. Thus, isoquinolinium **H29**-**H34** and pyridinium **H35**-**H44** (Scheme 58) were hydrogenated in 24-36 h, under the same conditions but at refluxing temperature. Again, isolated yields higher than 90 % were achieved [212].

Scheme 58 Isoquinolinium and pyridinium

The protocol of reduction of complex **81** was also efficiently applied to indoles **H63**-**H69** (Scheme 59) as well as to a range of diverse heterocycles **H58** (Scheme 60), **H72** (Scheme 61) and **H90**-**H92** (Scheme 62). These substrates were all reduced with excellent yield although quinoxaline **H90** was isolated as its mono *N*-formyl derivative [212].

Scheme 59 Indoles

Scheme 60 Isoquinolines and dehydroquinolines

Scheme 61 Phenanthrolines

Scheme 62 Other *N*-heterocycles

2-Methylquinoline was quantitatively reduced to 2-methyl-1,2,3,4-tetrahydroquinoline within 24 h at room temperature using 0.1 mol % loading of the iridium complex **82** (Scheme 56) and aqueous HCOOH/HCOONa as a solvent and a hydrogen source. The same result was obtained using $[Cp^*IrCl_2]_2$ with the ligand 8-aminoquinoline as the catalyst precursor. Application of the same conditions to unsubstituted quinoline led to the hydrogenation of the pyridinic ring along with the introduction of a formyl group on the nitrogen atom in 33 % yield [213].

The *N*,*C*,*P* pincer iridium complex **72** (Scheme 55), at 0.25 mol % catalyst loading, selectively reduced benzofurans **H95**-**H98** (Scheme 63) at 60 ºC in EtOH as a solvent and a hydrogen donor, using *t*BuONa (1 mol %) as a base. Dihydrobenzofurans were isolated in ≥ 95 yield [181]. *N*-Tosylindole, quinoline **H1** and its derivatives **H20** and **H21** (Scheme 57) were also reduced to the corresponding indoline and tetrahydroquinolines, respectively. Isoquinoline exhibited low reactivity (27 % isolated yield) [181].

Scheme 63 Benzofurans

Asymmetric TH of isoquinolines **H46** and **H47**, dehydroquinolines **H58**, **H61** and **H62** (Scheme 60), quinoline **H2** (Scheme 57) and sulfonyl imine **H94** (Scheme 62) was accomplished by using a combination of $[Cp^*IrCl_2]_2$ and chiral cyclic diamine ligands as the catalyst precursor [214]. The best results were obtained employing the cyclic diamine (*S*)-CAMPY (Scheme 64) as a ligand, in MES or MOPS buffer (1.2 M, pH 6-8), in the presence of HCOONa (6 M) at 20 ºC. Yields up to 99 % and e. r.'s from 65/35 to 88/12 were obtained. For the disubstituted isoquinoline **H47** (Scheme 60) the *syn* diastereomers were obtained in > 99 % d. r. with 86/14 e. r. [214].

Scheme 64 Chiral diamine (*S*)-CAMPY

The Vilhanová's group developed a protocol for the asymmetric TH of 1-aryl substituted dihydroquinolines **H48**-**H57**, **H59** and **H60** (Scheme 60) using anhydrous phosphoric acid as an additive and the iridium complex **83** (Scheme 56) as the catalyst. Reactions were performed in *i*PrOH at 30 ºC with 1 mol % of catalyst and using a 1/1 $HCOOH/NEt_3$ mixture as the hydrogen donor. Isolated yields up to 92 % and e. r's. from 75/25 to 93/7 were obtained [215].

Reduction of a wide variety of 2-substituted and 2,9-disubstituted 1,10-phenathrolines to exclusively give 1,2,3,4-tetrahydro-1,10-phenanthrolines was

achieved employing the dimer $[Cp^*IrCl_2]_2$ or combinations of $[Cp^*IrCl_2]_2$/chiral diamine ligand as a catalyst. The products were obtained in high yields using HCOOH as the hydrogen source. When the dimer $[Cp^*IrCl_2]_2$ in combination with the chiral diamine **I** (Scheme 56) was employed as a catalyst precursor e. r.'s up to 99.5/0.5 were achieved [216].

8 Transfer Hydrogenation and Sustainability

The design and development of efficient chemical processes that meet the requirements of the green chemistry principles [217] remain a global challenge. Nowadays, the vast majority of chemicals are derived from fossil resources which are limited and non-renewable. Sustainability has become an imperative issue and renewables are destined to increasingly replace fossil chemicals. Biomass is the major renewable feedstock on the planet and, consequently, biomass-derived chemicals are promising alternatives to replace them.

Levulinic acid (LA) is one of such chemicals that, in turn, can be converted to higher value compounds such as γ-valerolactone (GVL), 1,4-pentanediol or 2-methyl tetrahydrofuran. A number of homogeneous catalysts based on Ru, Ir, Pd, or Fe have been applied to the transformation of LA to GVL, an important green fuel additive, solvent and fine chemical intermediate [218]. However, reports dealing with homogeneous TH of LA are scarce. In particular, the generation of GLV from aqueous mixtures of LA and HCOOH catalysed by the half-sandwich iridium complex **84** (Scheme 65) has been reported [219].

Scheme 65 Iridium catalysts for the TH of levulinic acid

More recently, Fischmeister and co-workers reported on the solvent free reduction of LA to GVL (Scheme 66) mediated by the dipyridylamine iridium complexes **85**. Reactions were performed at 120-150 ºC, employing mixtures of $HCOOH/NEt_3$ as a hydrogen donor. Yields from 22 to 98 % were obtained within 16 h. Complex **85c** with the bulkiest ligand was found to be the less active catalyst [220].

Scheme 66 Transfer hydrogenation of levulinic acid

The half-sandwich complex **28** (Scheme 7) catalysed the transformation of LA to GVL. Under standard TH conditions (1 mol % of catalyst, *i*PrOH, 85 ºC) 69 % yield was obtained within 12 h [76].

Furfural is one of the organic compounds readily available from nonedible biomass (corncobs, oat hulls, bagasse, etc.) [221]. Furfural is mainly used as a raw material for the synthesis of a multitude of important non-petroleum derived chemicals such as furfuryl alcohol, methyltetrahydrofuran and furan [222]. In this line, Grushin, van Leeuween et al. reported a highly efficient chemo- and stereoselective synthesis of chiral hydrofuroins via asymmetric TH of racemic furoin that is prepared from furfural (Scheme 67) using the half-sandwich iridium complex [Cp*IrCl((*S*,*S*)-TsDPEN)] as catalyst precursor [223].

Scheme 67 Two steps synthesis of hydrofuroin from furfural

On the other hand, solvents often account for most of the mass wasted in syntheses and processes [224]. The utilisation of biogenetic alcohols such as glycerol as a H-donor solvent in catalytic TH reactions is an interesting contribution to the field of sustainable chemistry. Glycerol is a non-toxic and non-flammable by-product from biodiesel processing. Its physical and solvation properties [225] make glycerol a promising candidate to be employed as an environmentally friendly reaction medium for synthetic chemistry [226]. Furthermore, glycerol has advantages, for example, over ethanol, another H-donor also produced from biomass. Dihydroxyacetone, the thermodynamic product of the dehydrogenation of glycerol, has a low tendency to decarbolynation. Although glyceraldehyde can also be formed in glycerol dehydrogenation, it would tautomerize to dihydroxyacetone under the usual catalytic conditions (Scheme 68). However, dehydrogenation of ethanol renders acetaldehyde which is expected to have a much greater tendency than dihydroxyacetone to deactivate the catalyst by decarbonylation.

The last decade has witnessed an increasing use of glycerol as a solvent and a reducing agent in homogeneous TH reactions. In fact, carbon dioxide, carbonyl compounds, olefins, nitroarenes and carboxylic acids have been efficiently hydrogenated in glycerol using Ir, Ru, Pd, Rh and Mo complexes as the catalysts [227, 228].

Scheme 68 Dehydrogenation of glycerol

Recently, it has been reported the reduction of aldehydes, ketones, imines and, to a lesser extent, olefins mediated by iridium carbene complexes **86** and **50** (Scheme 69) with glycerol as a H-donor solvent. Imines were more readily reduced than carbonyl. This trend is opposite to that encountered in TH from *i*PrOH. TH was thought to proceed through a monohydride mechanism [229].

Scheme 69 Iridium catalysts used in TH from biomass-derived H-donors

The iridium precatalyst **51** (Scheme 69) bearing an abnormal carbene ligand converts CO_2 to formate salt at a TOF value of 90 h^{-1} in 12 h of reaction at 150 ºC, using glycerol as a hydrogen source [94].

Nishina reported on the $[Cp^*IrCl_2]_2$-catalysed reduction of carbonyl groups using biogenetic alcohols such as glycerol, monosaccharides and polysaccharides as a hydrogen source. This system did not require any base [230]. 2-Naphthaldehyde was reduced in 1,4-dioxane/water 1/1 (v/v) mixtures, at 85 ºC, at 5.0 mol % of catalyst loading using glycerol (1 equiv, 24 h, 87 % yield) or glucose (1 equiv, 24 h, 95 % yield) as a hydrogen source. Monosaccharides galactose and xylose, disaccharides lactose, sucrose and maltose and the trisaccharide raffiose can also be employed as a hydrogen source. Under the same conditions, yields from 79 to 92 % were obtained [230] with these biogenetic H-donors.

Aryl aldehydes bearing different substituents (**A7**, **A23**, **A31**, **A32**, **A35**), heterocyclic aldehydes such as 4-pyridine carboxaldehyde and 2-thiophene carboxaldehyde, alkyl aldehyde **A56** (Scheme 3) and diphenylketone were converted to the corresponding alcohols in yields ranging from 61 to 83 %, using 1 equiv of glucose as a hydrogen source [230].

Various aldehydes and ketones were efficiently converted to the corresponding alcohols with 2 equiv of glucose as a H-donor, in the presence of 0.1-1 mol % of the bipyridonate iridium complex **79** (Scheme 51). Reactions were carried out at 100 ºC, using water or *N*,*N*-dimethylacetamide as a solvent and Na_2CO_3 as a base. Aryl aldehydes (**A1**, **A10**, **A21**, **A23**, **A24**, **A28**, **A30**, **A31**, **A35**, **A37**, **A50**, **A51**), alkyl aryl (**B1**, **B3**, **B5**, **B8**, **B11**, **B18**, **B21**-**B24**, **B26**, **B27**, **B47**, **B58**), methyl alkyl (**B107**) and cyclic (**B118**, **B120**) ketones were reduced to the corresponding alcohols. Isolated yields from 54 to 91 % were obtained [231].

To determine which of the glucose OH groups functioned as a hydrogen donor, the reaction of acetophenone was conducted using α-glucopyranoside, in which only the hydroxyl group at the C1 position was methylated, or, alternatively, using 2,3,4,6-tetra-*O*-methyl α-glucopyranose, in which all the hydroxyl groups except that at C1 are methylated. The TH reaction did not proceed with the former but gave 97 % yield in the alcohol with the latter. These results suggested that TH of the CO group of the carbonyl substrates implied the hydroxyl group at the C1 position glucose [231].

9 Mechanistic Aspects

Despite the variety of substrates i. e. carbonyl compounds, imines, alkenes and alkynes, used in catalytic TH, mainly the mechanism of the TH of carbonyl compounds using 2-propanol as the hydrogen donor has been systematically studied by means of both experimental methods and theoretical calculations. For an overview of mechanistic aspects of TH see refs. 228, 232-234. In general, the different basicity and nucleophilicity of the substrates makes it difficult to apply the reaction map depicted for carbonyl compounds to imines, alkenes, or alkynes. In addition, as shown in the previous sections, besides the ubiquitous 2-propanol, different hydrogen donors have been successfully used as well, e. g. formic acid, 1,4-dioxane, glycerol, ethanol and diols.

As far as TH of carbonyl compounds using 2-propanol is concerned, overall, the formal transfer of a hydride and a hydrogen ion from the donor to the substrate takes place.

Three scenarios have been depicted so far:

i) in an inner sphere mechanism, a metal-alkoxide is the entry species of the catalytic cycle (Scheme 70), eventually undergoing a β-hydrogen elimination rendering a metal monohydride complex. The hydride moiety is transferred by means of the insertion of the substrate into the metal-hydride bond whereas the protonolysis of the resulting alkoxide intermediate enables the transfer of the hydrogen ion.

   Alternatively a metal dihydride species has been proposed as the active species along the catalytic cycle. In this case both hydride moieties come from the hydrogen donor thanks to the oxidative addition of the O–H bond followed by the β-hydrogen elimination in the resulting alkoxide (Scheme 70). In this case, the hydrogen atoms of the metal-dihydride moiety transfer to the substrate in a sequential way by means of the insertion of the substrate into the metal-hydride bond and the following reductive elimination of the hydrogenated substrate from the hydride-alkoxide intermediate.

   As a result, in the monohydride route the C-H hydrogen of the donor exclusively turns into the C-H hydrogen of the product, while in the dihydride route a scrambling of the C-H and O-H hydrogen atoms of the donor takes place.

Scheme 70 Metal monohydride (*top*) and metal dihydride routes (*bottom*) for the TH of carbonyl compounds using 2-propanol as the hydrogen donor

ii) the hydride moiety and the hydrogen ion are transferred to the substrate in an outer sphere mechanism implying both a metal-hydride moiety and a protic end

of one ligand at the metal centre (Scheme 71). This metal-ligand bifunctional mechanism was initially described by Noyori and coworkers [235] for ruthenium catalysts and has been later observed in a number of structurally related transition metal complexes as well as in metal-ligand platforms in which the ligand act as a non-innocent fragment. [236] Notably recent reviews on this mechanism have raised concerns about the concertedness of the H^+/H^- transfer to the substrate and the genuine non-innocence of the ancillary ligand [236-238]. It is worth mentioning that metal-ligand bifunctional catalysts are very competent in the asymmetric transfer hydrogenation (ATH) of either carbonyl compounds or imines. Nonetheless, it has been proposed that the origin of enantioselection is different for carbonyl compounds or imines. In the case of carbonyl compounds it relies on the formation of weak interactions between ancillary ligands and substituents at the substrate, while in the case of imines an ionic outer sphere mechanism could be operative [237].

Scheme 71 Metal-ligand bifunctional mechanism for the TH of carbonyl compounds using 2-propanol as the hydrogen donor (*left*) and the transition state for the concerted transfer of the two hydrogen atoms from the metal-ligand platform to the substrate (*right*)

iii) in an inner sphere mechanism, the hydride moiety is transferred directly from the donor to the substrate and the protonolysis of the resulting alkoxide intermediate enables the transfer of the hydrogen ion (Scheme 72). This route is known as the Meerwein-Ponndorf-Verley mechanism and was first reported for the TH reaction catalysed by aluminium 2-propoxide. Nontheless it has also been observed when transition metal complexes have been used as the catalysts.

Scheme 72 Meerwein-Ponndorf-Verley mechanism of the TH of carbonyl compounds using 2-propanol as the hydrogen donor (*left*) and the transition state of the direct hydrogen transfer (*right*)

As a milestone in the DFT-based elucidation of the mechanism of iridium catalysed TH of carbonyl compounds, back in 2003 the pioneering DFT study by Meijer [239] explored the viability of both the hydride route (inner/outer sphere) and the direct transfer when using iridium(I) catalysts of general formula Ir(COD)(L) (HL = 2-amino ethanol, 2-aminoethylmethylsulfide). The study concluded that the direct transfer exhibits the lowest activation barrier and consequently is the most accessible path (Scheme 73). Further, the hemilabile character of the amino ligand proved to be decisive given that the dissociation of either the SCH_3 or the OH moiety takes place generating the necessary coordination vacant for the coordination of the substrates to the iridium(I) centre.

Scheme 73 Intermediates and transition states for the TH of carbonyl compounds catalysed by Ir(COD)(HL) (HL = 2-amino ethanol, 2-aminoethylmethylsulfide) [239]

Within the time frame covered herein, namely from early 2015 to early 2020, a selection of mechanistic proposals, backed by experimental data and/or theoretical calculations, will be presented in the following in order to highlight different aspects of TH (or ATH) of different C=X (X = C, N, O) and C≡C bonds catalysed by iridium complexes using either alcohols or formic acid as the hydrogen donor.

In 2015 Xiao [212] explored the reaction mechanism of the TH of the C=N bond in *N*-heterocycles using κ^2*C,N*-iridacycle catalysts and formic acid as the hydrogen source. Using 2-methylquinoline as the model substrate, stoichiometric assays as well as isotopic labelling experiments allowed shedding light on the main steps of the TH reaction (Scheme 74). Indeed, the authors clearly demonstrated that the rate limiting step is the hydrogen transfer from the metal hydride to the substrate. Furthermore, the occurrence of both the 1,2-addition (Scheme 74, *bottom*) and the 1,4-addition of hydrogen (Scheme 74, *top*) to the H-heterocycle was proved.

Scheme 74 Catalytic cycle proposed by Xiao [212] for the TH of N-heterocycles: 1,4-addition (*top*), 1,2-addition (*bottom*)

Also, Xiao and Catlow [240] have described the remarkable activity of κ^2*C,N*-iridacycles in reducing imino groups by TH with formic acid. In this case, based on a combination of kinetic measurements, crystallographic studies and DFT calculations the metal hydride route depicted in Scheme 75 was proposed, pointing at that the rate limiting step is the hydride formation rather than the hydrogen transfer to the protonated substrate.

Scheme 75 Catalytic cycle and transition states proposed by Xiao [240] for the TH of imine catalysed by iridacycles using formic acid as the hydrogen donor

Stirling [241] reported the ATH of imines using formic acid as the hydrogen source (in the presence of NEt_3) using an iridium CATHy catalyst (Scheme 76). On one hand, under the experimental conditions the imine is expected to be protonated rendering the iminium ion, and, on the other one, the observed KIEs as well as the rate profiles point out that the order of the transfer hydrogenation kinetics of the iminium ion depends on the enantioface of the iminium implied in the hydride transfer, being first order when the *R* enantiomer is formed and zero order for the *S* enantiomer. On this background, one catalytic species could be operative for the formation of the two enantiomers, but there should exist different rate-limiting steps for each one, namely the slow dissociation of the *S* enantiomer, leading to a cero order kinetics, and the slow hydride transfer when the *R* enantiomer forms, leading to a first order kinetics.

Nonetheless, Stirling does not rule out the possibility that two different catalytic species could form, each one leading to a different enantiomer with its own activity.

Scheme 76 Catalytic cycle proposed by Stirling [241] for the TH of imines catalysed by an iridium CATHy catalyst. The rate determining steps (RDS) for the formation of the *R* and *S* enantiomers are indicated

Zhao and Lan [86] have investigated the ATH of imines catalysed by a chiral Cp*Ir platform using different alcohols as the hydrogen donor, focussing, among other things, on the influence of the hydrogen donor. In this study, the experimental data support that the iridium alkoxide pathway (direct transfer) prevails over the classical hydride pathway, and that the external phosphoric acid cocatalyst is necessary in order to activate the substrate (Scheme 77). As a confirmation, extensive DFT calculations nicely confirm that the activation barrier for the classical bifunctional mechanism is higher than that calculated for the outer sphere hydrogen transfer from the alkoxide moiety to the iminium ion (stabilised by a hydrogen bonded phosphate anion). In addition, the hydride route is discarded due to the significantly higher barrier calculated for the formation of the hydride via either β-hydrogen elimination in the alkoxide intermediate or transfer from the hydrogen source.

Scheme 77 Reaction paths and transition states for the ATH of imines proposed by Zhao and Lan [86]. Cycle I: iridium-alkoxide path; cycle II: iridium-hydride path

Iglesias and Oro [178] have explored the TH of both carbonyl compounds and imines using 2-propanol as the hydrogen donor, catalysed by novel iridium complexes containing an *N*-heterocyclic olefin (NHO) as the ligand. DFT calculations indicate that the inner sphere metal hydride route is operative (Scheme 78, cycle I). It is worth a mention that the proposed catalytic cycle only implies iridium(I) complexes as the active species. In addition the NHO ligand plays a crucial role switching between the coordination modes κ^3*C,P,P'* and κ^2*P,P'*, thus allowing the β-hydrogen elimination in the alkoxide intermediate and the insertion of the substrate into the metal-hydride bond. For the sake of comparison, the energy profile of the inner sphere direct hydrogen transfer has also been computed (Scheme 78, cycle II), thus ruling out that this route could be operative under the experimental conditions.

Scheme 78 Reaction paths and transition states for the TH of carbonyl compounds proposed by Iglesias and Oro [178]. Cycle I: monohydride route; cycle II: direct transfer

The TH of carbonyl compounds, imines and alkenes with a family of triazolylidene iridium complexes (Scheme 79) has been studied by Pámies, Albrecht and Diéguez [155]. A combination of isotope labelling experiments, KIE measurements and Hammet

parameter correlations reveals that the reaction takes place via a monohydride route and that the turn-over limiting step is the hydride transfer from the metal to the substrate.

Scheme 79 Triazolylidene iridium complexes used as the catalysts for the TH of carbonyl groups, imines and alkenes [155]

More recently, in 2018 Huang [181] described a family of *N,C,P* pincer iridium catalysts for the TH of alkenes, alkynes and heteroarenes using ethanol as the hydrogen source. As for the TH of alkene a thorough experimental and computational study shed light on the operating mechanism. A metal dihydride route is proposed and remarkably the nature of the alkene determines the resting state of the cycle. Indeed, strongly bound alkenes give rise to a square planar iridium(I) complex (Scheme 80, **A**), whereas weakly bound alkenes lead to an unprecedented iridium(III) hydride alkoxide as the resting state (Scheme 80, **B**). Both DFT data and crystallographic studies reveal that this resting state contains two hydrogen bonded ethanol molecules forming a six member iridacycle.

Scheme 80 Catalytic cycle for the TH of alkenes using ethanol as the hydrogen donor and an iridium *P*,*C,N* pincer catalyst, proposed by Huang [181]

In 2019, in a related study, Huang [182] delved into the application of *P,C,N*-pincer iridium(III) complexes to the catalytic TH of alkynes to *E*-alkenes using ethanol as the hydrogen source. Remarkably the authors make the most of a finely balanced catalytic cycle in order to gain control over the selective hydrogenation of alkynes to *E*-alkenes. Crystallographic studies, KIE measurements and kinetic studies reveal that a metal dihydride mechanism operates. As a matter of fact, the dihydride intermediate is responsible for both the TH of alkyne to *Z*-alkene and the following (fast) *Z*-*E* isomerization of the formed alkene. In addition, two crucial resting states have been proposed for the formation of the *Z*-alkene, namely the iridium(I) alkyne complex **C** (Scheme 81) and the iridium(III) hydride alkoxide derivative **B** stabilised by two hydrogen bonded ethanol molecules (Scheme 81, **B**). It is worth a mention that this two resting states differ in their colour and their relative stability in the presence of the alkyne. Indeed, as long as the alkyne is present, **C** forms and the reaction mixture has a green colour. On the other hand, when the full conversion of the alkyne is reached the solution turns yellow as a result of the formation of **B**.

Scheme 81 Catalytic cycles, proposed by Huang [182], for the TH of alkynes to *Z*-alkene (*top*) and *Z*-*E* isomerization (*bottom*) catalysed by an iridium *P*,*C*,*N* pincer complex using ethanol as the hydrogen donor

In 2019, Sawamura and Iwai [194] have reported the use of 1,4-dioxane as the hydrogen source in the TH of alkenes and alkyne catalysed by an in situ generated

diphosphino iridium(I) catalyst. Isotopic labelling tests and KIE measurements point to a dihydride route (Scheme 82).

Scheme 82 Catalytic cycle for the TH of alkenes using 1,4-dioxane as the hydrogen donor with an in situ generated iridium(I) catalyst [194]

Very recently Williams [242] described the TH of ketones catalysed by a family of Cp*Ir derivatives using 2-propanol as the hydrogen donor (Scheme 83). Isotopic labelling experiments, KIE measurements and NMR kinetic studies allow the authors to propose the occurrence of a single kinetically relevant step in which a concerted proton-hydride abstraction takes place in an associative event implying two molecules of donor. Further synthetic studies and DFT calculations pointed out that the active species should imply the pyridinyl ligand acting as a non-innocent platform.

Scheme 83 Cp*Ir catalysts used by Williams [242] for the TH of carbonyl compouds using 2-propanol as the hydrogen donor (*top*) and outer sphere metal-ligand bifunctional reaction sequence (*bottom*).

10 Conclusions

Although the first examples of TH date back to the first quarter of the 20th century, the systematic development of this methodology started in the early 1970s. Despite the inherent advantage that the use of a sacrificial hydrogen donor presents over the employ of hazardous molecular hydrogen, the good results that were obtained in hydrogenation placed TH as a non-competitive variant with respect to H_2-hydrogenation for the reduction of unsaturated substrates.

Two fundamental milestones changed the landscape of the TH in the 1990s. In 1991, Bäckwall, based on mechanistic proposals, introduced the use of bases as an additive in TH reactions. Increases of several orders of magnitude in reaction rate supported this innovation. In the second half of the 90s, Noyori presented a new catalytic system that meant a conceptual change in the mechanism of TH reactions and allowed almost perfect enantioselectivities to be achieved. These events gave rise to an explosive and fruitful development of the area in which HT has become a powerful and efficient alternative in the field of the reduction of unsaturated species. Iridium catalysts have played a fundamental role in this process since, after ruthenium catalysts, they have been the most widely used.

Most of the catalytic processes, including TH reactions, are carried out in organic media. HT reactions in water can make the process cheaper and environmentally more friendly. In this regard, some iridium catalysts show a high tolerance towards water and

acids. Therefore, they are appealing candidates to develop TH reactions in water as a solvent and with formic acid as a hydrogen source.

Along with the search for more robust and efficient catalysts, the development of environmentally benign catalytic systems is currently another key point. Iridium catalysts have been shown to be compatible with the use of biomass-derived compounds, such as glycerol or ethanol, as the solvents and the hydrogen donors in TH reactions. Likewise, iridium-based catalysts have been successfully applied in the transformation of this type of compounds into high added value products.

Half-sandwich iridium compounds are among the most widely used as the metallic part of metalloenzymes that have been successfully applied in TH reactions. Artificial metalloenzymes have the unique characteristic of being able to be improved both from a chemical and a genetic point of view. This feature provides them with immense room for improvement in order to optimise them and obtain catalysts with the desired capabilities. On the other hand, new anticancer strategies associated with the use of NADH or NAD(P)H as hydrogen donor in TH reactions mediated by iridium complexes have also been developed.

Nowadays, the field of HT has a solid and proven mechanistic basis that allows for the design, development and optimization of new catalytic systems to tackle new issues, fulfillng efficiency and sustainability criteria, with a high possibility of success.

In summary, TH affords an effective alternative for the reduction of unsaturated substrates and the last five years has witnessed great efforts to develop iridium catalysts for this purpose. In particular, iridium catalysts have substantially contributed to the development of green and sustainable as well as new anticancer strategies associated with TH processes. Without a doubt, in the coming years, in this rapidly evolving area there will be interesting findings for both academia and industry.

References

1. Meervein H, Schmidt R (1925) Liebigs Ann Chem 444:221-238
2. Verley A (1925) Bull Soc Chim Fr 37:537-542
3. Ponndorf W (1926) Angew Chem 39:138-143
4. Addadh YMY, Henbest HB, Husbands J, Mitchell TRB (1964) Proc Chem Soc London 361-361
5. Trocha-Grimshaw J, Henbest HB (1967) Chem Commun 544-544
6. Sasson Y, Blum J (1971) Tetrahedron Lett 12:2167-2170
7. Sasson Y, Blum J (1975) J Org Chem 40:1887-1896
8. Blum J, Sasson Y, Iflah S (1972) Tetrahedron Lett 13:1015-1018
9. Chowdhury RL, Bäckvall JE (1991) J Chem Soc, Chem Commun 1063-1064
10. Hashiguchi S, Fujii A, Takehara J, Ikariya T, Noyori R (1995) J Am Chem Soc 117:7562-7563
11. Noyori R, Yamakawa M, Hashiguchi S (2001) J Org Chem 66:7931-7944
12 Li YY, Yu SL, Shen WY, Gao JX (2015) Acc Chem Res 48:2587-2598
13. Magubane MN, Nyamato GS, Ojwach SO, Munro OQ (2016) RSC Adv 6:65205-65221
14. Dubey P, Gupta S, Singh AK (2019) Organometallics 38:944-961
15. Shaikh MN (2019) RSC Adv 9:28199-28206
16. Foubelo F, Nájera C, Yus M (2015) Tetrahedron: Asymmetry 26:769-790
17. Chelucci G, Baldino S, Baratta W (2015) Acc Chem Res 48:363-379
18. Gichumbi JM, Friedrich HB (2018) 866:123-143
19. Wang F, Lin Xu L, Sun C, Yu L, Xu Q (2018) Appl Organometal Chem 32:e4505
20. Tang Z, Liu P, Cao H, S Bals S, Heeres HJ, Pescarmona PP (2019) ACS Catal 9:9953-9963
21. Vilhanová B, van Bokhoven JA, Ranocchiaric M (2017) Adv Synth Catal 359:677-686
22. Zhao J, Li Q, Zhuang S, Song Y, Morris DJ, Zhou M, Wu Z, Zhang P, Jin R, (2018) J Phys Chem Lett 9:7173-7179
23. Hou SF, Chen JY, Xue M, Jia M, Zhai X, Liao RZ, Tung CH, Wang W (2020) ACS Catal 10:380-390
24. Wu W, Seki T, Walker KL, Waymouth RM (2018) Organometallics 37:1428-1431
25. Ma F, Chen J, Yang F, Shinde MV, Zhoua Y, Fan B (2017) Org Biomol Chem 15:2359-2362
26. Xu Y, Long J, Zhao W, Li H, Yang S (2019) Frontiers in Chemistry 7:590
27. Mishra AA, Bhanage BM (2019) New J Chem 43:6160-6167

28. Cabanillas M, Franco A, Lázaro N, Balu AM, Luque R, Pineda A (2019) Molecular Catalysis 477:110522
29. Wang F, Planas O, Cornella J (2019) J Am Chem Soc 141:4235-4240
30. Bolm C (2009) Nat Chem 1:420-420
31. Bullock RM (2013) Science 342:1054-1055
32. Zuo WW, Lough AJ, Li YF, Morris RH (2013) Science 342:1080-1083
33. Morris RH (2015) Acc Chem Res 48:1494-1502
34. Zuo W, Morris RH (2015) Nat Protoc 10:241-257
35. Demmans K Z, Seo CSG, Lough AJ, Morris RH (2017) Chem Sci 8:6531-6541
36. Morris RH (2018) Dalton Trans 47:10809-10826
37. De Luca L, Passera A, Mezzetti A (2019) J Am Chem Soc 141:2545-255
38. Farrar-Tobar RA, Wozniak B, Savini A, Hinze S, Tin S, de Vries JG (2019) Angew Chem Int Ed 58:1129-1133
39. Liang Q, Song D (2020) Chem Soc Rev 49:1209-1232
40. Jiang BL, Ma SS, Wang ML, Liu DS, Xu BH, Zhang SJ (2019) ChemCatChem 11:1701-1706
41. Gao Y, Zhang X, Laishram RD, Chen J, Li K, Zhang K, Zeng G, Fan B (2019) Adv Synth Catal 361:3991-3997
42. Bruneau-Voisine A, Wang D, Dorcet V, Roisnel T, Darcel C, Sortais J-B (2017) Org Lett 19:3656-3659
43. Demmans KZ, Olson ME, Morris RH (2018) Organometallics 37:4608-4618
44. Zhou Y-P, Mo Z, Luecke M-P, Driess M (2018) Chem Eur J 24:4780-4784
45. Wei D, Bruneau-Voisine A, Dubois M, Bastin S, Sortais JB (2019) ChemCatChem 11:5256-5259
46. Schneekönig J, Junge K, Beller M (2019) Synlett 30:503-507
47. Putten RV, Benschop J, Munck VJ, Weber M, Müller C, Filonenko GA, Pidko EA (2019) ChemCatChem 11:5232-5235
48. Dubey A, Rahaman SMW, Fayzullin RR, Khusnutdinova JR (2019) ChemCatChem 11: 3844-3852
49. Garduño JA, Flores-Alamo M, García JJ (2019) ChemCatChem 11:5330-5338
50. Nikita V. Shvydkiy NV, Vyhivskyi O, Nelyubina YV, Perekalin DS (2019) ChemCatChem 11:1602-1605
51. Ganguli K, Shee S, Panja D, Kundu S (2019) Dalton Trans 48:7358-7366
52. Vigneswaran V, MacMillan SN, Lacy DC (2019) Organometallics 38:4387-4391
53. Zhang C, Hu B, Chen D, Xia H (2019) Organometallics 38:3218-3226
54. Zhou L, Liu D, Lan H, Wang X, Zhao C, Ke Z, Hou C (2020) Catal Sci Technol 10: 169-179
55. Passera A, Mezzetti A (2020) Angew Chem Int Ed 59:187-191

56. Uematsu N, Fujii A, Hashiguchi S, Ikariya T, Noyori R (1996) J Am Chem Soc 118:4916-4917
57. Wang C, Pettman A, Bacsa J, Xiao J (2010) Angew Chem Int Ed 49:7548-7552
58. Liu Z, Romero-Canelón I, Qamar B, Hearn JM, Habtemariam A, Barry NPE, Pizarro AM, Clarkson G. J, Sadler PJ (2014) Angew Chem Int Ed 53:3941-3946
59. Wang C, Li C, Wu X, Pettman A, Xiao J (2009) Angew Chem Int Ed. 48:6524-6528
60. Wang D, Astruc D (2015) Chem Rev 115:6621-6686
61. Mashima K, Abe T, Tani K (1998) Chem Lett 1199-1200
62. Bolje A, Hohloch S, van der Meer M, Kosmrlj J, Sarkar B (2015) Chem Eur J 21:6756-6764
63. Bolje A, Hohloch S, Kosmrlj J, Sarkar B (2016) Dalton Trans 45:15983-15993
64. Maity R, Hohloch S, Su C-Y, van der Meer M, Sarkar B (2014) Chem Eur J 20:9952-9961
65. Maity R, van der Meer M, Hohloch S, Sarkar B (2015) Organometallics 34:3090-3096
66. Maity R, Mekic A, van der Meer M, Verma A, Sarkar B (2015) Chem Commun 51:15106-15109
67. Volpe A, Baldino S, Tubaro C, Baratta W, Basato M, Graiff C (2016) Eur J Inorg Chem 247-251
68. Müller AL, Bleith T, Roth T, Wadepohl H, Gade LH (2015) Organometallics 34:2326-2342
69. Gómez-López JL, Chávez D, Parra-Hake M, Royappa AT, Rheingold AL, Grotjahn DB, Miranda-Soto V (2016) Organometallics 35:3148-3153
70. Vivancos Á, Albrecht M (2017) Organometallics 36:1580-1590
71. Pretorius R, Mazloomi Z, Albrecht M (2017) J Organomet Chem 845:196-205
72. Navarro M, Smith CA, Albrecht M (2017) Inorg Chem 56:11688-11701
73. Sato Y, Kayaki Y, Ikariya T (2016) Chem Asian J 11:2924-2931
74. Holmes J, Pask CM, Willans CE (2016) Dalton Trans 45:15818-15827
75. Sun M, Campbell J, Kang G, Wang H, Ni B (2016) J Organomet Chem 810:12-14
76. Ruff A, Kirby C, Chan BC, O'Connor AR (2016) Organometallics 35:327-335
77. Townsend TM, Kirby C, Ruff A, O'Connor AR (2017) J Organomet Chem 843:7-13
78. Meriç N, Aydemir M (2016) J Organomet Chem 819:120-128
79. Ak B, Aydemir M, Durap F, Meriç N, Elma D, Baysal A (2015) Tetrahedron: Asymmetry 26:1307-1313

80. Durap F, Karakas DE¸ Ak B, Baysal A, Aydemir M (2016) J Organometal Chem 818:92-97
81. Baysal A, Karakas DE, Meriç N, Ak B, Aydemir M, Durap F (2017) Transit Met Chem 42:365-372
82. Chen HJ, Teo RHX, Li Y, Pullarkat SA, Leung P-H (2018) Organometallics 37:99-106
83. Dubey P, Gupta S, Singh AK (2108) Dalton Trans 47:3764-3774
84. Zhou G, Aboo AH, Robertson CM, Liu R, Li Z, Luzyanin K, Berry NG, Chen W, Xiao J (2018) ACS Catal 8:8020-8026
85. Camarena-Díaz JP, Iglesias AL, Chávez D, Aguirre G, Grotjahn DB, Rheingold AL, Parra-Hake M, Miranda-Soto V (2019) Organometallics 38:844-851
86. Pan H-J, Zhang Y, Shan C, Yu Z, Lan Y, Zhao Y (2016) Angew Chem Int Ed 55:9615-9619
87. Wang W-H, Himeda Y, Muckerman JT, Manbeck GF, Fujita E (2015) Chem Rev 115:12936-12973
88. Sordakis K, Tang C, Vogt LK, Junge H, Dyson PJ, Beller M, Laurenczy G (2018) Chem Rev 118:372-433
89. Bernskotter WH, Hazari N (2017) Acc Chem Res 50:1049-1058
90. Klankermayer J, Wesselbaum S, Beydoun K, Leitner W (2016) Angew Chem Int Ed 55:7296-7343
91. Goeppert A, Czaun M, Jones J-P, Prakash GKS, Olah GA (2014) Chem Soc Rev 43:7995-8048
92. Sanz S, Benítez M, Peris E (2010) Organometallics 29:275-277
93. Azua A, Sanz S, Peris E (2011) Chem Eur J 17:3963-3967
94. Kumar A, Semwal S, Choudhury J (2019) ACS Catal 9:2164-2168
95. Bar R, Sasson Y (1981) Tetrahedron Lett 22:1709-1710
96. Bar R, Sasson Y, Blum J (1984) J Mol Catal 26:327-332
97. Bar R, Bar LK, Sasson Y, Blum J (1985) J Mol Catal 33:161-177
98. Joó F, Csuhai E, Quinn PJ, Vigh L (1988) J Mol Catal 49:L1-L5
99. Joó F, Bényei A (1989) J Organomet Chem 363:C19-C21
100. Bényei A, Joó F (1990) J Mol Catal 58:151-163
101. Wu X, Xiao J (2007) Chem Commun 2449-2466
102. Wang C, Wu X, Xiao J (2008) Chem Asian J 3:1750-1770
103. Wu X, Wang C, Xiao J (2010) Platinum Met Rev 54:3-19
104. Robertson A, Matsumoto T, Ogo S (2011) Dalton Trans 40:10304-10310
105. Wei Y, Wub X, Wanga C, Xiao J (2015) Catal Today 247:104-115
106. He Y-M, Fan Q-H (2015) ChemCatChem 7:398-400
107. Wu X, Wang C, Xiao J (2016) Chem Rec 16:2772-2786

108. Wang C, Xiao J (2017) Chem Commun 53:3399-3411
109. Thangavel S, Friedrich HB, Omondi B (2017) J Mol Caltal A: Chem 429:27-42
110. Yang Z, Zhu Z, Luo R, Qiu X, Liu J-t, Yang J-K, Tang W (2017) Green Chem 19:3296-3301
111. Liu J-t, Yang S, Tang W, Yang Z, Xu J (2018) Green Chem 20:2118-2124
112. Liu Q, Wang C, Zhou H, Wang B, Lv J, Cao L, Fu Y (2018) Org Lett 20:971-974
113. Yang Z, Cheng W, Li Z (2018) Catal Commun 117:38-42
114. Davis HJ, Ward TR (2019) ACS Cent Sci 5:1120-1136
115. Schwizer F, Okamoto Y, Heinisch T, Gu Y, Pellizzoni MM, Lebrun V, Reuter R, Köhler V, Lewis JC, Ward TR (2018) Chem Rev 118:142-231]
116. Letondor C, Humbert N, Ward TR (2005) Proc Natl Acad Sci USA 102:4683-4687
117. Dürrenberger M, Heinisch T, Wilson YM, Rossel T, Nogueira E, Knörr L, Mutschler A, Kersten K, Zimbron MJ, Pierron J, Schirmer T, Ward TR (2011) Angew Chem Int Ed 50:3026-3029
118. Hestericov M, Heinisch T, Alonso-Cotchico L, Maréchal J-D, Vidossich P, Ward TR (2018) Angew Chem Int Ed 57:1863-1868
119. Scott JD, Williams RM, (2002) Chem Rev 102:1669-1730
120. Ward TR (2011) Acc Chem Res 44:47-57
121. Heinisch T, Ward TR (2016) Acc Chem Res 49:1711-1721
122. Liang AD, Serrano-Plana J, Peterson RL, Ward TR (2019) Acc Chem Res 52:585-595
123. Pellizzoni M, Facchetti G, Gandolfi R, Fusé M, Contini A, Rimoldi I (2016) ChemCatChem 8:1665-1670
124. Facchetti G, Rimoldi I (2018) New J Chem 42:18773-18776
125. Reetz MT, Wu S, Zheng H, Prasad S (2010) Pure Appl Chem 82:1575-1584
126. Denard CA, Ren H, Zhao H (2015) Curr Opin Chem Biol 25:55-64
127. Quinto T, Häussinger D, Köhler V, Ward TR (2015) Org Biomol Chem 13:357-360
128. Okamoto Y, Köhler V, Paul CE, Hollmann F, Ward TR (2016) ACS Catal 6:3553-3557
129. Okamoto Y, Köhler V, Ward TR (2016) J Am Chem Soc 138:5781-5784
130. Monnard FW, Nogueira ES, Heinisch T, Schirmerb T, Ward TR (2013) Chem Sci 4:3269-3274
131. Monnard FW, Heinisch T, Nogueira ES, Schirmerb T, Ward TR (2011) Chem Commun 47:8238-8240

132. Tinberg CE, Khare SD, Dou J, Doyle L, Nelson JW, Schena A, Jankowski W, Kalodimos CG, Johnsson K, Stoddard BL, Baker D (2013) Nature 501:212-218
133. Heinisch T, Pellizzoni M, Dürrenberger M, Tinberg CE, Köhler V, Klehr J, Häussinger D, Baker D, Ward TR (2018) J Am Chem Soc 137:10414-10419
134. Raines DJ, Clarke JE, Blagova EV, Dodson EJ, Wilson KS, Duhme-Klair A-K (2018) Nat Catal 1:680-688
135. Lin S-J, Guarente L (2003) Curr Opin Cell Biol 15:241-246
136. Betanzos-Lara S, Liu Z, Habtemariam A, Pizarro AM, Qamar B, Sadler PJ (2012) Angew Chem Int Ed 51:3897-3900
137. Maenaka Y, Suenobu T, Fukuzumi S (2014) J Am Chem Soc 134:367-374
138. Soldevila-Barreda JJ, Romero-Canelón I, Habtemariam A, Sadler PJ (2015) Nat Commun 6:6582-6590
139. Ngo AH, Ibáñez M, Do LH (2016) ACS Catal 6:2637-2641
140. Bose S, Ngo AH, Do LH (2017) J Am Chem Soc 139:8792-8795
141. Jang B, Kwon H, Katila P, Lee SJ, Lee H (2016) Adv Drug Delivery Rev 98:113-133
142. Yang L, Bose S, Ngo AH, Do LH (2017) ChemMedChem 12:292-299
143. Wang C, Liu J, Tian Z, Tian M, Tian L, Zhao W, Liu Z (2017) Dalton Trans 46:6870-6883
144. Li JJ, Tian M, Tian Z, Zhang S, Yan C, Shao C, Liu Z (2018) Inorg Chem 57:1705-1716
145. Li JJ, Guo L, Tian Z, Zhang S, Xu Z, Han Y, Li R, Li Y, Liu Z (2018) Inorg Chem 57:13552-13563
146. Du Q, Guo L, Tian M, Ge X, Yang Y, Jian X, Xu Z, Tian Z, Liu Z (2018) Organometallics 37:2880-2889
147. Du Q, Yang Y, Guo L, Tian M, Ge X, Tian Z, Zhao L, Xu Z, Li J, Liu Z (2019) Dyes Pigm 162: 821-830
148. Soetens M, Drouet F, Riant O (2017) ChemCatChem 9:929-933
149. Stringer T, Melis DR, Smith GS (2019) Dalton Trans 13143-13148
150. Facchetti G, Pellegrino S, Bucci R, Nava D, Gandolfi R, Christodoulou MS, Rimoldi I (2019) Molecules 2:2771-2779
151. Campos J, Sharninghausen LS, Manas MG, Crabtree RH (2015) Inorg Chem 54:5079-5084
152. Jiménez MV, Fernández-Tornos J, Pérez-Torrente JJ, Modrego FJ, García-Orduña P, Oro LA (2015) Organometallics 34:926-940
153. García N, E. A. Jaseer EA, Munarriz J, Sanz Miguel PJ, Polo V, Iglesias M, Oro LA (2015) Eur J Inorg Chem 4388-4395
154. Ramasamy B, Gangwar MK, Ghosh P (2017) Eur J Inorg Chem 3253-3268

155. Mazloomi Z, Pretorius R, Pàmies O, Albrecht M, Diéguez M (2017) Inorg Chem 57:11282-11298
156. Wang H, Jiang T, Xu M-H (2013) J Am Chem Soc 135:971-974
157. Li Y, Lei M, Yuan W, Meggers E, Lei Gong L (2017) Chem Commun 53:8089-8092
158. Albrecht M, van Koten G (2001) Angew Chem Int Ed 40:3650-3781
159. Peris E, Crabtree RH (2004) Coord Chem Rev 248:2239-2246
160. Leis W, Mayera HA, Kaska WC (2008) Coord Cherm Rev 252:1787-1797
161. Morales-Morales D (2008) Mini-Rev Org Chem 5:141-152
162. van der Boom ME, Milstein D (2003) Chem Rev 103:1759-1792
163. Benito-Garagorri D, Kirchner K (2008) Acc Chem Res 41:201-213
164. Choi J, MacArthur AHR, Brookhart M, Goldman AS (2011) Chem Rev 111:1761-1779
165. Selander N, Szabó KJ (2011) Chem Rev 111:2048-2076
166. Gunanathan C, Milstein D (2011) Acc Chem Res 44:588-602
167. Ito J-i, Nishiyama H (2011) Tetrahedron Lett 55:3133-3145
168. Gunanathan C, Milstein D (2014) Chem Rev 114:12024-12087
169. Younus HA, Ahmad N, Su W, Verpoort F (2014) Coord Chem Rev 276:112-152
170. Werkmeister S, Neumann J, Junge K, Beller M (2015) Chem Eur J 21:12226-12250
171. Clarke ZE, Maragh PT, Dasgupta TP, Gusev DG, Lough AJ, Abdur-Rashid K (2006) Organometallics 25:4113-4117
172. Paredes P, Díez J, Gamasa P (2008) Organometallics 27:2597-2607
173. Bi S, Xie Q, Zhao X, Zhao Y, Kong X (2008) J Organomet Chem 693:633-638
174. Azerraf C, Gelman D (2008) Chem Eur J 14:10364-10368
175. Li Y-H, Zhang Y, Ding X-H (2011) Inorg Chem Commun 14:1306-1310
176. Liu W-P, Yuan M-L, Yang X-H, Li K, Xie J-H, Zhou Q-L (2015) Chem Commun 51:6123-6125
177. Zhang Y-M, Yuan M-L, Liu W-P, Xie J-H, Zhou Q-L (2018) Org Lett 20:4486-4489
178. Iturmendi A, García N, Jaseer EA, Munárriz J, Sanz Miguel PJ, Polo V, Iglesias M, Oro LA (2016) Dalton Trans 45:12835-12845
179. Pandrala M, Resendez A, Malhotra SV (2019) J Catal 378:283-288
180. Cohen S, Bilyachenko AN, Gelman D (2019) Eur J Inorg Chem 3203-3209
181. Wang Y, Huang Z, Leng X, Zhu H, Liu G, Huang Z (2018) J Am Chem Soc 140:4417-4429
182. Wang Y, Huang Z, Huang Z (2019) Nature Catal 2:529-536

183. Zweifel T, Naubron JV, Büttner T, Ott T, Grützmacher, H (2008) Angew Chem Int Ed 47:3245-3249
184. Reddy AS, Swarmy KCK (2017) Angew Chem Int Ed 56:6984-6988
185. Chen S, Lu G, Cai C (2015) New J Chem 39:5360-5365
186. Wang D, Zhao K, Yang S, Ding Y (2015) Z Anorg Allg Chem 641:400-404
187. El-Asaad B, Guicheret B, Métay E, Karamé I, Marc Lemaire M (2016) J Mol Catal A: Chemical 411:196-202
188. Tian C, Gong L, Meggers E (2016) Chem Commun 52:4207-4210
189. Ikariya K, Murata K, Noyori R, (2006) Org Biomol Chem 4:393-406
190. Ikariya K, Blacker AJ (2007) Acc Chem Res 40:1300-1308
191. Landaeta VR, Salazar-La Rosa AD, Rodríguez-Lugo RE (2018) Inorg Chim Acta 470:303-311
192. Zhang YM, Li PQ, Liu P (2018) Russ J Coord Chem 44:688-692
193. Günnaz S, Gökçe AG, Türkmen H (2018) Dalton Trans 47:17317-17328
194. Zhang D, Iwai T, Sawamura M (2019) Org Lett 21:5867-5872
195. Yang J, Wang C, Sun Y, Man X, Li J, Sun F (2019) Chem Commun 55:1903-1906
196. Wang C, Gong S, Liang Z, Sun Y, Cheng R, Yang B, Liu Y, Jinfei Yang J, Sun F (2019) ACS Omega 4:16045-16051
197. Farrar-Tobar RA, Tin S, de Vries JG (2018) Selective Transfer Hydrogenation of α,β-Unsaturated Carbonyl Compounds. In: Dixneuf P., Soulé JF. (eds) Organometallics for Green Catalysis. Topics in Organometallic Chemistry, vol 63. Springer, Cham
198. Wang R, Tang Y, Xu M, Meng C, Li F (2018) J Org Chem 83:2274-2281
199. Luo N, Liao J, Ouyang L, Wen H, Liu J, Tang W, Luo R (2019) Organometallics 38:3025-3011
200. Chen S-j, Lu G-p, and Chun Cai C (2015) RSC Adv 5:13208-13211
201. Ramasamy B, Prakasham AP, Gangwar MK, Ghosh P (2019) Chem Select 4:357-365
202. Chrzanowska M, Rozwadowska M (2004) Chem Rev 104:3341-3370
203. Augustine RL, Heterogeneous Catalysis for the Synthetic Chemist, CRC Press, Boca Raton, FL, 1995
204. Zhou Y-G (2007) Acc Chem Res 40:1357-1366
205. Wang D-S, Chen Q-A, Lu S-M, Zhou Y-G (2012) Chem Rev 112:2557-2590
206. Matsunami A, Kayaki Y (2018) Tetrahedron Lett 59:504-513
207. Wu J, Tang W, Pettman A, Xiao J (2013) Adv Synth Catal 355:35-40
208. Wu J, Wang C, Tang W, Pettman A, Xiao J (2012) Chem Eur J 18:9525-9529
209. Voutchkova AM, Gnanamgari D, Jakobsche CE, Butler C, Miller SJ, Parr J, Crabtree RH (2008) J Organomet Chem 693:1815-1821

210. Frediani P, Rosi L, Cetarini L, Frediani M (2006) Inorg Chim Acta 359:2650-2657
211. Fujita K-I, Kitatsuji C, Furukawa S, Yamaguchi R (2004) Tetrahedron Lett 45:3215-3217
212. Talwar D, Li HY, Durham E, Xiao J (2015) Chem Eur J 21:5370-5379
213. Fidalgo J, Ruiz-Castañeda M, García-Herbosa G, Carbayo A, Jalón FA, Rodríguez AM, Manzano BR, Espino G (2018) Inorg Chem 57:14186-14198
214. Facchetti G, Bucci R, Fusè M, Rimoldi I (2018) Chem Select 3:8797-8800
215. Vilhanová BV, Budinská A, Václavík J, Matoušek V, Kuzma M, Červený L (2017) Eur J Org Chem 5131-5134
216. Xu C, Zhang L, Dong C, Xu J, Pan Y, Li Y, Zhang H, Li H, Yu Z, Xu L (2016) Adv Synth Catal 358:567-572
217. Anastas P, Eghbali N (2010) Chem Soc Rev 39:301-312
218. Omoruyi U, Page S, Hallett J, Miller PW (2016) ChemSusChem 9:2037-2047
219. Deng J, Wang Y, Pan T, Xu Q, Guo Q-X, Fu Y (2013) ChemSusChem 6:1163-1167
220. Wang S, Dorcet V, Roisnel T, Bruneau C, Fischmeister C (2017 Organometallics 36:708-713
221. Xing R, Qi W, Huber GW (2011) Energy Environ Sci 4:2193-2205
222. Karinen R, Kati Vilonen K, Niemel M (2011) ChemSusChem 4: 1002-1016
223. Kabro A, Escudero-Adán EC, Grushin VV, Leeuwen PWNM (2012) Org Lett 14:4014-4017
224. Constable DJC, Jiménez-González C, Henderson RK (2007) Org Process Res Dev 11:133-137
225. Gu Y, Jérôme F (2010) Green Chem 12:1127-1138
226. Wolfson A, Dlugy C, Tavor D (2011) Trends Org Chem 15:41-50
227. Díaz-Álvarez AE, Cadierno V (2013) Appl Sci 3:55-69
228. Crabtree RH (2019) ACS Sustainable Chem Eng 7:15845-15853
229. Azua A, Finn M, Yi H, Dantas AB, Voutchkova-Kostal A (2017) ACS Sustainable Chem Eng 5:3963-3972
230. Nishina Y (2019) Inorganics 7:114
231. Yoshida M, Hirahata R, Inoue T, Shimbayashi T, Fujita K-i (2019) Catalysts 9:503
232. Mwansa JM, Page MI (2020) Catal Sci Technol 10:590–612
233. Cheng-Xing C, Chen H, Li SJ, Zhang T, Qu LB, Lan Y (2020) Coord Chem Rev 412:213251
234. Samec JSM, Bäckvall JE, Andersson PG, Brandt P (2006) Chem Soc Rev 35:237-248

235. Noyori R, Ohkuma T (2001) Angew Chem Int Ed 40:40-73, and references therein
236. Dub, PA. Gordon JC (2016) Dalton Trans 45:6756–6781
237. Dub, PA. Gordon JC (2017) ACS Catal 7:6635–6655
238. Dub, PA. Gordon JC (2018) Nature Rev Chem 2:396–408
239. Handgraaf, JW, Reek JNH, Meijer EJ (2003) Organometallics 22: 3150–3157
240. Chen HYT, Wang C, Wu X, Jiang X, Catlow CRA, Xiao J (2015) Chem Eur J 21:16564–16577
241. Stirling MJ, Sweeney G, MacRory K, Blacker AJ, Page MI (2016) Org Biomol Chem 14:3614–3622
242. Demianets I, Cherepakhin V, Maertens A, Lauridsen PJ, Sharada SM, Williams TJ (2020) Polyhedron 182:114508

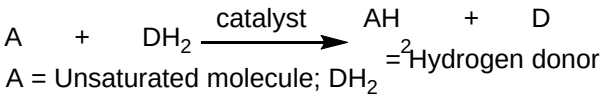

Scheme 1 Catalysed transfer hydrogenation reaction

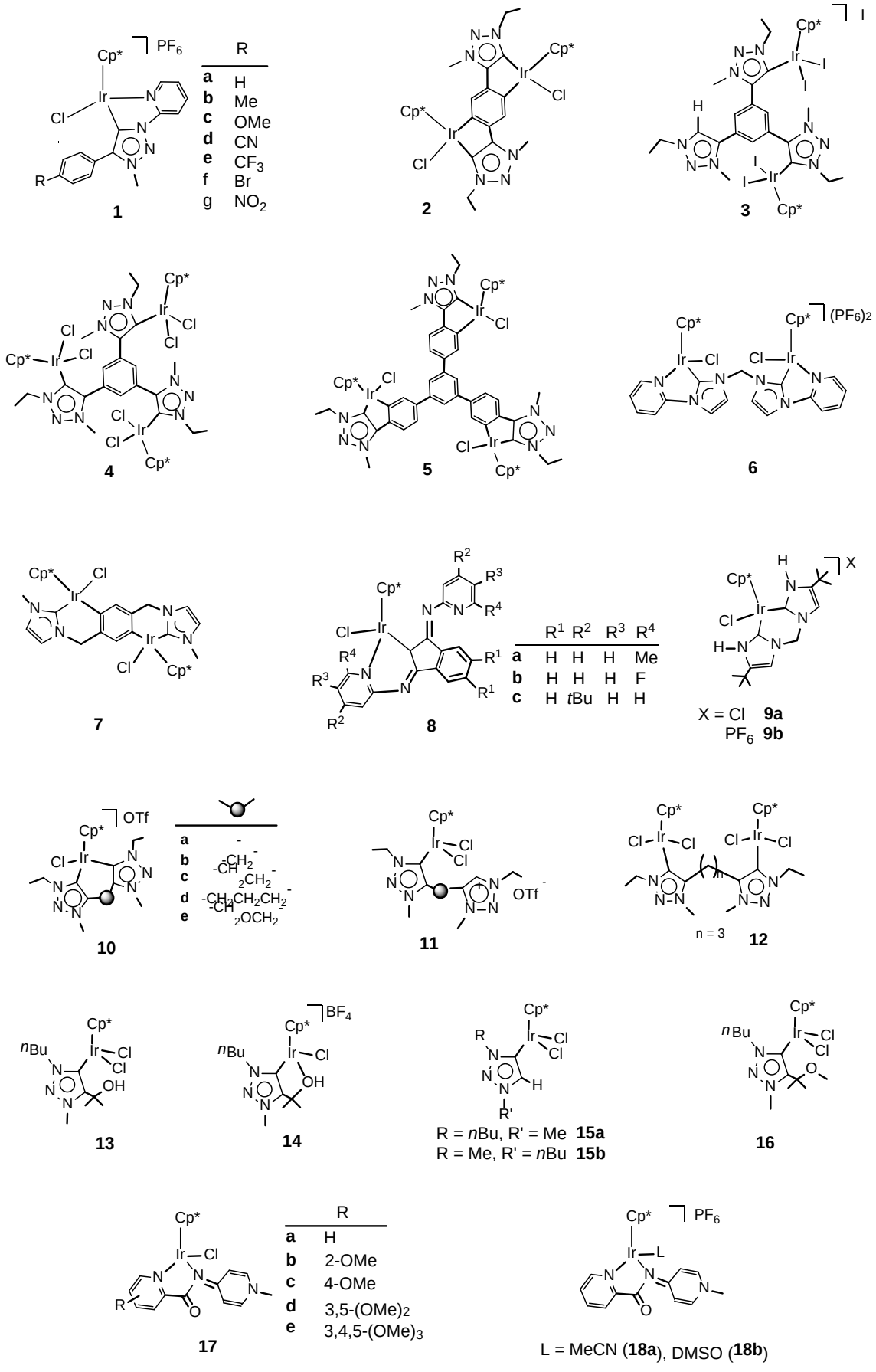

Scheme 2 Half-sandwich iridium catalyst precursors (**1**-**18**)

Aryl aldehydes

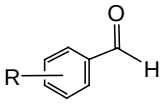

R		R		R	
H	**A1**	3-F	**A14**	4-*i*Pr	**A27**
2-OH	**A2**	3-Cl	**A15**	4-*t*Bu	**A28**
2-OMe	**A3**	3-Br	**A16**	4-F	**A29**
2-*i*Pr	**A4**	3-CF_3	**A17**	4-Cl	**A30**
2-F	**A5**	3-COMe	**A18**	4-Br	**A31**
2-Cl	**A6**	3-CN	**A19**	4-CF_3	**A32**
2-Br	**A7**	3-COOH	**A20**	4-CHO	**A33**
2-CF_3	**A8**	3-NO_2	**A21**	4-COMe	**A34**
2-COOH	**A9**	4-OH	**A22**	4-CN	**A35**
2-NO_2	**A10**	4-Me	**A23**	4-COOH	**A36**
3-OH	**A11**	4-OMe	**A24**	4-COOMe	**A37**
3-OMe	**A12**	4-OC_3H_5	**A25**	4-NO_2	**A38**
3- *i*Pr	**A13**	4-OC_5H_{11}	**A26**		

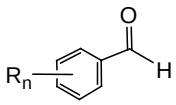

R_2		R_3	
2,5-$(OMe)_2$	**A39**	2,4,6-Me_3	**A46**
3,4-$(OMe)_2$	**A40**	2,4,6-$(OMe)_3$	**A47**
2-OH,5-F	**A41**	3,4,5-$(OMe)_3$	**A48**
2-Br,5-OH	**A42**	3,5-$(OMe)_2$,4-OH	**A49**
2-Cl,5-NO_2	**A43**		
2-Cl,6-NO_2	**A44**		
3-OPh,4-F	**A45**		

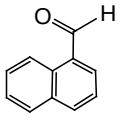

A50

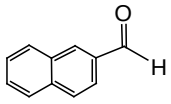

A51

Alkyl aldehydes

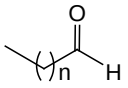

n	
3	**A52**
4	**A53**
6	**A54**
7	**A55**
8	**A56**
9	**A57**

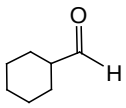

A58

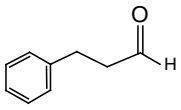

A59

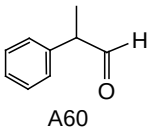

A60

Heteroaryl aldehydes

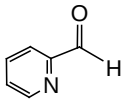

A61

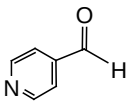

A62

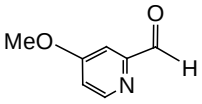

A63

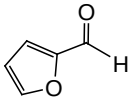

A64

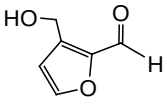

A65

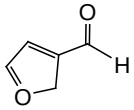

A66

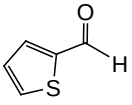

A67

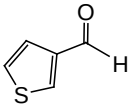

A68

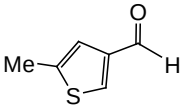

A69

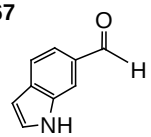

A70

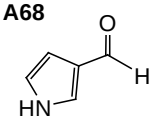

A71

Scheme 3 Aldehydes

Methyl aryl ketones

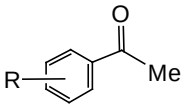

R		R		R	
H	**B1**	3-OMe	**B10**	4-SMe	**B19**
2-Me	**B2**	3-Cl	**B11**	4-F	**B20**
2-OMe	**B3**	3-Br	**B12**	4-Cl	**B21**
2-F	**B4**	3-CF_3	**B13**	4-Br	**B22**
2-Cl	**B5**	3-NO_2	**B14**	4-CF_3	**B23**
2-Br	**B6**	4-Me	**B15**	4-CN	**B24**
2-CF_3	**B7**	4-*t*Bu	**B16**	4-COOH	**B25**
3-Me	**B8**	4-OH	**B17**	4-COOMe	**B26**
3-OH	**B9**	4-OMe	**B18**	4-NO_2	**B27**

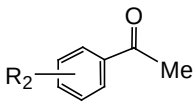

R_2		R_2	
3,4-Me_2	**B28**	2,4-Cl_2	**B31**
3,5-Me_2	**B29**	2-Cl,4-F	**B32**
2,4-$(OMe)_2$	**B30**	2,5-F_2	**B33**
		3,5-$(CF_3)_2$	**B34**

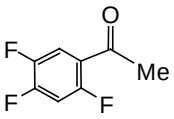

B35

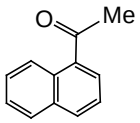

B36

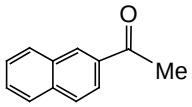

B37

Methyl heteroaryl ketones

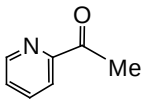

B38

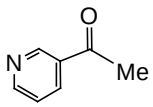

B39

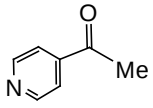

B40

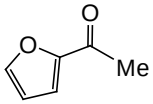

B41

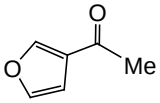

B42

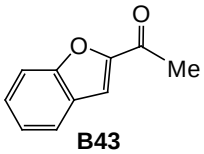

B43

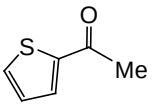

B44

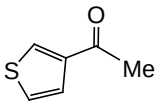

B45

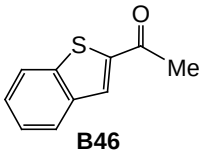

B46

Alkyl aryl ketones

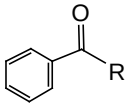

R		R		R	
Et	**B47**	CH_2OH	**B53**	Bn	**B59**
*n*Pr	**B48**	CH_2OCOMe	**B54**	CPh_3	**B60**
*i*Pr	**B49**	CH_2Cl	**B55**	COOEt	**B61**
*t*Bu	**B50**	$CHCl_2$	**B56**	CH_2COOEt	**B62**
*n*Hex	**B51**	CH_2F	**B57**	CH_2CN	**B63**
Cy	**B52**	CF_3	**B58**		

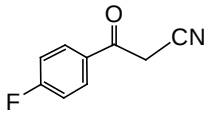

B64

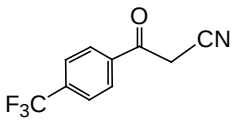

B65

Diaryl ketones

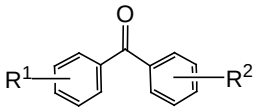

R^1	R^2	
H	H	**B66**
H	4-Br	**B67**
2-Me	H	**B68**
2-F	H	**B69**

R^1	R^2	
4-Me	4-Me	**B70**
4-OMe	H	**B71**
4-CF_3	H	**B72**

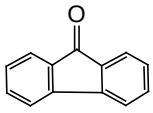

B73

Aryl heteroaryl ketones

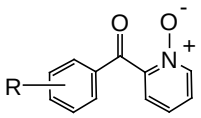

R	
H	**B74**
3-Me	**B75**
3-OMe	**B76**
3-CF_3	**B77**
4-Me	**B78**
4-F	**B79**

R	
4-Cl	**B80**
4-Br	**B81**
4-CF_3	**B82**
3,5-Me_2	**B83**
3,5-$(OMe)_2$	**B84**
3,5-$(CF_3)_2$	**B85**

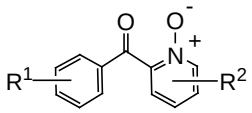

R^1	R^2	
H	3-Me	**B86**
H	4-Me	**B87**
3,5-$(CF_3)_2$	3-Me	**B88**
3,5-$(CF_3)_2$	4-Me	**B89**

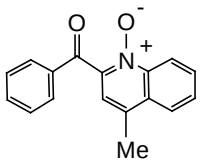

B90

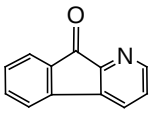

B91

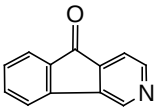

B92

Methyl alkyl ketones

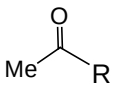

R		R		R	
Me	**B93**	*t*Bu	**B99**	Cy	**B104**
Et	**B94**	*n*Pent	**B100**	CH_2CH_2OH	**B105**
*n*Pr	**B95**	*n*Hex	**B101**	CH_2OPh	**B106**
*i*Pr	**B96**	*n*Hep	**B102**	$(CH_2)Ph$	**B107**
*n*Bu	**B97**	*n*Oct	**B103**	CH_2COOEt	**B108**
*i*Bu	**B98**				

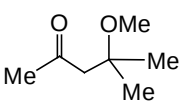

B109

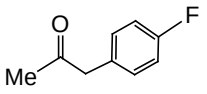

B110

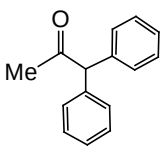

B111

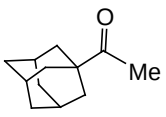

B112

Dialkyl ketones

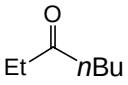

B113

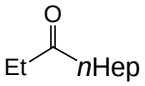

B114

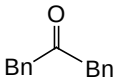

B115

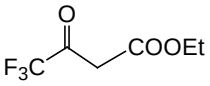

B116

Cyclic ketones

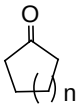

n	
1	**B117**
2	**B118**
3	**B119**
4	**B120**

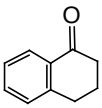

B121

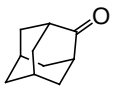

B122

Alkynyl ketones

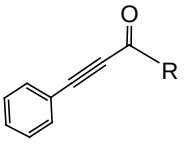

R		R	
Me	**B123**	CF_3	**B126**
Et	**B124**	$(CH_2)_2COOEt$	**B127**
*i*Pr	**B125**	$(CH_2)_3COOEt$	**B128**

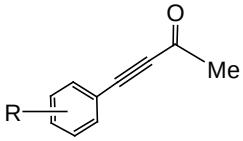

R		R	
2-OMe	**B129**	4-Me	**B133**
2-Cl	**B130**	4-OMe	**B134**
3-Me	**B131**	4-Cl	**B135**
3-Cl	**B132**	4-Br	**B136**

α-Ketophosphonates

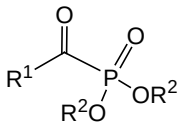

R^1	R^2		R^1	R^2	
Ph	Me	**B137**	4-$(OMe)C_6H_4$	*i*Pr	**B143**
Ph	Et	**B138**	4-FC_6H_4	*i*Pr	**B144**
Ph	*i*Pr	**B139**	4-ClC_6H_4	*i*Pr	**B145**
2-BrC_6H_4	*i*Pr	**B140**	4-BrC_6H_4	*i*Pr	**B146**
3-BrC_6H_4	*i*Pr	**B141**	Bn	*i*Pr	**B147**
4-MeC_6H_4	*i*Pr	**B142**	$(CH_2)_2Ph$	*i*Pr	**B148**

Scheme 4 Ketones

Aldimines

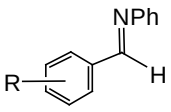

R	
H	**C1**
2-OMe	**C2**
3-OMe	**C3**
4-OMe	**C4**

R	
3-Cl	**C5**
3-Br	**C6**
4-Cl	**C7**
4-Br	**C8**

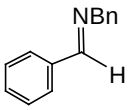

C9

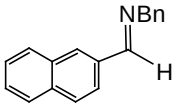

C10

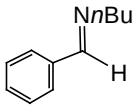

C11

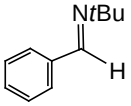

C12

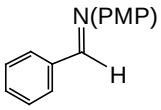

C13

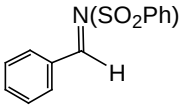

C14

PMP = *p*-metoxyphenyl

Ketimines

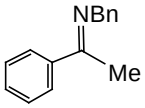

C15

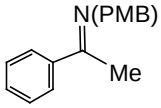

C16

PMB = *p*-metoxybenzyl

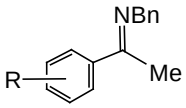

R	
H	**C17**
3-Me	**C18**
4-Me	**C19**

R	
4-OMe	**C20**
3-Br	**C21**
3-CF_3	**C22**

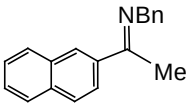

C23

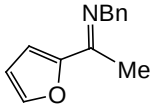

C24

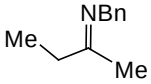

C25

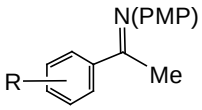

R	
H	**C26**
4-Me	**C27**
4-OMe	**C28**

R	
3-Br	**C29**
4-CF_3	**C30**

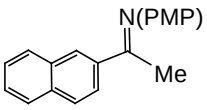

C31

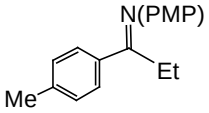

C32

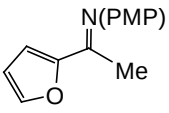

C33

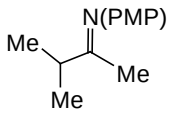

C34

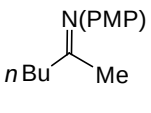

C35

Cyclic *N*-sulfonylimines

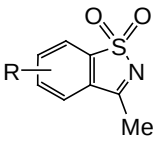

R		R	
H	**C36**	6-Br	**C42**
3-F	**C37**	4-I	**C43**
4-Cl	**C38**	3-Me	**C44**
3-Br	**C39**	3-CF_3	**C45**
4-Br	**C40**	4,5-$(OMe)_2$	**C46**
5-Br	**C41**		

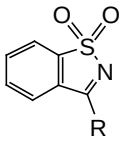

R		R	
Et	**C47**	Cy	**C50**
*i*Pr	**C48**	$(CH_2)_2Ph$	**C51**
*n*Bu	**C49**		

Benzofused *N*-sulfonylimines

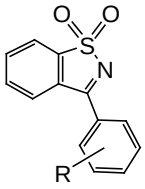

R		R	
H	**C52**	4-OMe	**C56**
2-Me	**C53**	4-F	**C57**
3-Me	**C54**	2-CH_2OH	**C58**
4-Me	**C55**	2-OTBS	**C59**

TBS = *t*Butyldimethylsilyl

Scheme 5 Imines

Alkenes

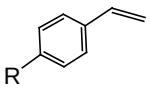

R		R	
H	**D1**	Cl	**D6**
*t*Bu	**D2**	Br	**D7**
OMe	**D3**	COOMe	**D8**
OBn	**D4**	NO_2	**D9**
SMe	**D5**		

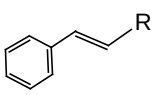

R	
Me	**D10**
Ph	**D11**

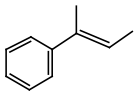

D12

D13

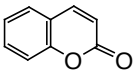

D14

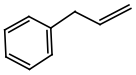

D15

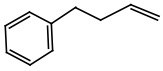

D16

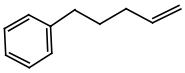

D17

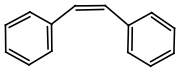

D18

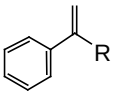

R		R	
Me	**D19**	*t*Bu	**D22**
*i*Pr	**D20**	Ph	**D23**
*i*Bu	**D21**		

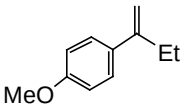

D24

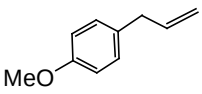

D25

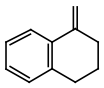

D26

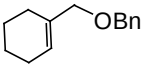

D27

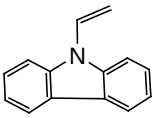

D28

D29

D30

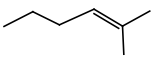

D31

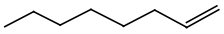

D32

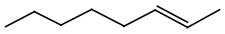

D33

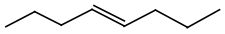

D34

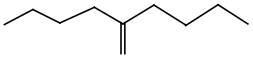

D35

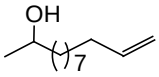

D36

D37

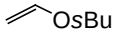

D38

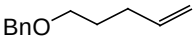

D39

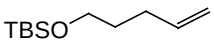

D40

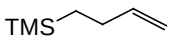

D41

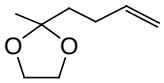

D42

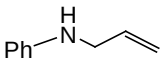

D43

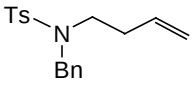

D44

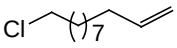

D45

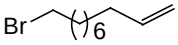

D46

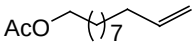

D47

D48

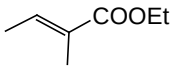

D49

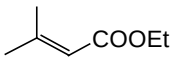

D50

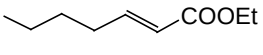

D51

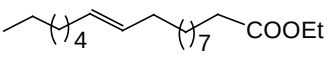

D52

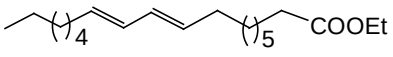

D53

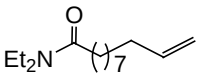

D54

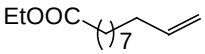

D55

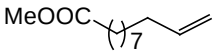

D56

TBS = Tris(tertbutoxy)silanoxy

TMS = Trimethylsilyl

Ts = Tosyl

1,2-Disubstituted alkynes

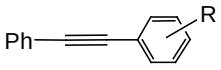

R	
H	**D57**
2-Me	**D58**
3-Me	**D59**
4-Me	**D60**
2-OMe	**D61**
4-OMe	**D62**
4-SMe	**D63**
4-NMe_2	**D64**

R	
4-TMS	**D65**
2-Ph	**D66**
2-F	**D67**
4-F	**D68**
2-Cl	**D69**
3-Cl	**D70**
4-Cl	**D71**

R	
3-Br	**D72**
4-Br	**D73**
4-CF_3	**D74**
4-$CONEt_2$	**D75**
4-COOEt	**D76**
2,6-Me_2	**D77**
3,5-$(CF_3)_2$	**D78**

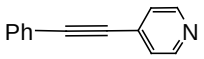

D79

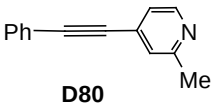

D80

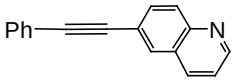

D81

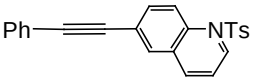

D82

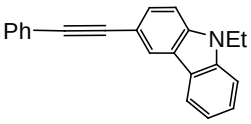

D83

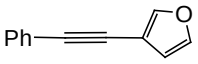

D84

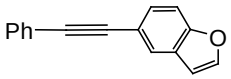

D85

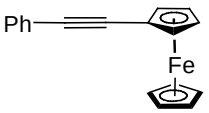

D86

R	
Me	**D87**
*n*Bu	**D88**
*t*Bu	**D89**
Cy	**D90**

R	
1-Naphthyl	**D91**
2-Naphthyl	**D92**
COOMe	**D93**

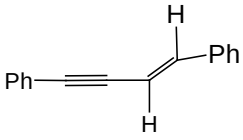

D94

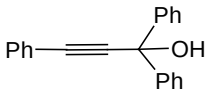

D95

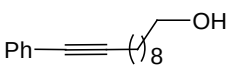

D96

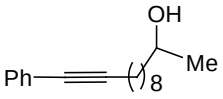

D97

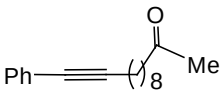

D98

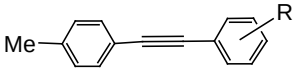

R	
2-Me	**D99**
3-Cl	**D100**
4-Cl	**D101**
3-Br	**D102**
4-Br	**D103**

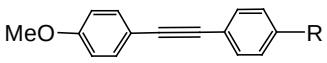

R	
*n*Pr	**D104**
OMe	**D105**

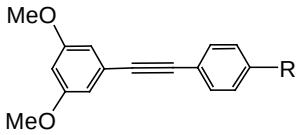

R	
H	**D106**
F	**D107**

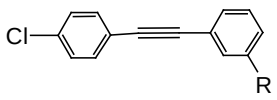

R	
Me	**D108**
Cl	**D109**
Br	**D110**

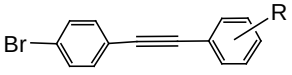

R	
3-Me	**D111**
4-Me	**D112**
4-F	**D113**
3-Cl	**D114**
4-Cl	**D115**
3-Br	**D116**
4-Br	**D117**

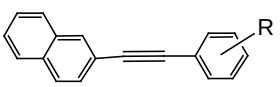

R	
4-Cl	**D118**
3-Br	**D119**
4-Br	**D120**

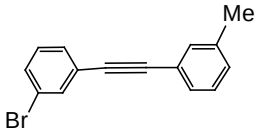

D121

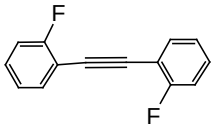

D122

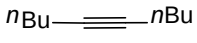

D123

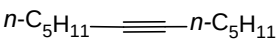

D124

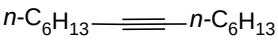

D125

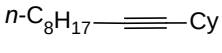

D126

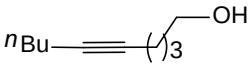

D127

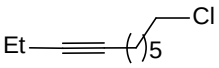

D128

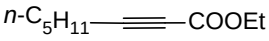

D129

Terminal alkynes

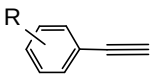

R		R		R	
H	**D130**	4-Ph	**D138**	3-Br	**D146**
2-Me	**D131**	2-F	**D139**	4-Br	**D147**
3-Me	**D132**	3-F	**D140**	3-CF_3	**D148**
4-Me	**D133**	4-F	**D141**	4-CF_3	**D149**
2-OMe	**D134**	2-Cl	**D142**	4-CN	**D150**
3-OMe	**D135**	3-Cl	**D143**	3-NO_2	**D151**
4-OMe	**D136**	4-Cl	**D144**	4-NO_2	**D152**
4-*t*Bu	**D137**	2-Br	**D145**	3,5-$(CF_3)_2$	**D153**

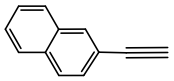

D154

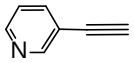

D155

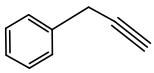

D156

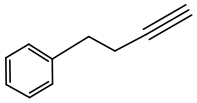

D157

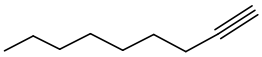

D158

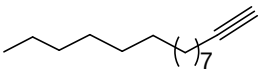

D159

Scheme 6 Alkenes and alkynes

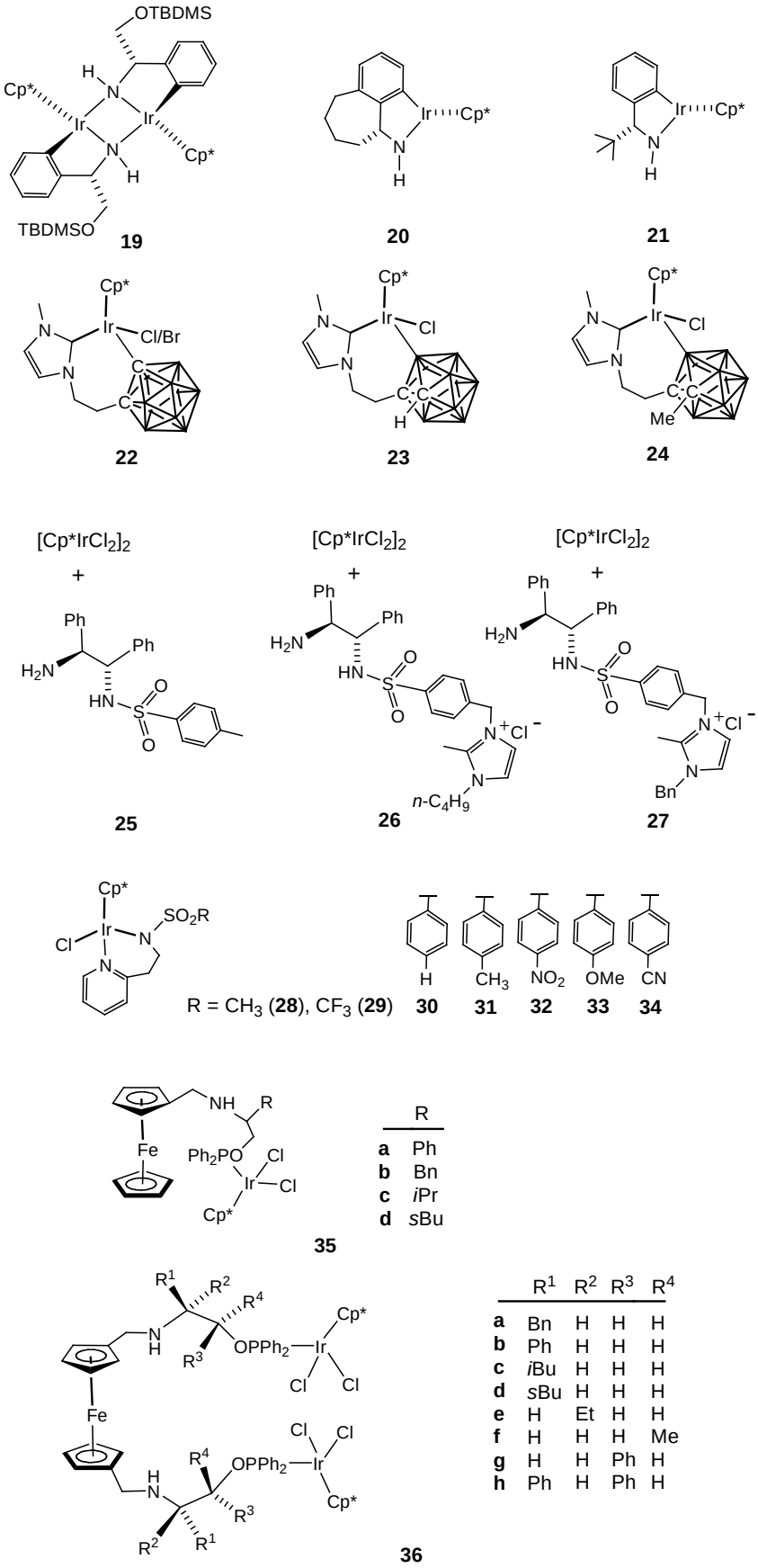

	R
a	Ph
b	Bn
c	*i*Pr
d	*s*Bu

	R^1	R^2	R^3	R^4
a	Bn	H	H	H
b	Ph	H	H	H
c	*i*Bu	H	H	H
d	*s*Bu	H	H	H
e	H	Et	H	H
f	H	H	H	Me
g	H	H	Ph	H
h	Ph	H	Ph	H

Scheme 7 Half-sandwich iridium catalyst precursors (**19-36)**

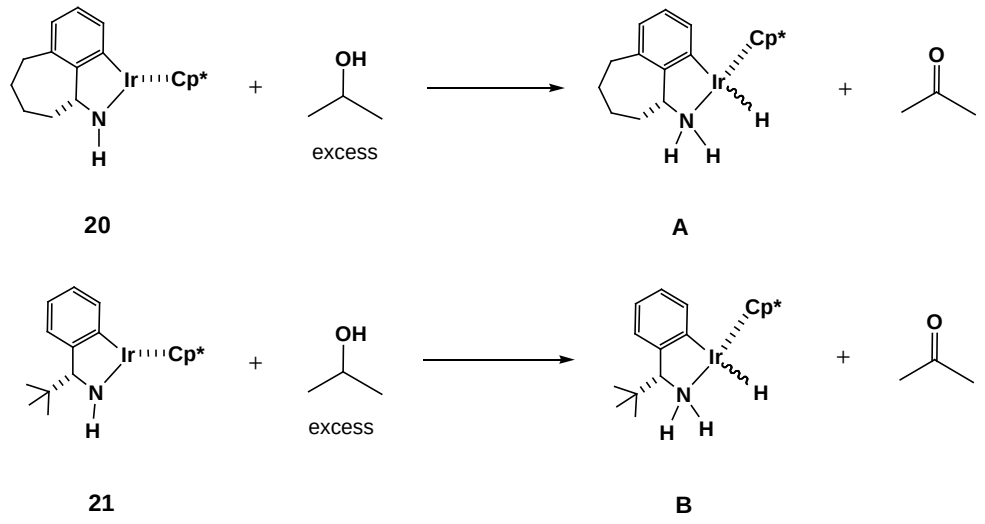

Scheme 8 Dehydrogenation of 2-propanol by the amido complexes **20** and **21**

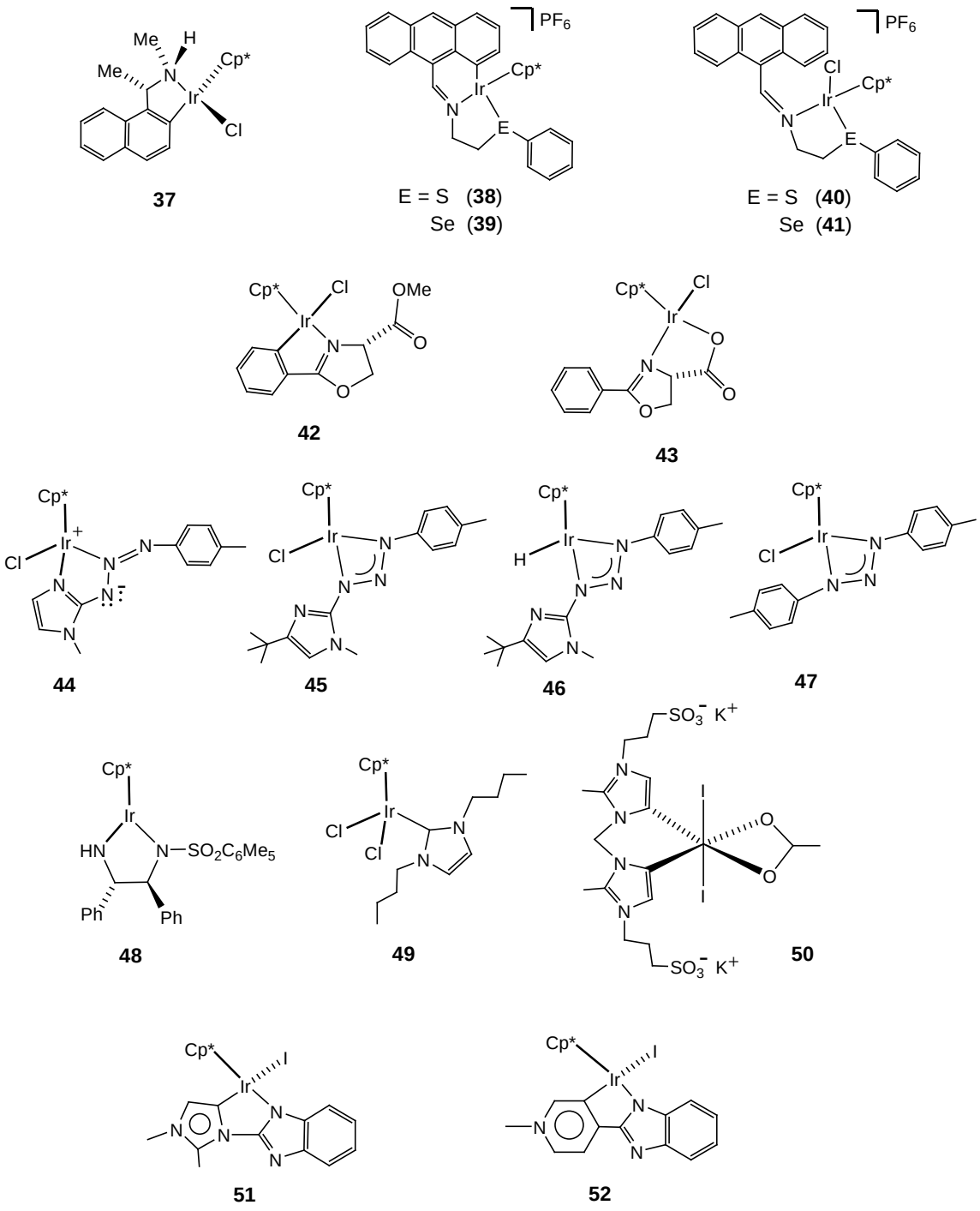

Scheme 9 Half-sandwich iridium catalyst precursors (**37**-**52**)

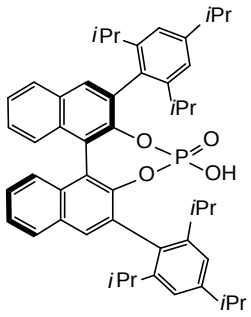

Scheme 10 Chiral phosphoric acid used as additive in the TH of imines

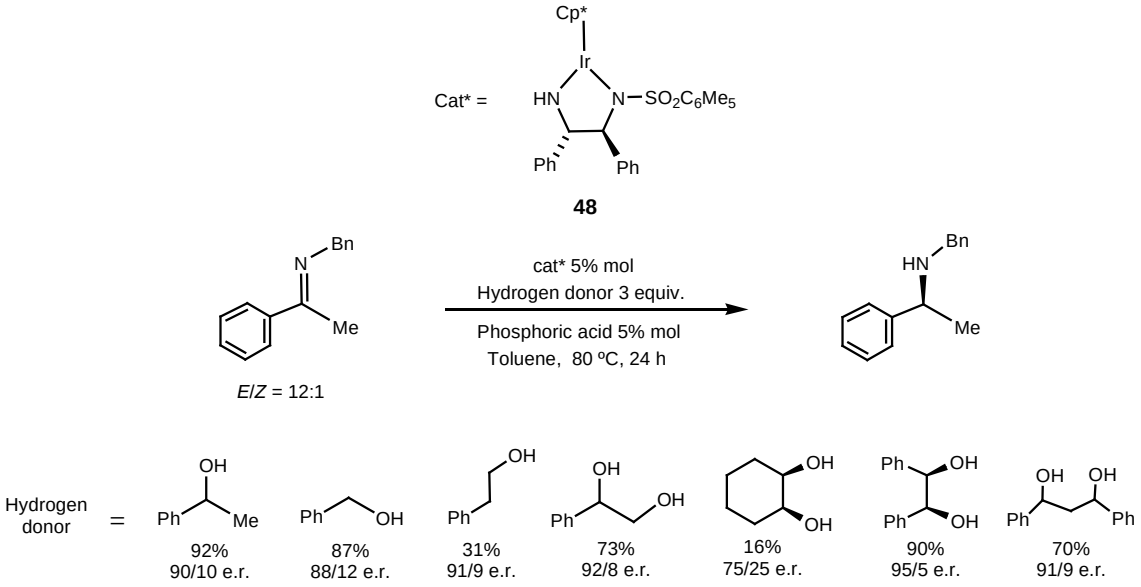

Scheme 11 Screening of hydrogen donors for the TH of imines

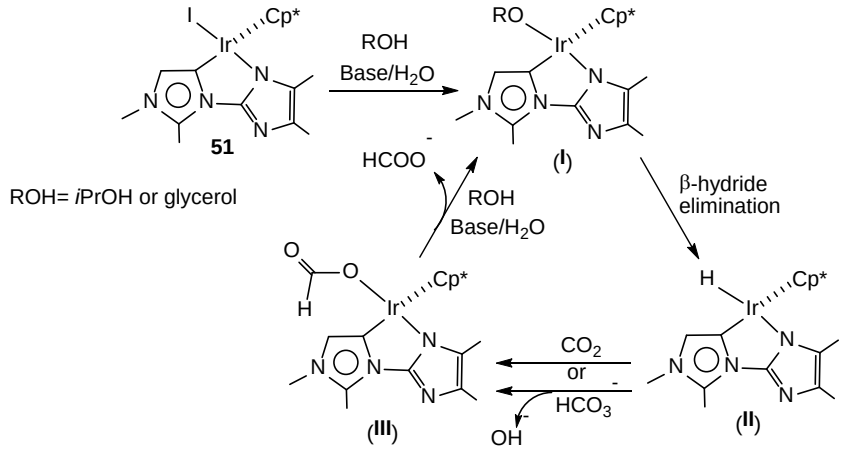

Scheme 12 Proposed catalytic cycle for the TH of CO_2

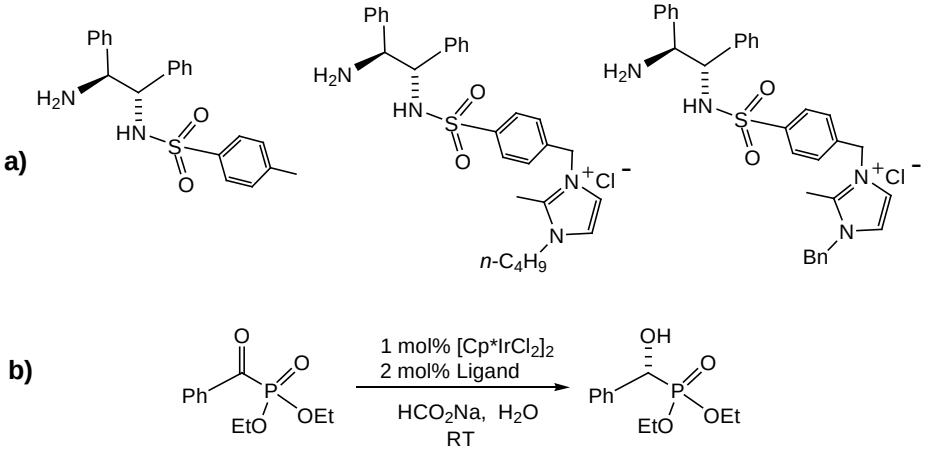

Scheme 13 a) TsDPEN and imidazolium ion tethered TsDPEN ligands b) Phosphonate reduction

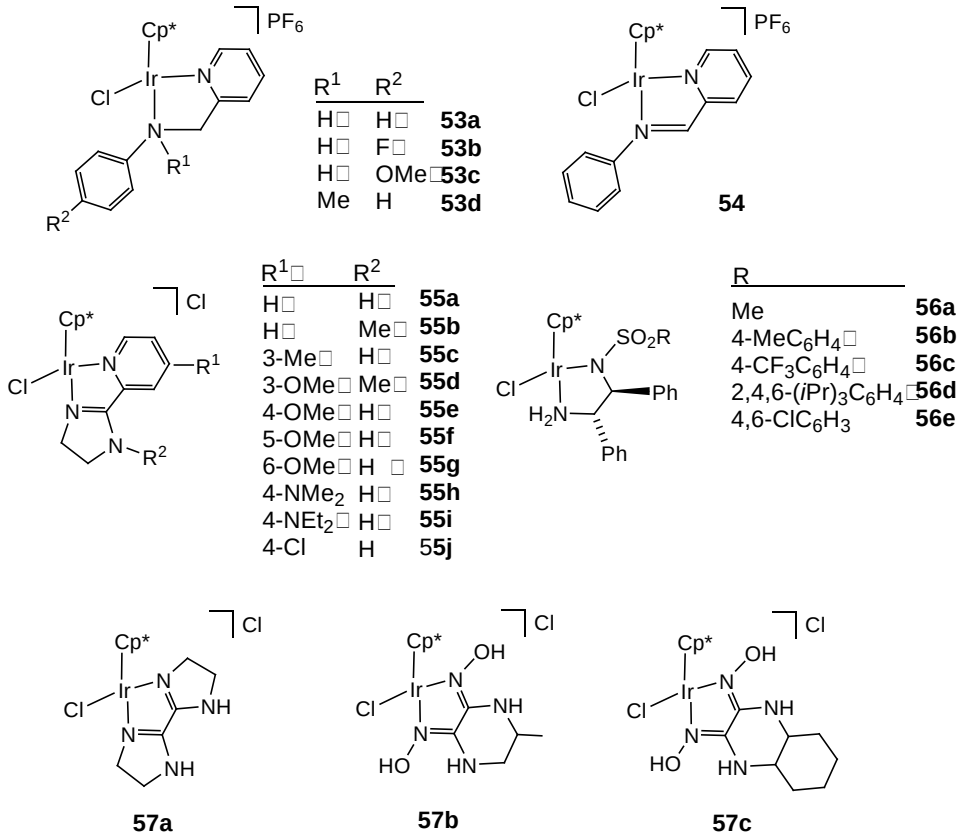

Scheme 14 Half-sandwich iridium catalyst precursors (**53-57)**

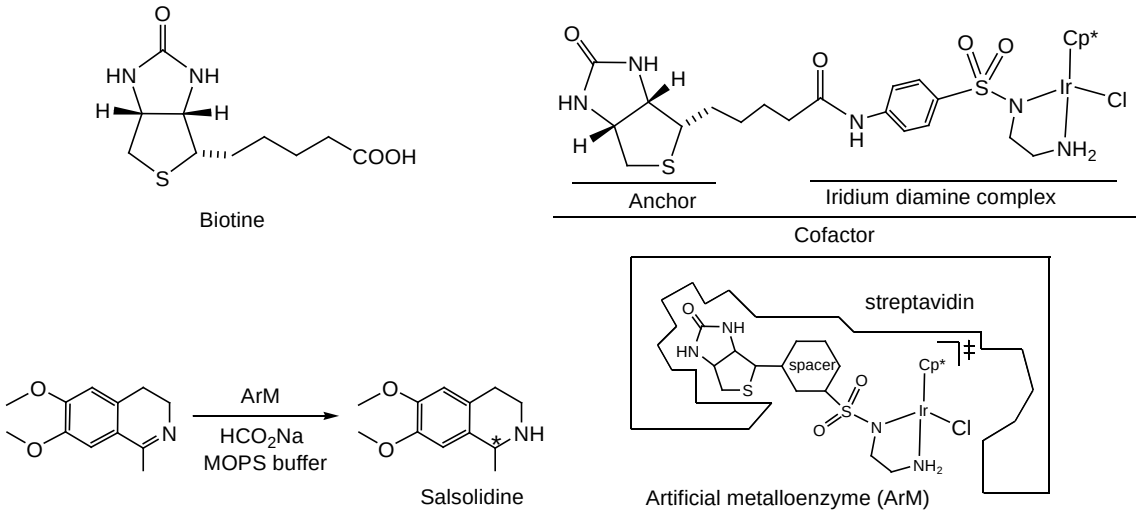

Scheme 15 Transfer hydrogenation of imines catalysed by artificial metalloenzymes

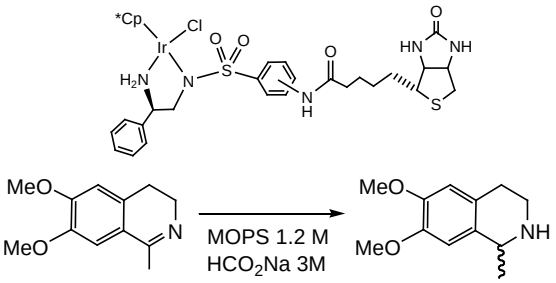

Host protein
Sav WT
S112X
S112R
S112C
S112Y
S112E
S112M
S112Q

Scheme 16 Artificial metalloenzymes for the TH of the salsolidine precursor developed by Rimoldi et al. [123]

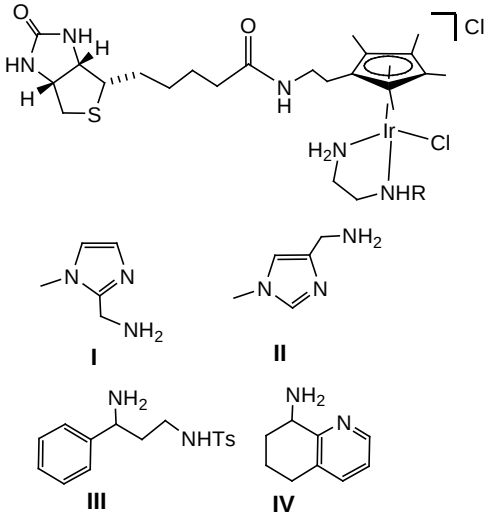

Host protein
Sav WT□S112K
S112Q□ S112W
S112R□ K121R
S112M□ K121M
S112C□ K121H
S112H□ K121F
S112A□ K121A
S112E□ S112Y + K121R
S112T□ S112K + L124E
S112Y□ S112C + K121H

Scheme 17 Artificial metalloenzymes for the TH of imines [124]

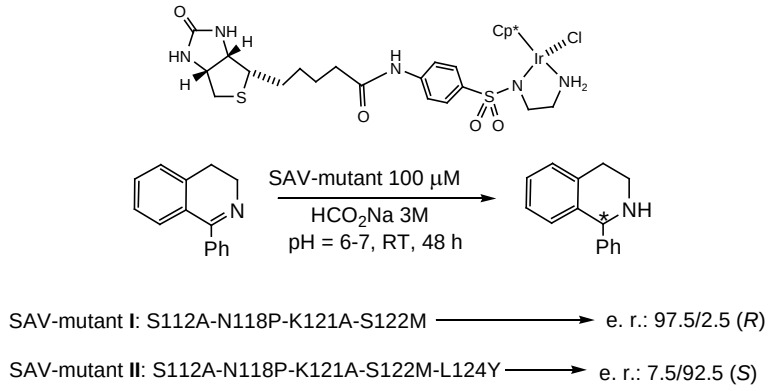

Scheme 18 Observed enantiodivergence with two selected Sav-mutants obtained by directed evolution

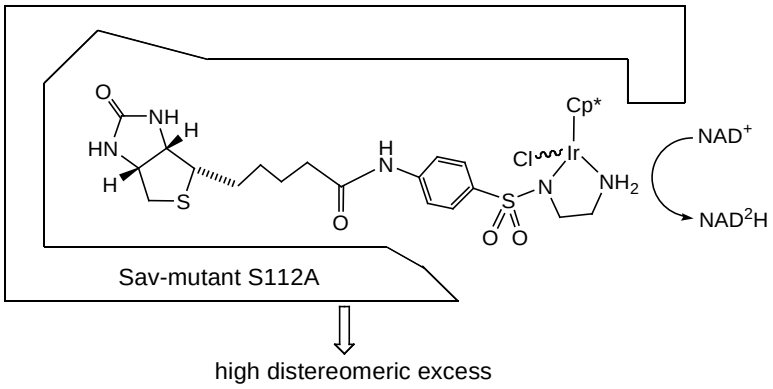

Scheme 19 Diastereoselective reduction of NAD^+

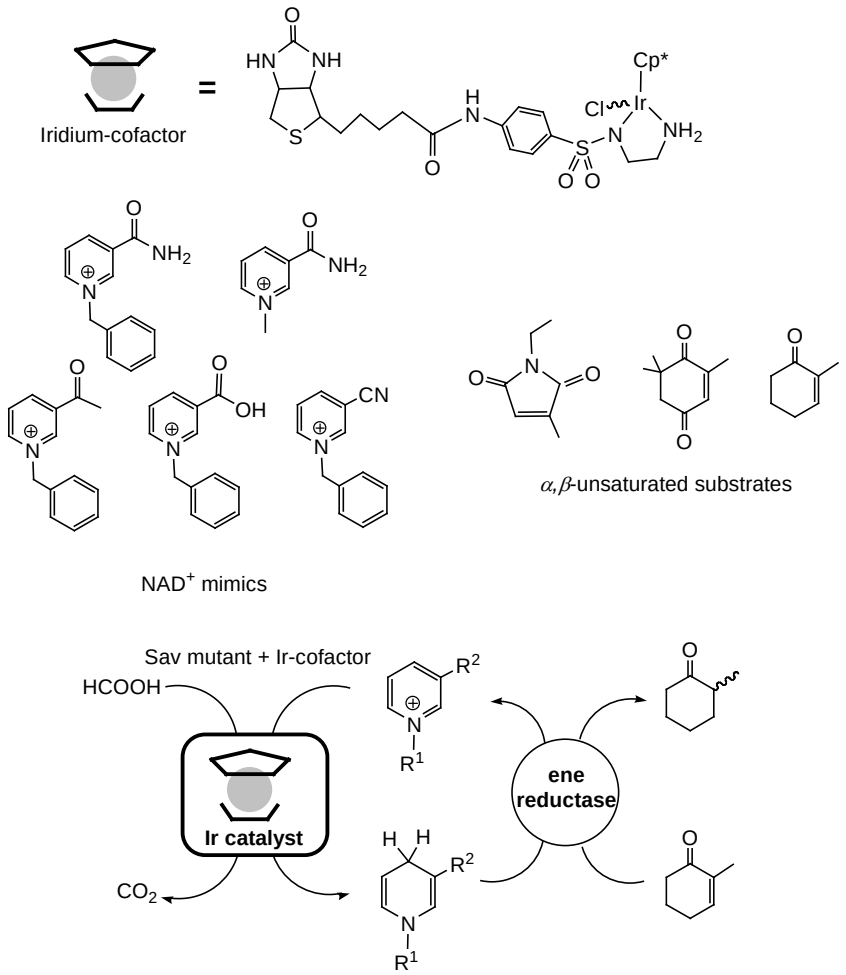

Scheme 20 Reduction of a NAD^+ mimics by the Sav 112K mutant combined with the iridium cofactor shown (top). The reduction is coupled with the enzymatic hydrogenation of an α,β-unsaturated substrate

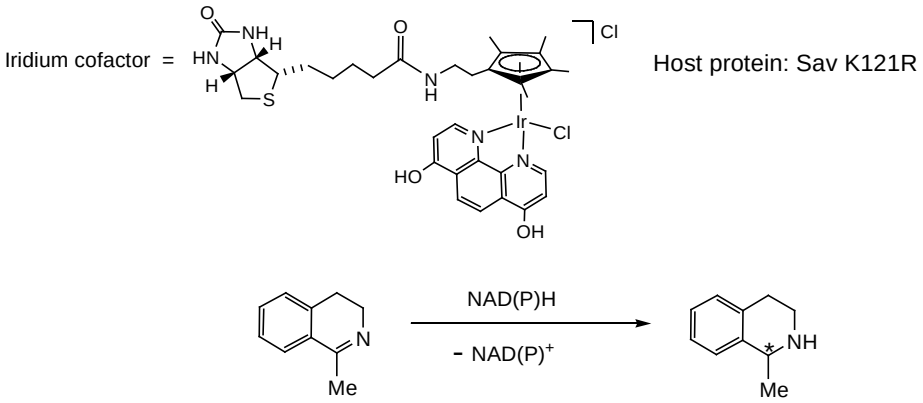

Scheme 21 TH employing NAD(P)H as a hydrogen source. Sav K121R combined with the Ir-cofactor shown (top) was used as catalyst. The glucose dehydrogenase, monoamine oxidase and catalase are not integrated in the Scheme

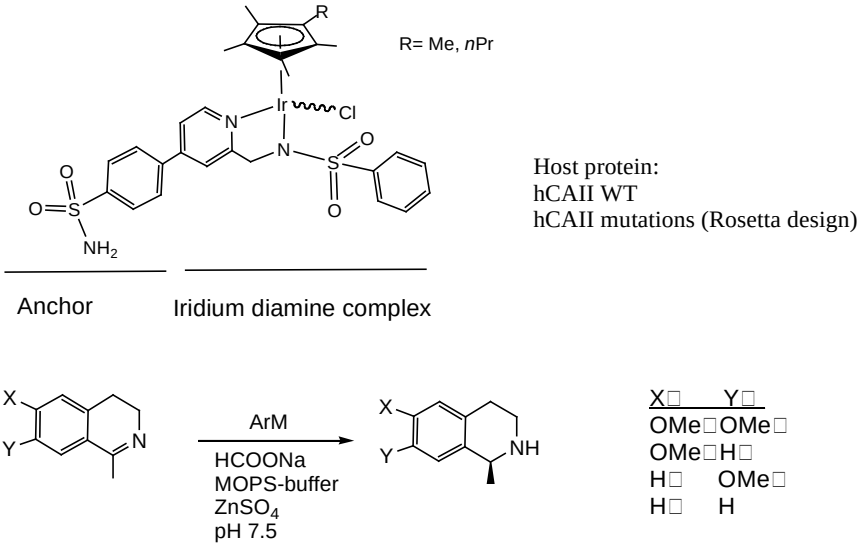

Scheme 22 TH of isoquinolines mediated by ArMs. The Ir-cofactors are shown (top) and the host proteins employed are hCAII WT or mutants computationally designed

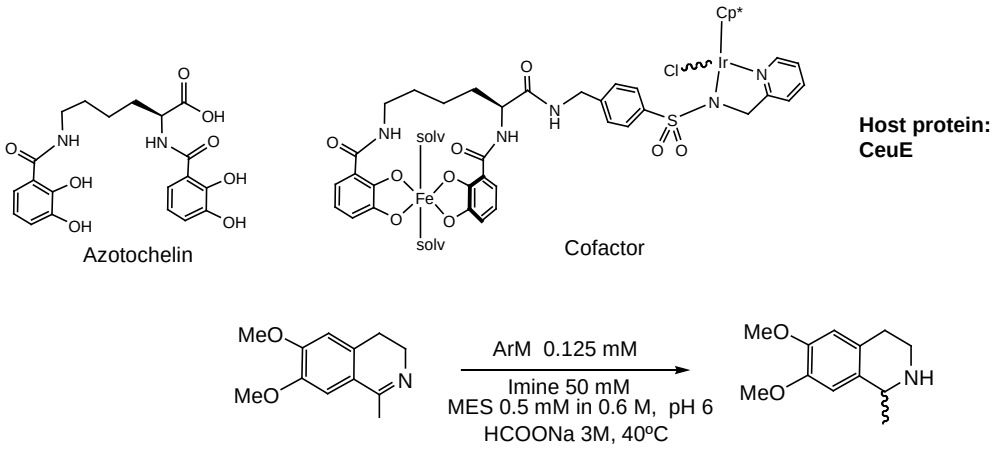

Scheme 23 TH of 1-methyl-6,7-dihydroxy-3,4-dihydroisoquinoline by the ArM formed by combination of the Ir-cofactor and host protein shown at the top

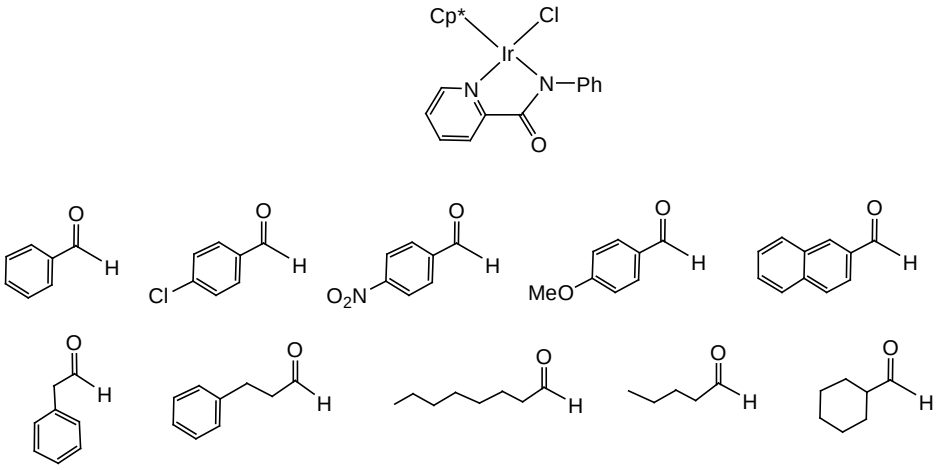

Scheme 24 Iridium catalyst and aldehydes that are hydrogenated. NADH was employed as a hydrogen donor

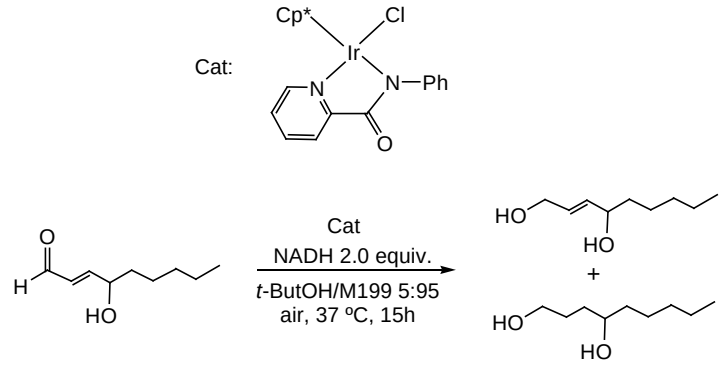

Scheme 25 TH of 4-hydroxynon-2-enal pyridine catalysed by the carboxamidate iridium complex shown. NADH was the H-donor

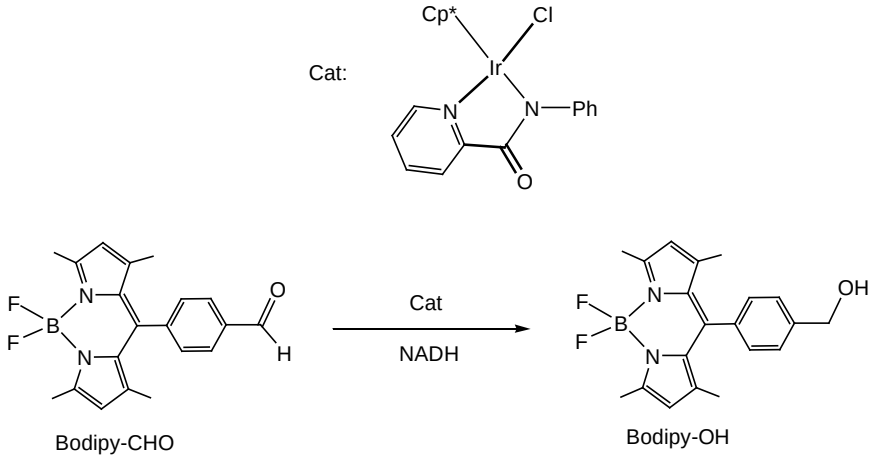

Scheme 26 Reduction of Bodipy-CHO

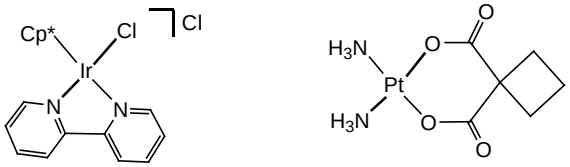

Scheme 27 Bipyridine iridium complex and carboplatin

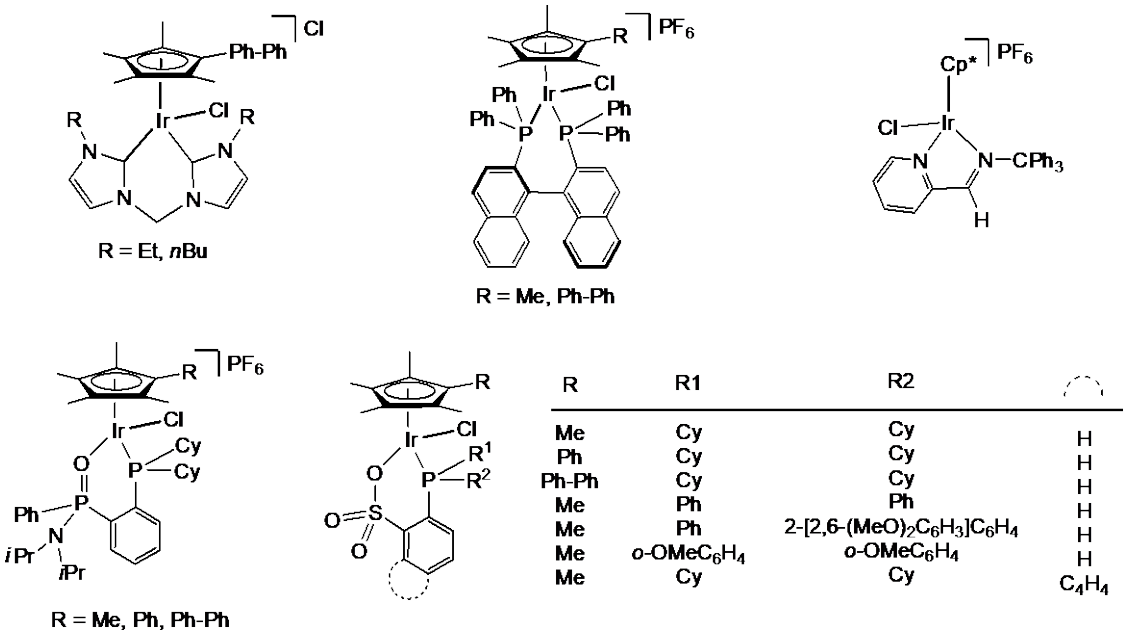

Scheme 28 Iridium complexes with anticancer activity

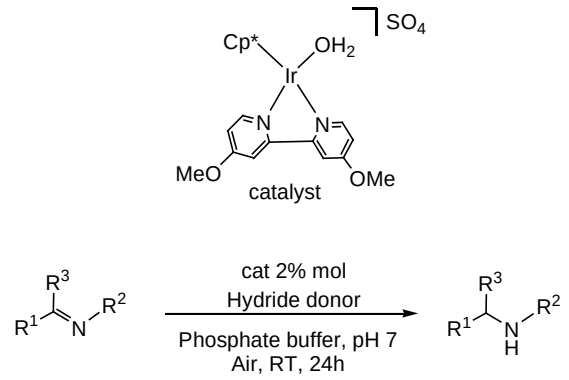

Scheme 29 Reduction of imines with a half-sandwich iridium catalyst with NADH and an NADH mimic as a hydrogen donor

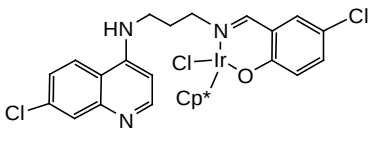

Scheme 30 Quinoline-based half-sandwich organoiridium complex

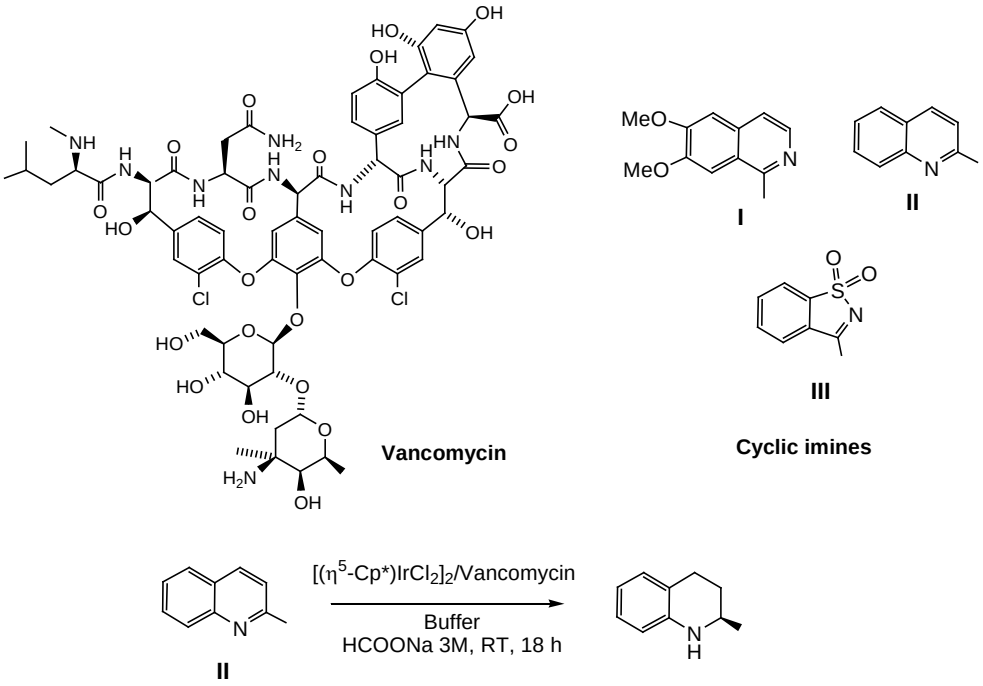

Scheme 31 Structure of vancomycin and application of the [(η^5-Cp*)$IrCl_2$]$_2$/Vancomycin system to the TH of cyclic imines

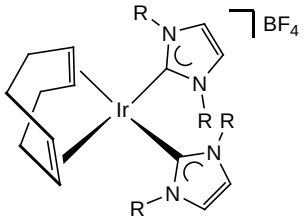

R = Me (**58a**), Et (**58b**), *n*Bu (**58c**)

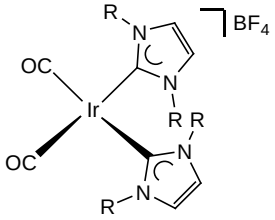

R = Me (**59a**), Et (**59b**), *n*Bu (**59c**)

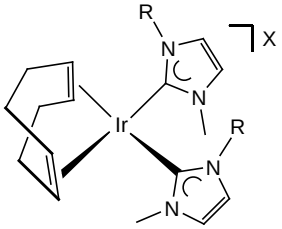

R = 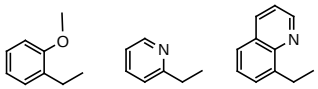

X =	Br **60a**	Br **60b**	Br **60c**
X =	PF_6 **60d**	PF_6 **60e**	

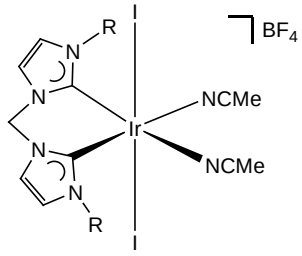

R = Me (**61a**), *n*Bu (**61b**), CH_2-CH_2OPh (**61c**)

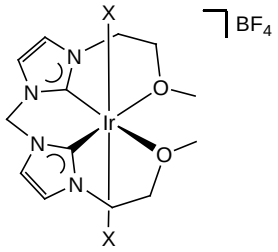

X = I (**61d**), CF_3-COO (**61e**)

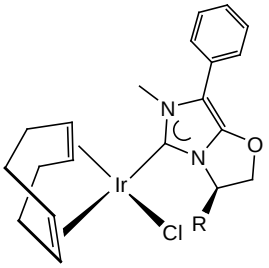

R = *s*Bu (**62a**), *i*Bu (**62b**), *i*Pr (**62c**)

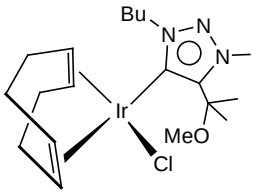

63

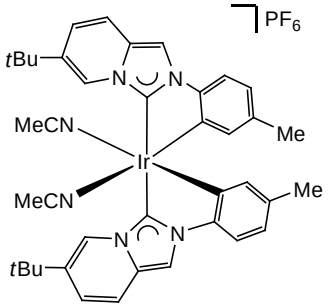

64

Scheme 32 Carbene iridium catalysts (**58**-**64**)

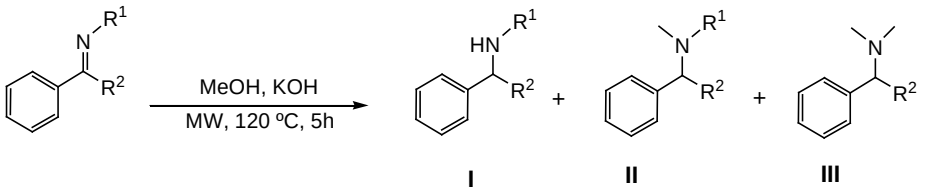

R^1	R^2	Yield (%) I	Yield (%) II	Yield (%) III
Ph	H	>95	>1	--
Bn	H	15	70	--
Me	H	<1	63	--
*n*Bu	H	<1	50	--
H	Ph	20	34	20

Scheme 33 Reduction of imines by catalyst **59a**

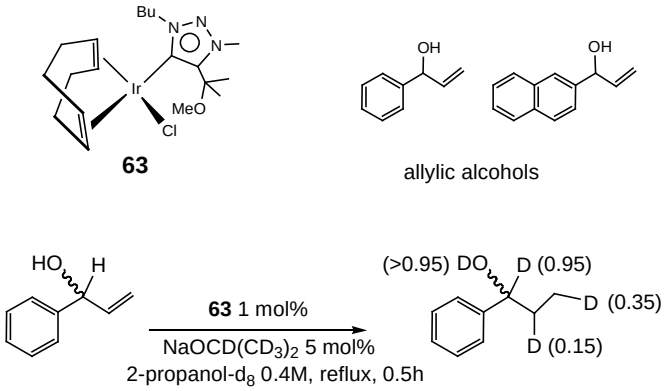

Scheme 34 Deuterium labelling experiments in the reduction of allylic alcohols by complex **63**

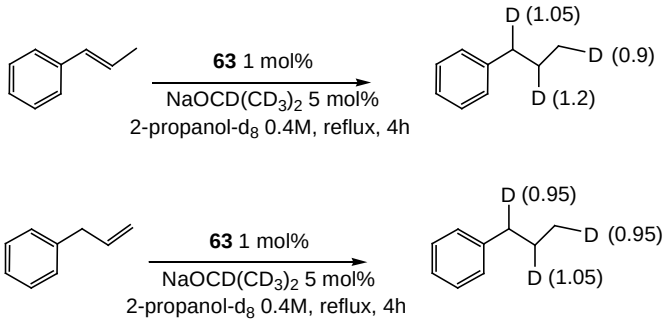

Scheme 35 Deuterium labelling experiments in the reduction of olefins by complex **63**

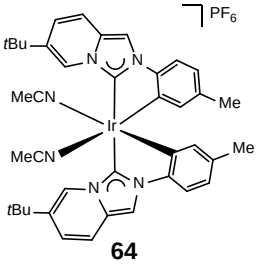

64

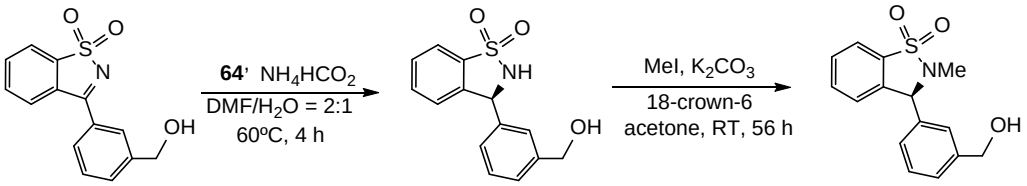

C58 **sultam I**

Scheme 36 Enantioselective synthesis of sultam **I**

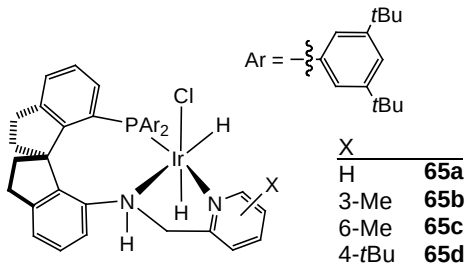

X	
H	**65a**
3-Me	**65b**
6-Me	**65c**
4-*t*Bu	**65d**

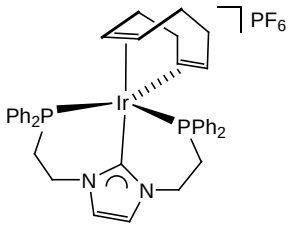

66

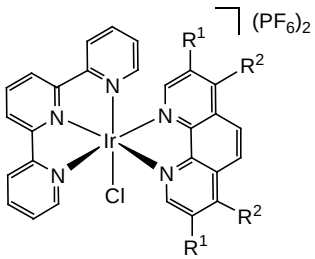

R^1 = R^2 = H (**67a**)
R^1 = H, R^2 = Me (**67b**)
R^1 = R^2 = Me (**67c**)

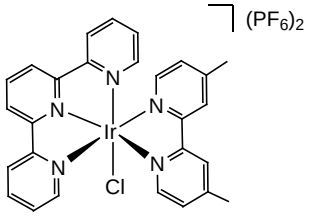

68

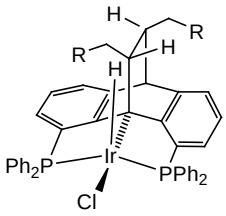

R = NH_2 (**69a**), OMe (**69b**)

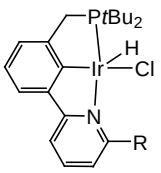

R = H (**70a**), *t*Bu (**70b**)

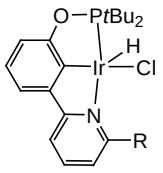

R = H (**71a**), *t*Bu (**71b**)

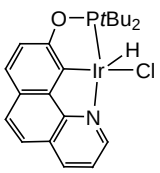

72

Scheme 37 Pincer iridium TH catalysts (**65-72**)

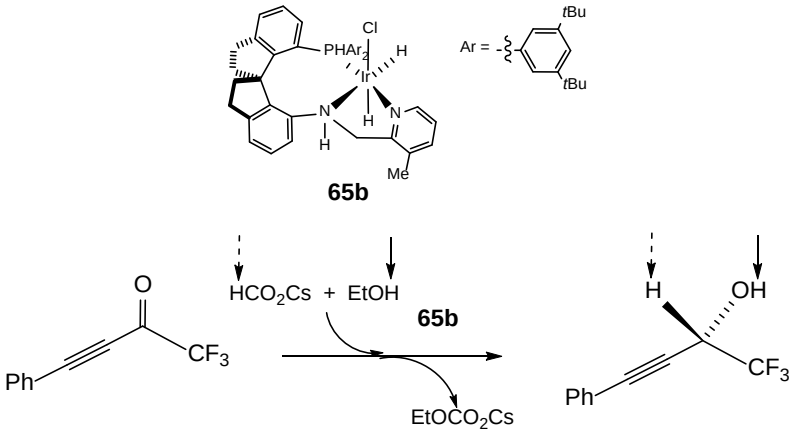

Scheme 38 Transfer hydrogenation of ketone **B126** with HCO_2Cs in EtOH

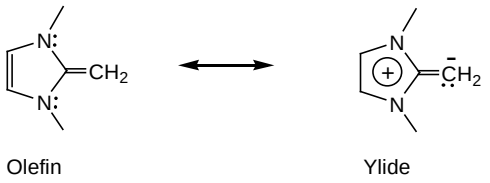

Scheme 39 Resonance structures of *N*-heterocyclic olefins

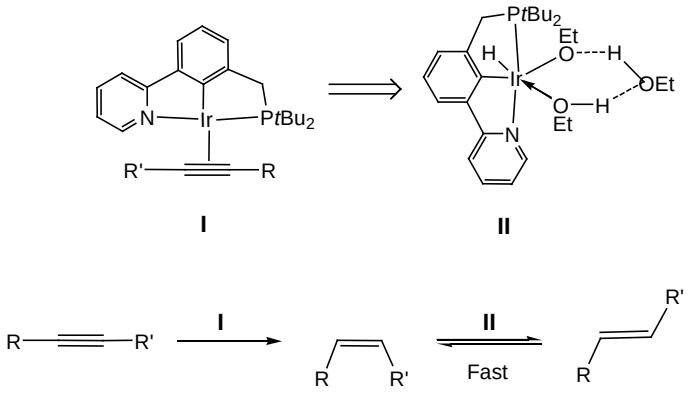

Scheme 40 Selective TH of alkynes to *E*-alkenes with EtOH

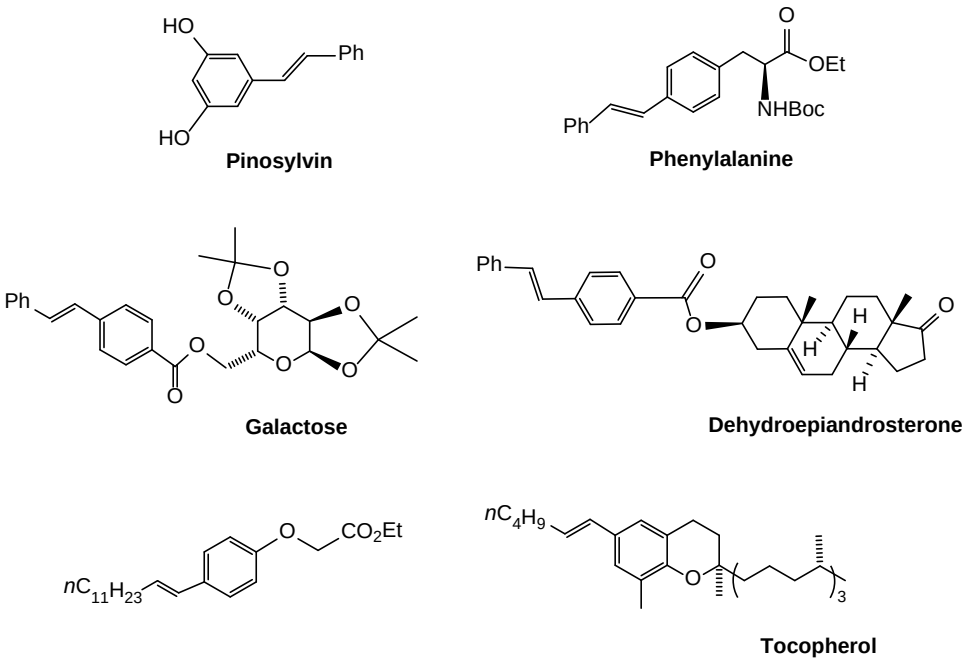

Scheme 41 Alkenes containing biologically active skeletons

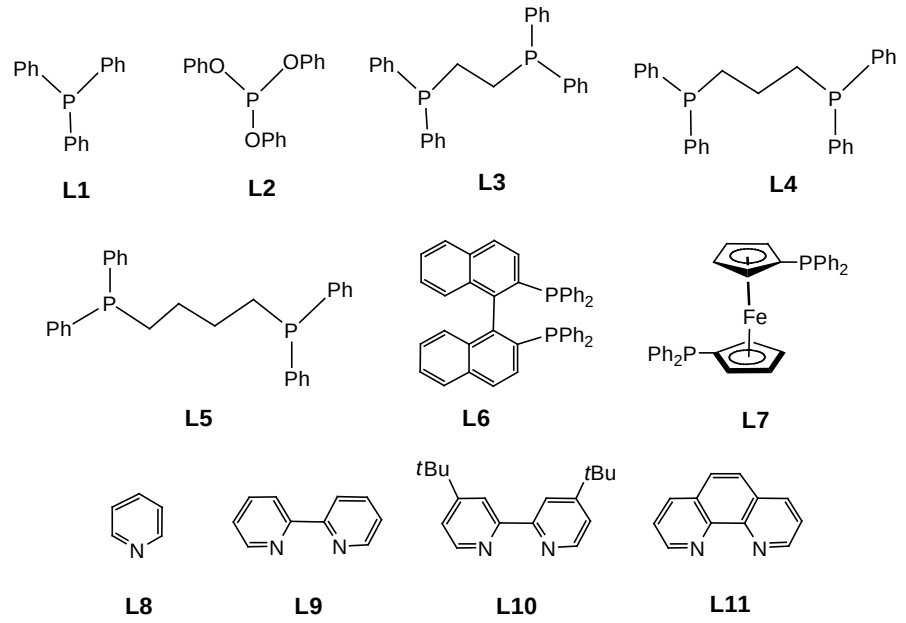

Scheme 42 Phosphorus and nitrogen donor ligands employed in combination with $[IrCl(COD)]_2$ in the TH of ketones

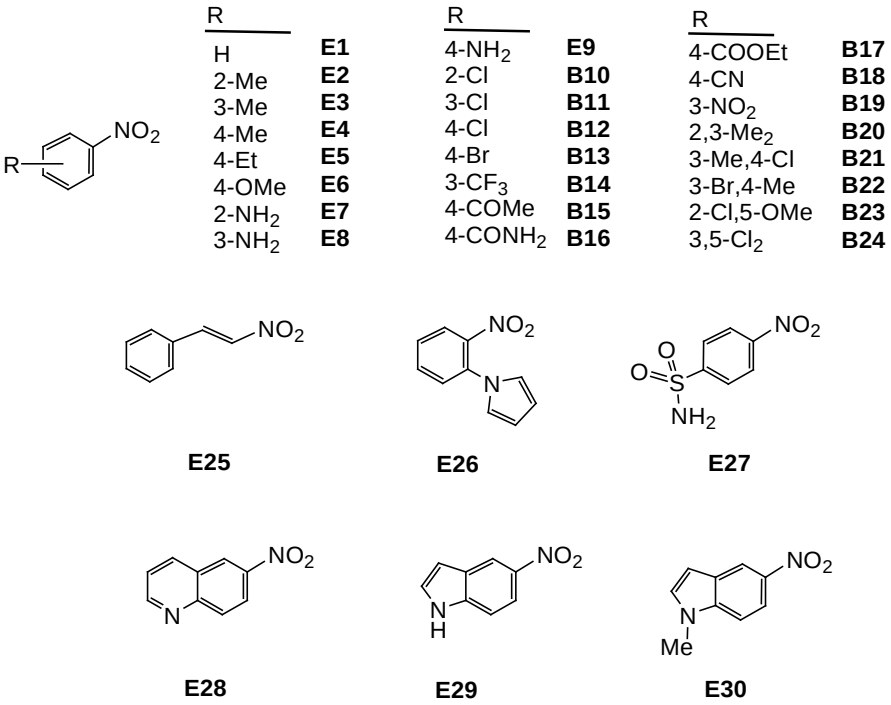

Scheme 43 Nitroarenes

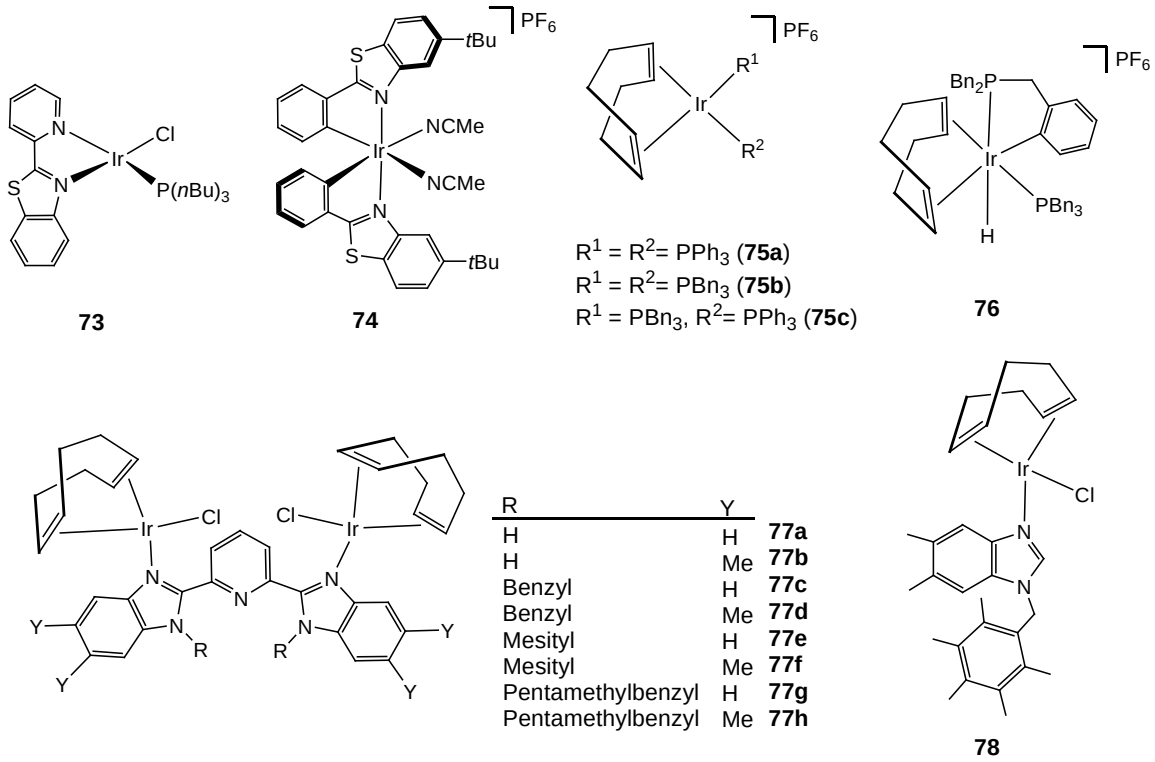

Scheme 44 Other iridium complexes employed as TH catalysts (**73**-**78)**

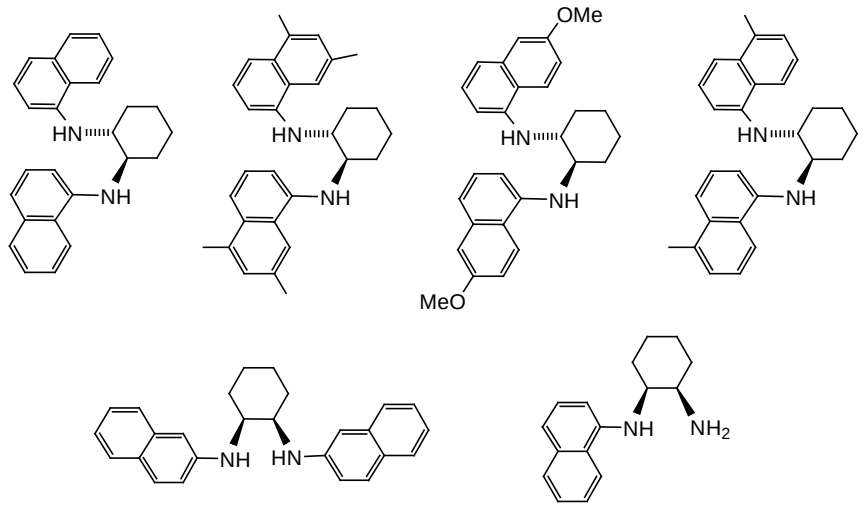

Scheme 45 Chiral amine ligands employed in combination with $[IrCl(COD)]_2$ in the TH of ketones

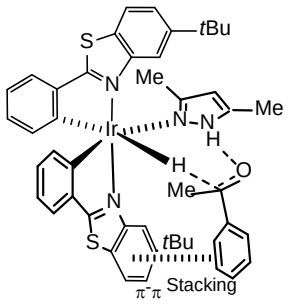

Scheme 46 Proposed transition state state for the TH of ketones catalysed by complex **74**

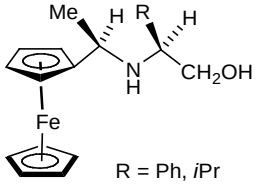

Scheme 47 Chiral ferrocenyl amino alcohols employed in combination with $[IrCl(COD)]_2$ in the TH of ketones

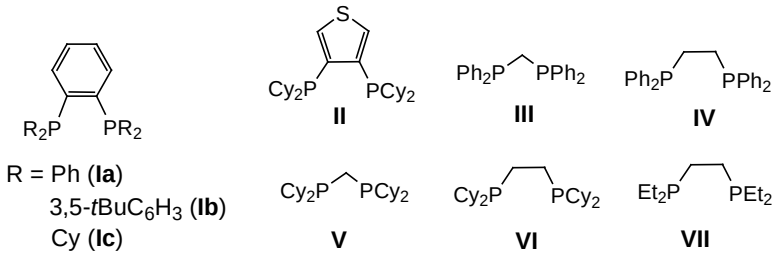

Scheme 48 Investigated diphosphines employed in combination with $[IrCl(COD)]_2$ in the TH of alkenes and alkynes

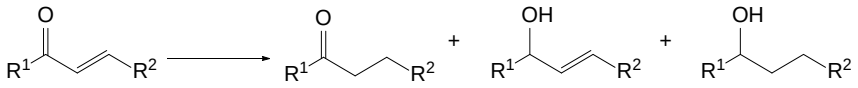

Scheme 49 Partial and complete reduction of α,β-unsaturated carbonyl compounds

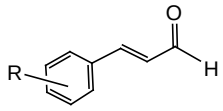

R		R	
H	**F1**	4-F	**F7**
3-Me	**F2**	2-Cl	**F8**
4-Me	**F3**	3-Cl	**F9**
2-OMe	**F4**	4-Cl	**F10**
4-OMe	**F5**	4-Br	**F11**
4-NMe_2	**F6**	2-NO_2	**F12**

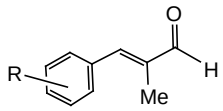

R		R	
H	**F13**	2-OMe	**F17**
2-Me	**F14**	3-OMe	**F18**
3-Me	**F15**	4-OMe	**F19**
4-Me	**F16**	4-Cl	**F20**

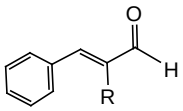

R	
Et	**F21**
*n*Pen	**F22**
*n*Hex	**F23**
Cy	**F24**

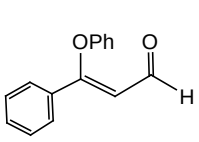

F25

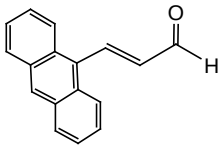

F26

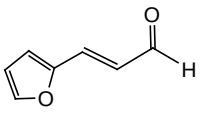

F27

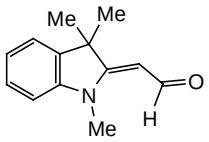

F28

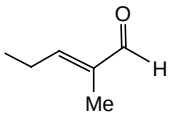

F29

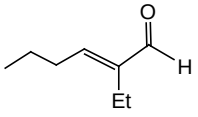

F30

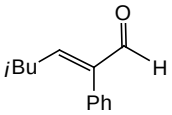

F31

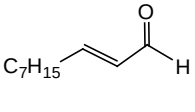

F32

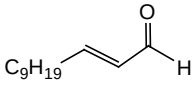

F33

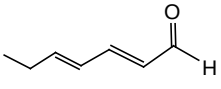

F34

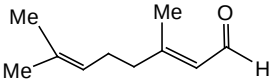

F35

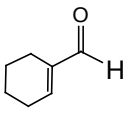

F36

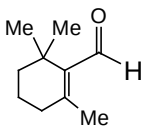

F37

Scheme 50 α,β-Unsaturated aldehydes

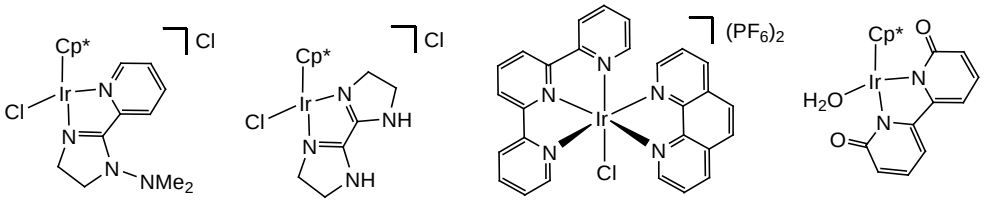

55h **57a** **67a** **79**

Scheme 51 Catalysts for the reduction of α,β-unsaturated aldehydes

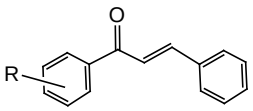

R		R	
H	**G1**	3,4-Me_2	**G7**
2-Me	**G2**	4-F	**G8**
4-Me	**G3**	3-Cl	**G9**
4-*t*Bu	**G4**	4-Cl	**G10**
2-OMe	**G5**	4-Br	**G11**
4-OMe	**G6**		

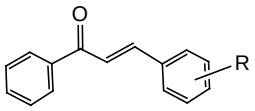

R		R	
4-Me	**G12**	2-CF_3	**G15**
4-OMe	**G13**	3-CF_3	**G16**
4-Cl	**G14**	4-CF_3	**G17**

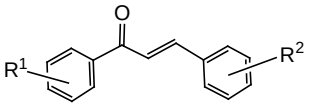

R^1	R^2		R^1	R^2	
2-Me	2-Me	**G18**	4-*t*Bu	2-Me	**G20**
4-Me	4-*t*Bu	**G19**	4-Cl	2-CF_3	**G21**

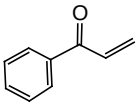

G22

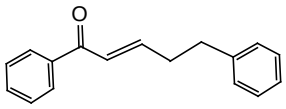

G23

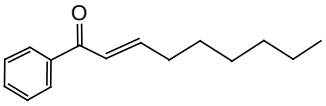

G24

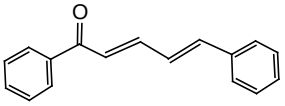

G25

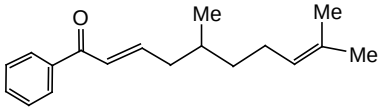

G26

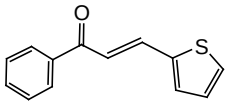

G27

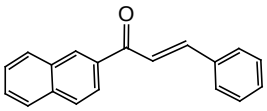

G28

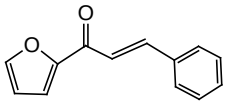

G29

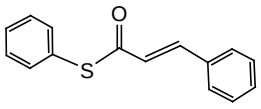

G30

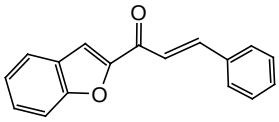

G31

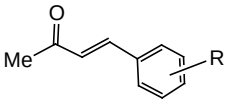

R		R	
H	**G32**	4-F	**G36**
2-Me	**G33**	4-Cl	**G37**
4-OMe	**G34**	4-CF_3	**G38**
4-SMe	**G35**		

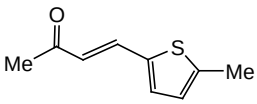

G39

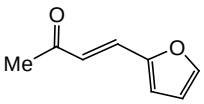

G40

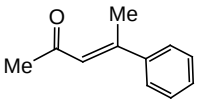

G41

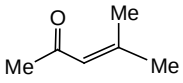

G42

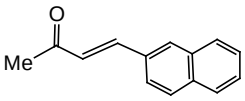

G43

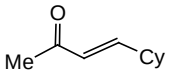

G44

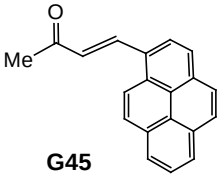

G45

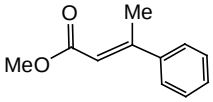

G46

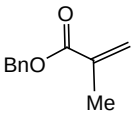

G47

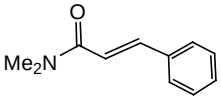

G48

G49

G50

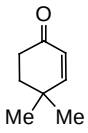

G51

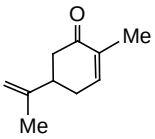

G52

Scheme 52 α,β-Unsaturated ketones

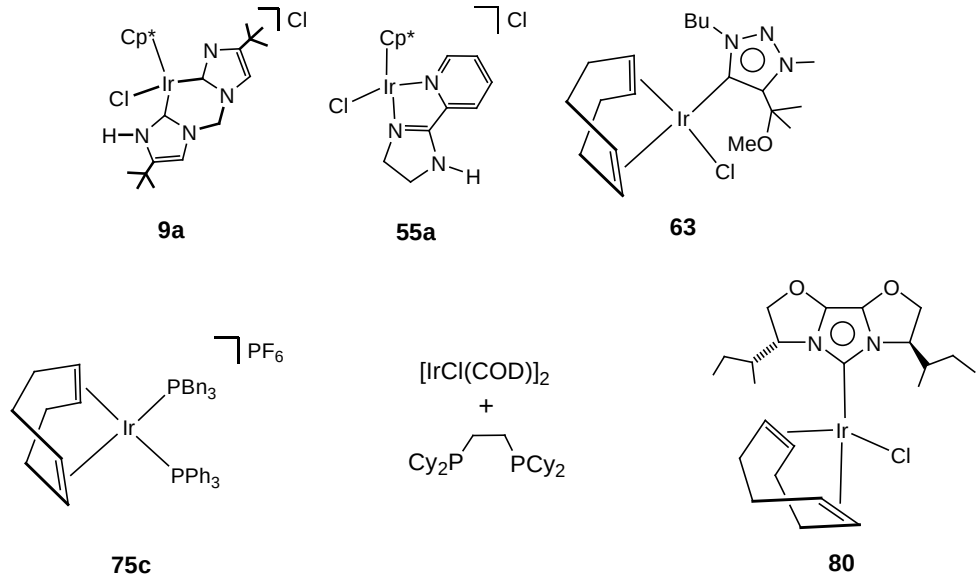

9a **55a** **63**

75c **80**

Scheme 53 Catalysts for the reduction of α,β-unsaturated ketones

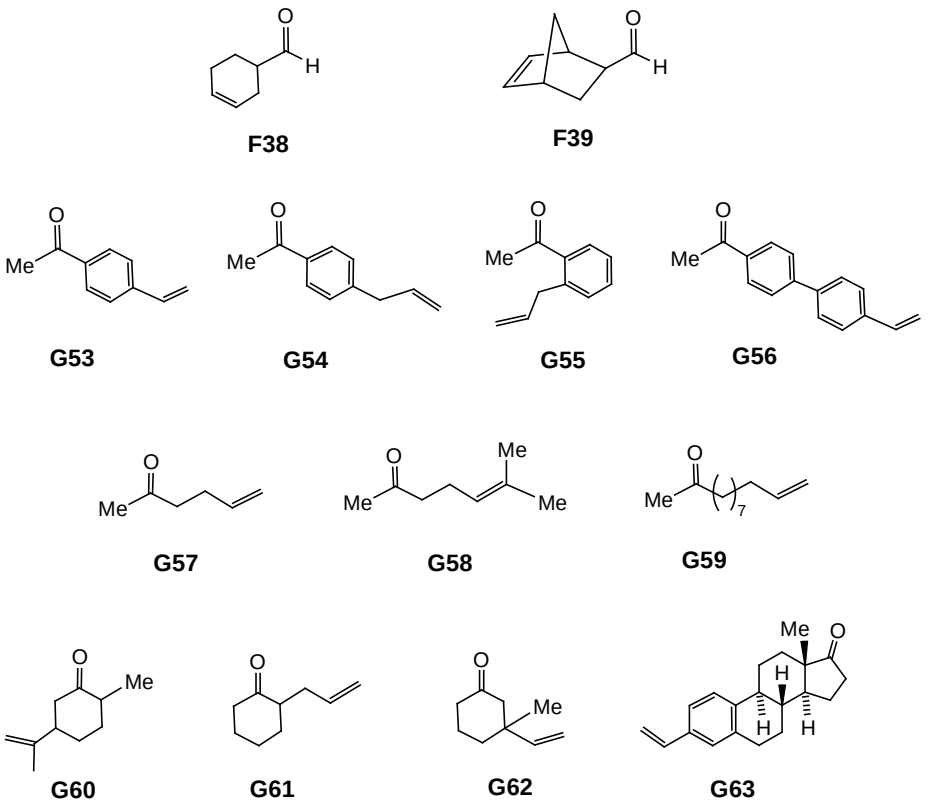

F38 **F39**

G53 **G54** **G55** **G56**

G57 **G58** **G59**

G60 **G61** **G62** **G63**

Scheme 54 Non-conjugated unsaturated aldehydes and ketones

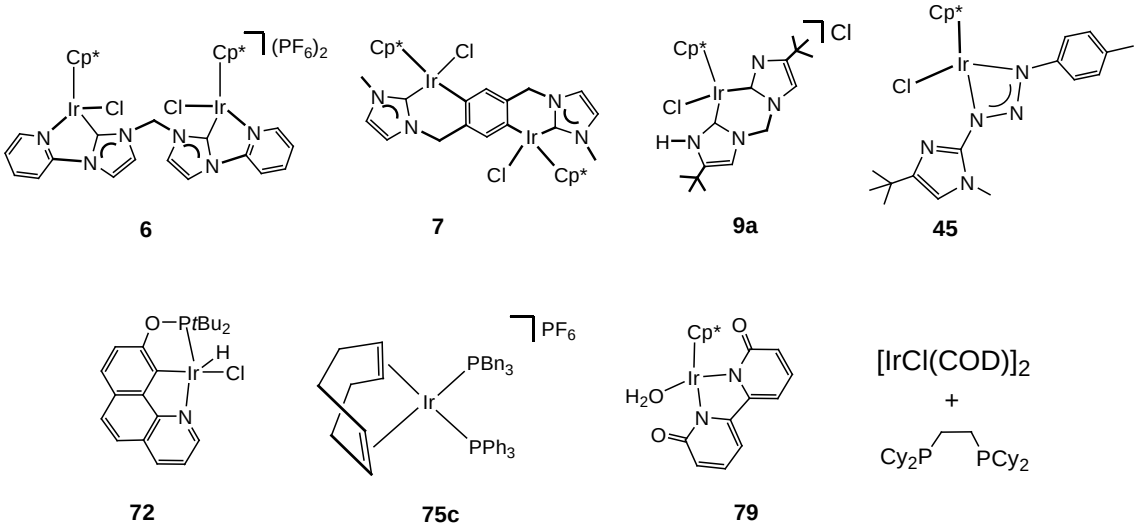

Scheme 55 Catalysts for the reduction of non-conjugated unsaturated aldehydes and ketones

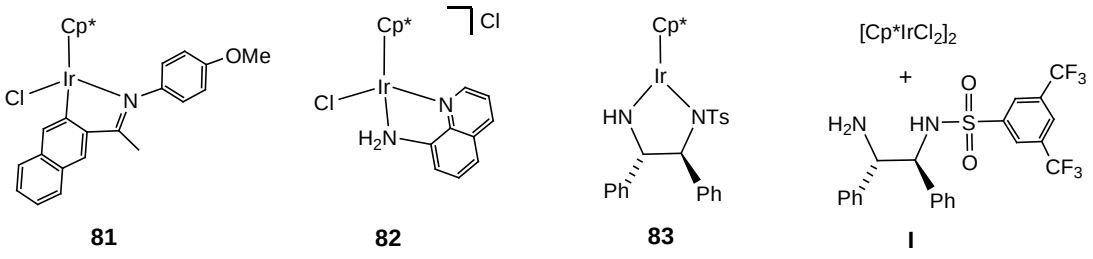

Scheme 56 Iridium complexes for the reduction of *N*-heterocycles

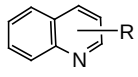

R	
H	**H1**
2-Me	**H2**
3-Me	**H3**
4-Me	**H4**
2-Ph	**H5**

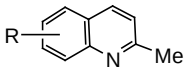

R		R	
6-Me	**H6**	6-CONEt$_2$	**H13**
6-OMe	**H7**	6-F	**H14**
6-OBn	**H8**	6-Cl	**H15**
6-OAllyl	**H9**	6-Br	**H16**
6-NHBoc	**H10**	7-F	**H17**
6-COOH	**H11**	8-Cl	**H18**
6-COOMe	**H12**	6-CF$_3$	**H19**

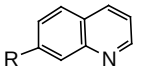

R	
Me	**H20**
Cl	**H21**

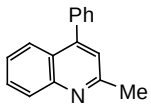

H22

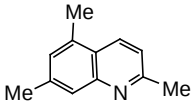

H23

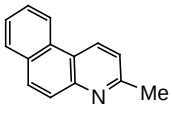

H24

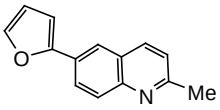

H25

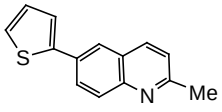

H26

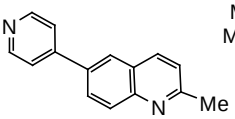

H27

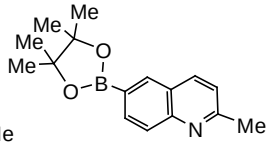

H28

Scheme 57 Quinolines

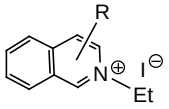

R	
H	**H29**
1-Me	**H30**
3-Me	**H31**
6-Me	**H32**
6-Br	**H33**

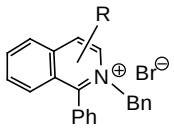

H34

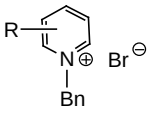

R		R	
2-Ph	**H35**	3-COOEt	**H40**
2-C(Ph)$_2$OH	**H36**	4-Bn	**H41**
2-CH$_2$NHCbz	**H37**	4-CF$_3$	**H42**
6-CH$_2$NHBoc	**H38**	4-COOEt	**H43**
6-*p*-C$_6$H$_4$(OMe)	**H39**	3,4-Me$_2$	**H44**

Scheme 58 Isoquinolinium and pyridinium

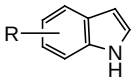

R	
H	**H63**
5-OMe	**H64**
5-Br	**H65**

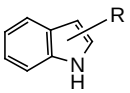

R	
2-Me	**H66**
3-Me	**H67**
2-Ph	**H68**

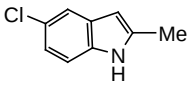

H69

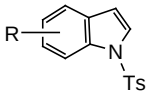

H70

Scheme 59 Indoles

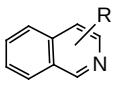

R	
H	**H45**
4-CO_2Et	**H46**
3-Ph,4-CO_2Et	**H47**

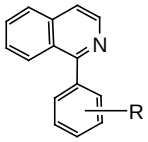

R		R	
H	**H48**	3-CF_3	**H53**
2-Me	**H49**	4-CF_3	**H54**
4-Me	**H50**	4-COOMe	**H55**
4-OMe	**H51**	4-NO_2	**H56**
4-Br	**H52**	3,4,5-$(OMe)_3$	**H57**

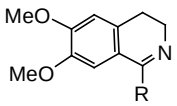

R		R	
Me	**H58**	4-$(OMe)C_6H_4CH_2$	**H61**
Ph	**H59**	3,4-$(OMe)_2C_6H_3CH_2$	**H62**
2,3,4,5-$(OMe)_4C_6H$	**H60**		

Scheme 60 Isoquinolines and dehydroisoquinolines

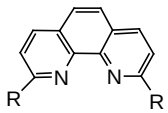

R		R	
H	**H71**	*n*Bu	**H76**
Me	**H72**	*i*Bu	**H77**
Et	**H73**	*t*Bu	**H78**
*n*Pr	**H74**	*n*-C_6H_{13}	**H79**
*i*Pr	**H75**	Ph	**H80**

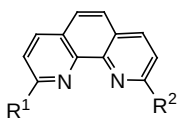

R^1	R^2		R^1	R^2	
Et	H	**H81**	*t*Bu	H	**H86**
*n*Pr	H	**H82**	*n*-C_6H_{13}	H	**H87**
*i*Pr	H	**H83**	Ph	H	**H88**
*n*Bu	H	**H84**	*i*Bu	Me	**H89**
*i*Bu	H	**H85**			

Scheme 61 Phenanthrolines

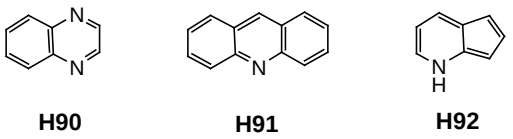

H90 **H91** **H92**

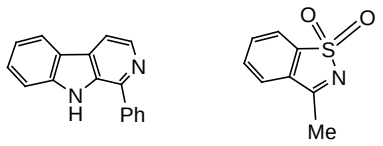

H93 **H94**

Scheme 62 Other *N*-heterocycles

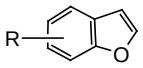

R	
H	**H95**
6-Me	**H96**
5-*t*Bu	**H97**
5-OMe	**H98**

Scheme 63 Benzofurans

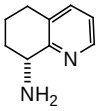

Scheme 64 Chiral diamine (*S*)-CAMPY

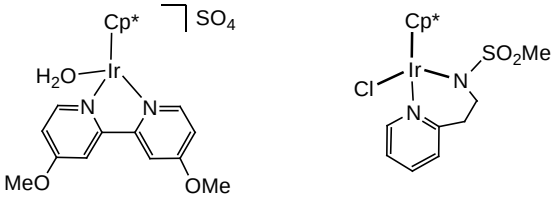

84 **28**

Scheme 65 Iridium catalysts for the TH of levulinic acid

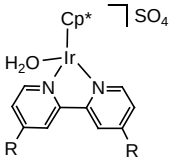

R = H **(85a)**, CH_2Ph **(85b)**, $CH(CH_3)Ph$ **(85c)**

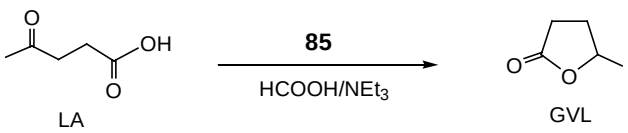

LA GVL

Scheme 66 Transfer hydrogenation of levulinic acid

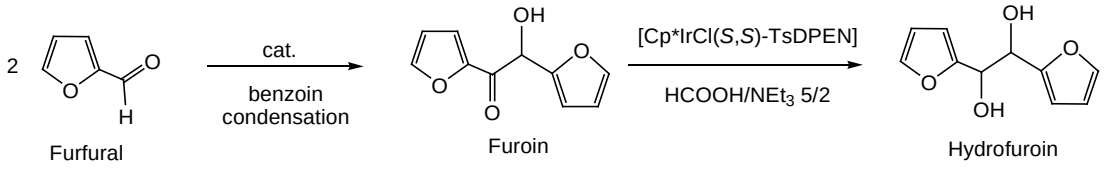

Scheme 67 Two steps synthesis of hydrofuroin from furfural

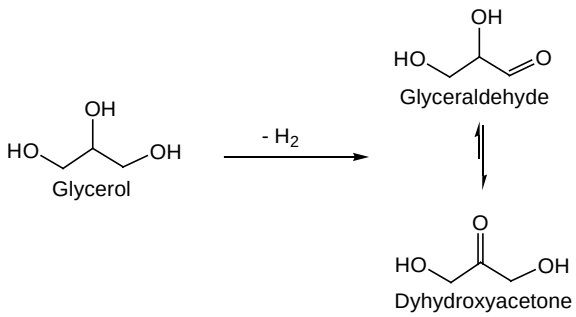

Scheme 68 Dehydrogenation of glycerol

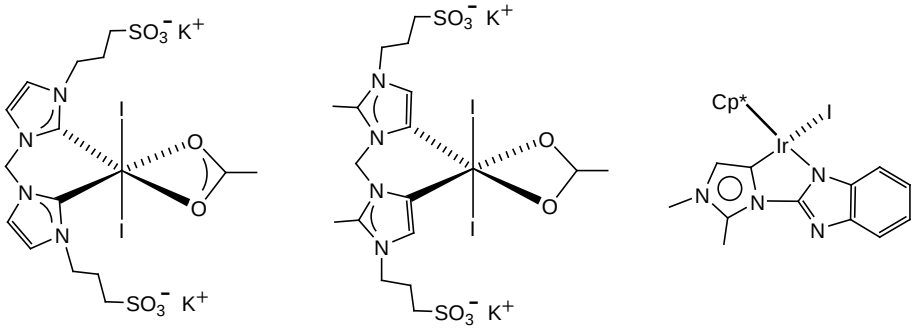

Scheme 69 Iridium catalysts used in TH from biomass-derived H-donors

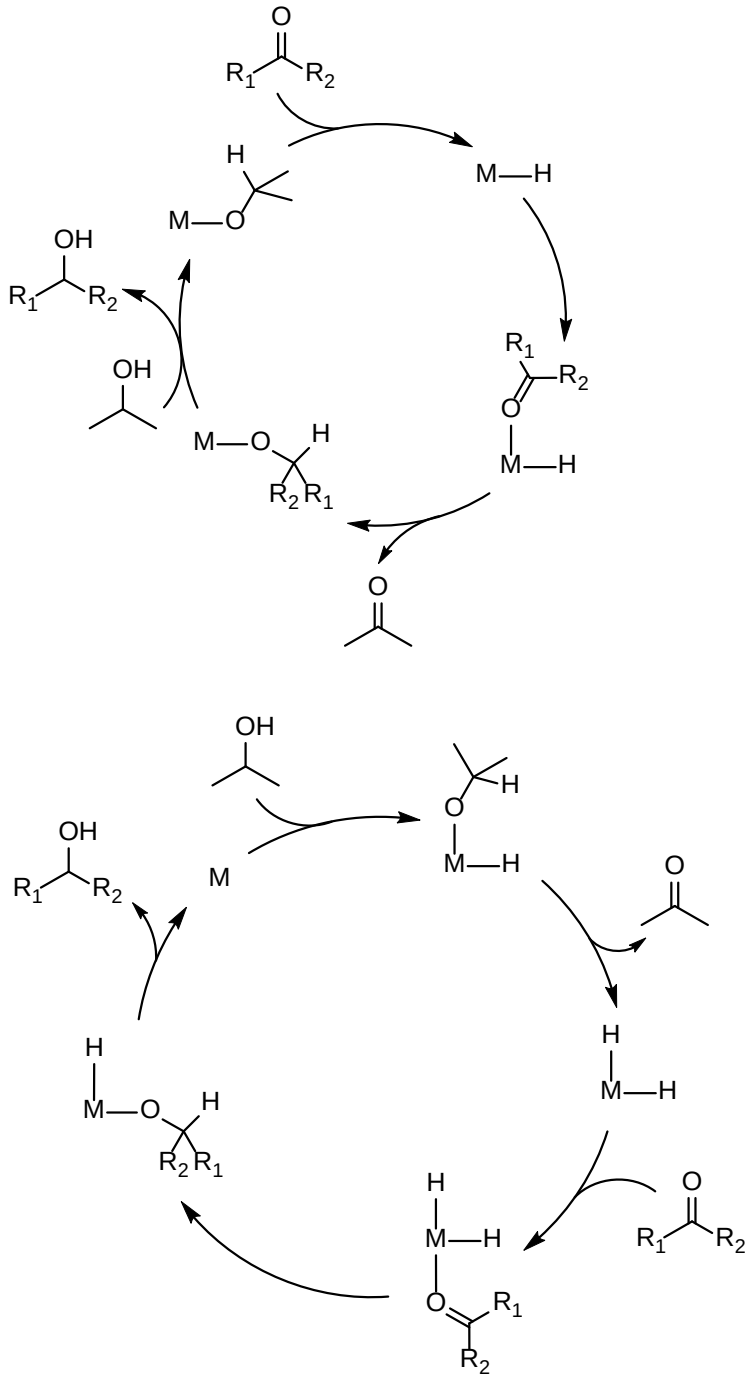

Scheme 70 Metal monohydride (*top*) and metal dihydride routes (*bottom*) for the TH of carbonyl compounds using 2-propanol as the hydrogen donor

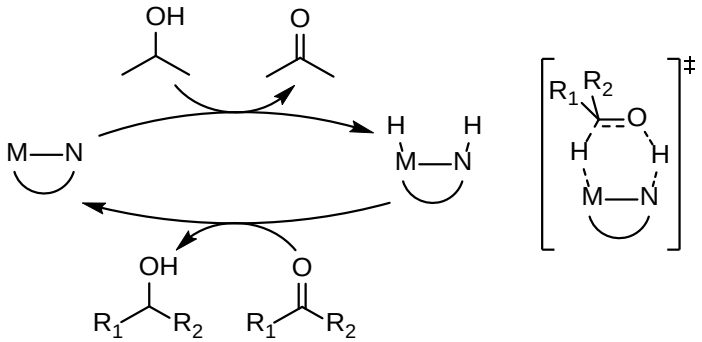

Scheme 71 Metal-ligand bifunctional mechanism for the TH of carbonyl compounds using 2-propanol as the hydrogen donor (*left*) and the transition state for the concerted transfer of the two hydrogen atoms from the metal-ligand platform to the substrate (*right*)

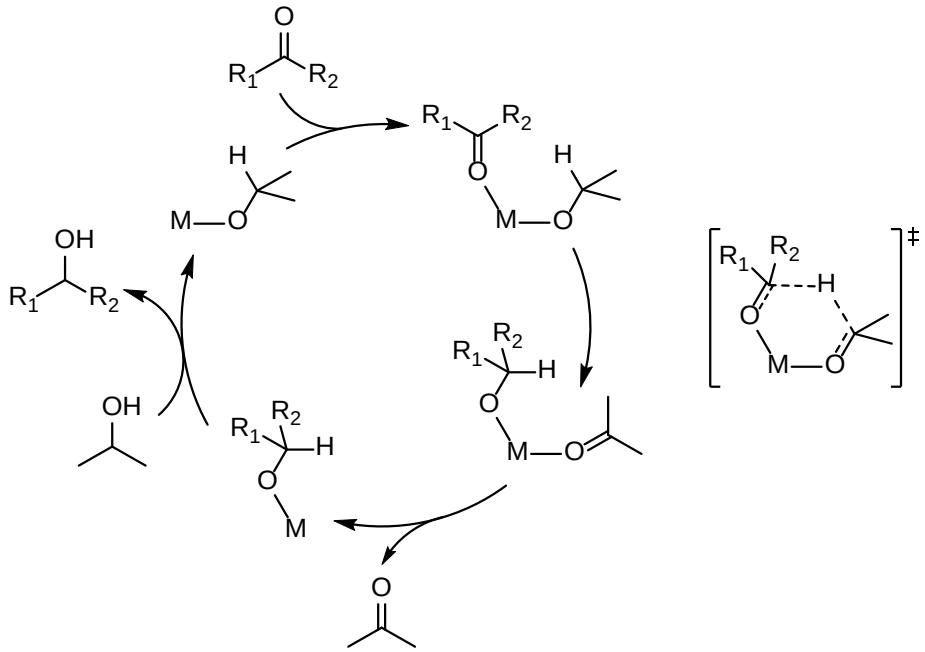

Scheme 72 Meerwein-Ponndorf-Verley mechanism of the TH of carbonyl compounds using 2-propanol as the hydrogen donor (*left*) and the transition state of the direct hydrogen transfer (*right*)

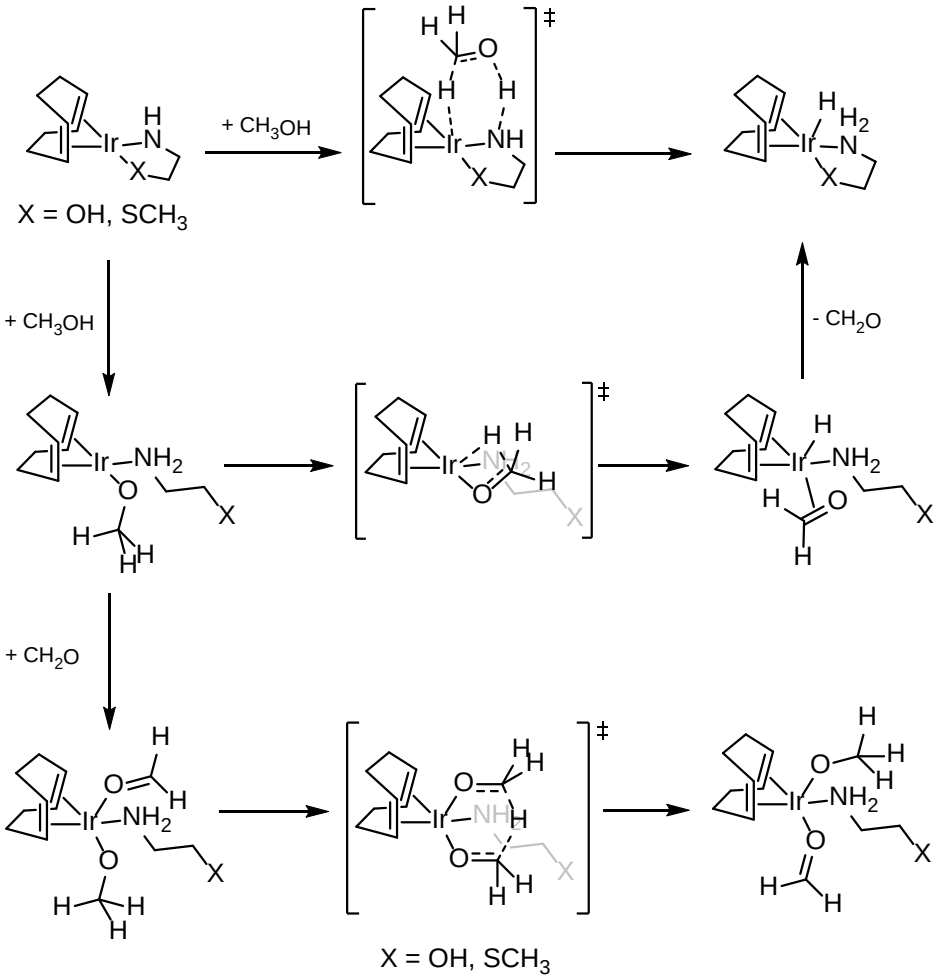

Scheme 73 Intermediates and transition states for the TH catalysed by Ir(cod)(HL) (HL = 2-amino ethanol, 2-aminoethylmethylsulfide) [239]

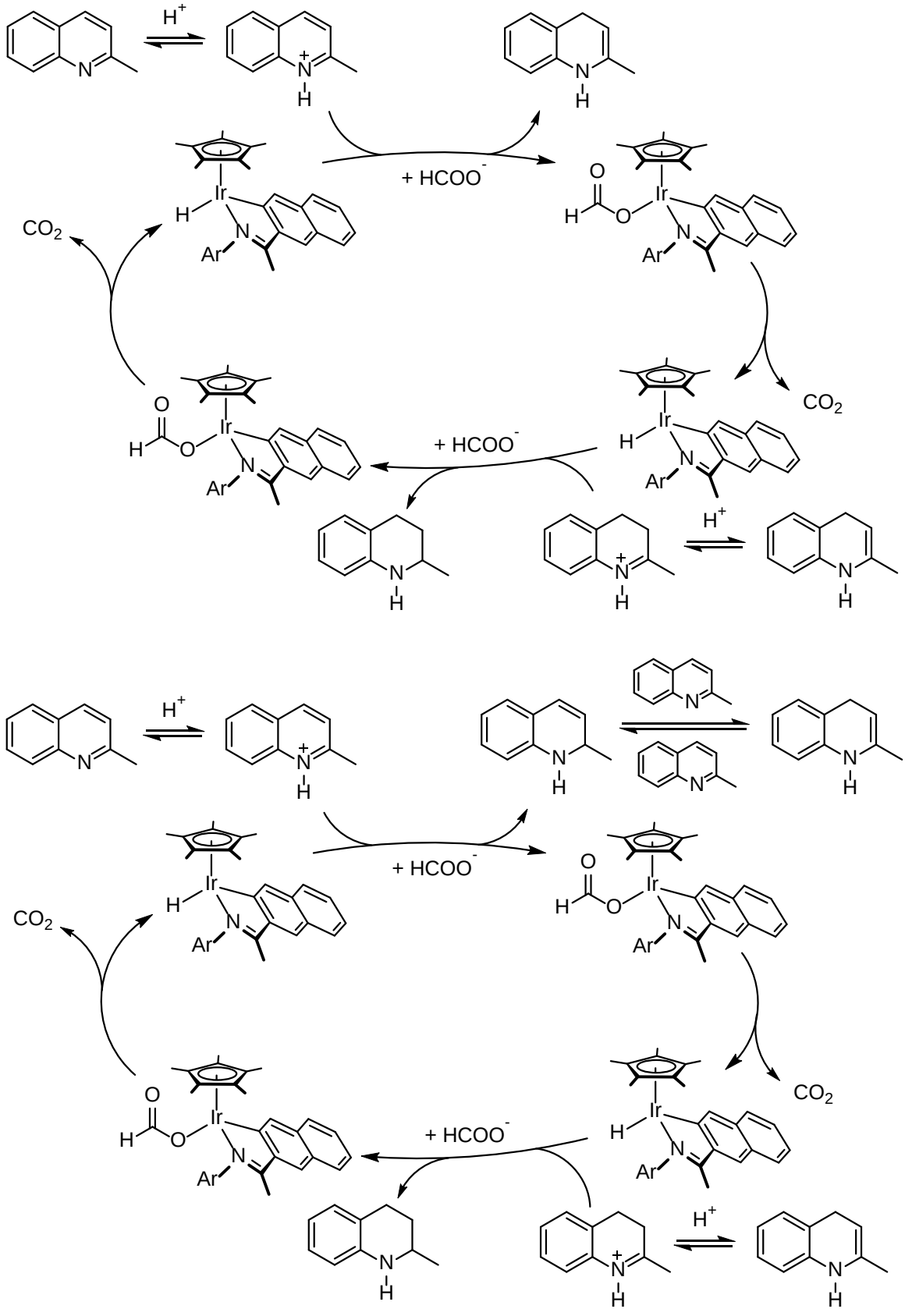

Scheme 74 Catalytic cycle proposed by Xiao [212] for the TH of *N*-heterocycles: 1,4-addition (*top*), 1,2-addition (*bottom*)

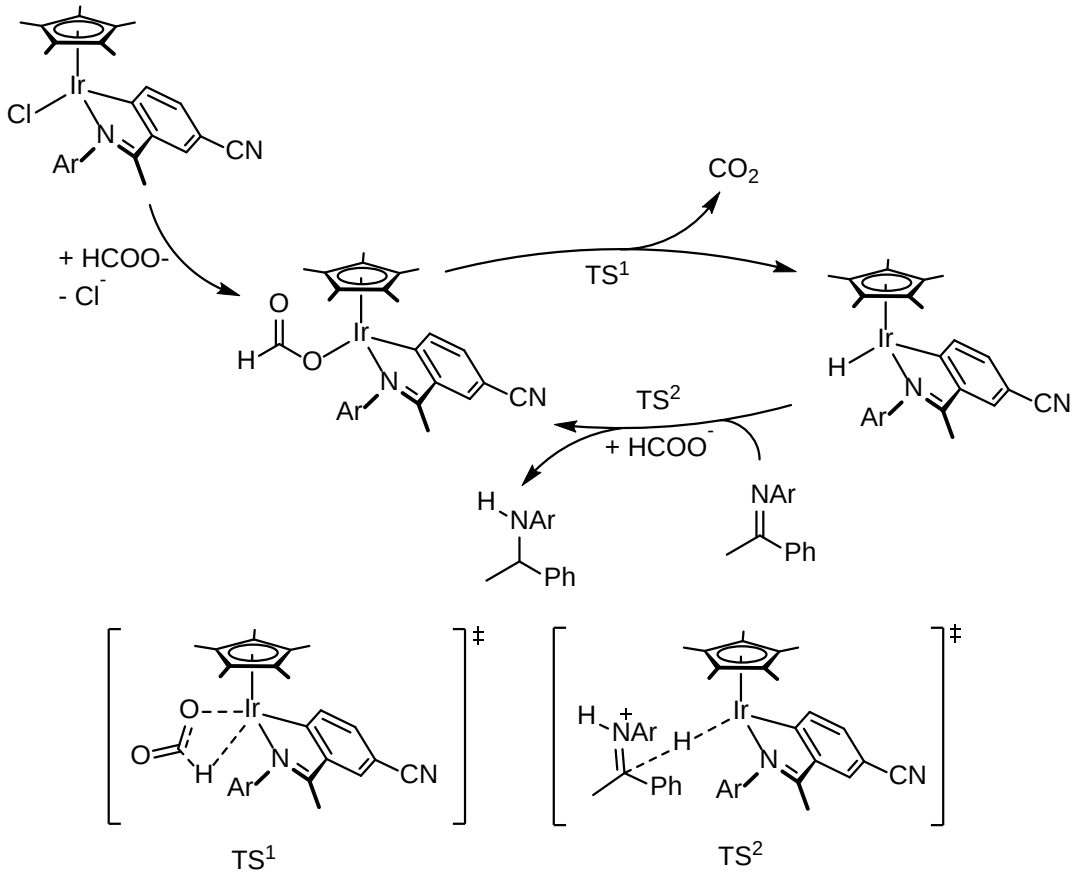

Scheme 75 Catalytic cycle and transition states proposed by Xiao [240] for the TH of imine catalysed by iridacycles using formic acid as the hydrogen donor

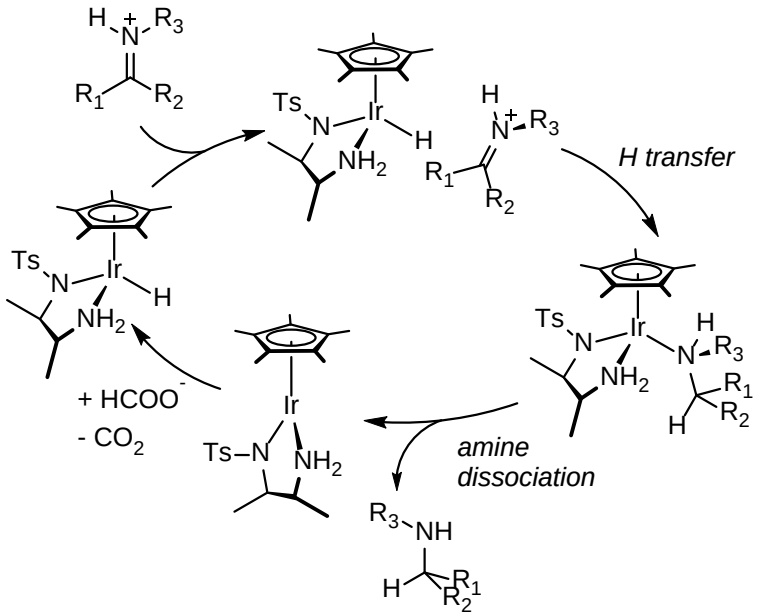

Scheme 76 Catalytic cycle proposed by Stirling [241] for the TH of imines catalysed by an iridium CATHy catalyst. The rate determining steps (RDS) for the formation of the *R* and *S* enantiomers are indicated

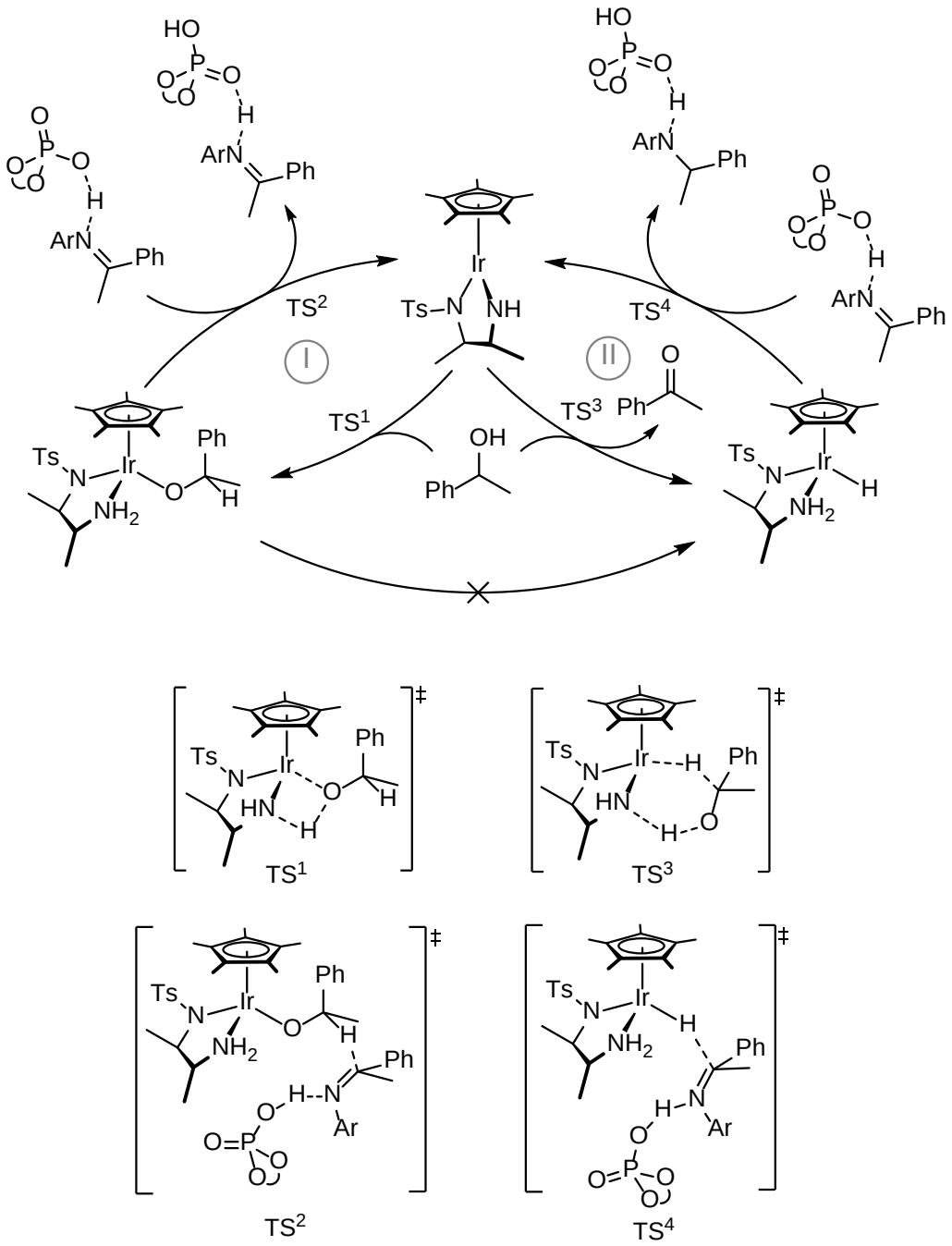

Scheme 77 Reaction paths and transition states for the ATH of imines proposed by Zhao and Lan [86]. Cycle I: iridium-alkoxide path; cycle II: iridium-hydride path

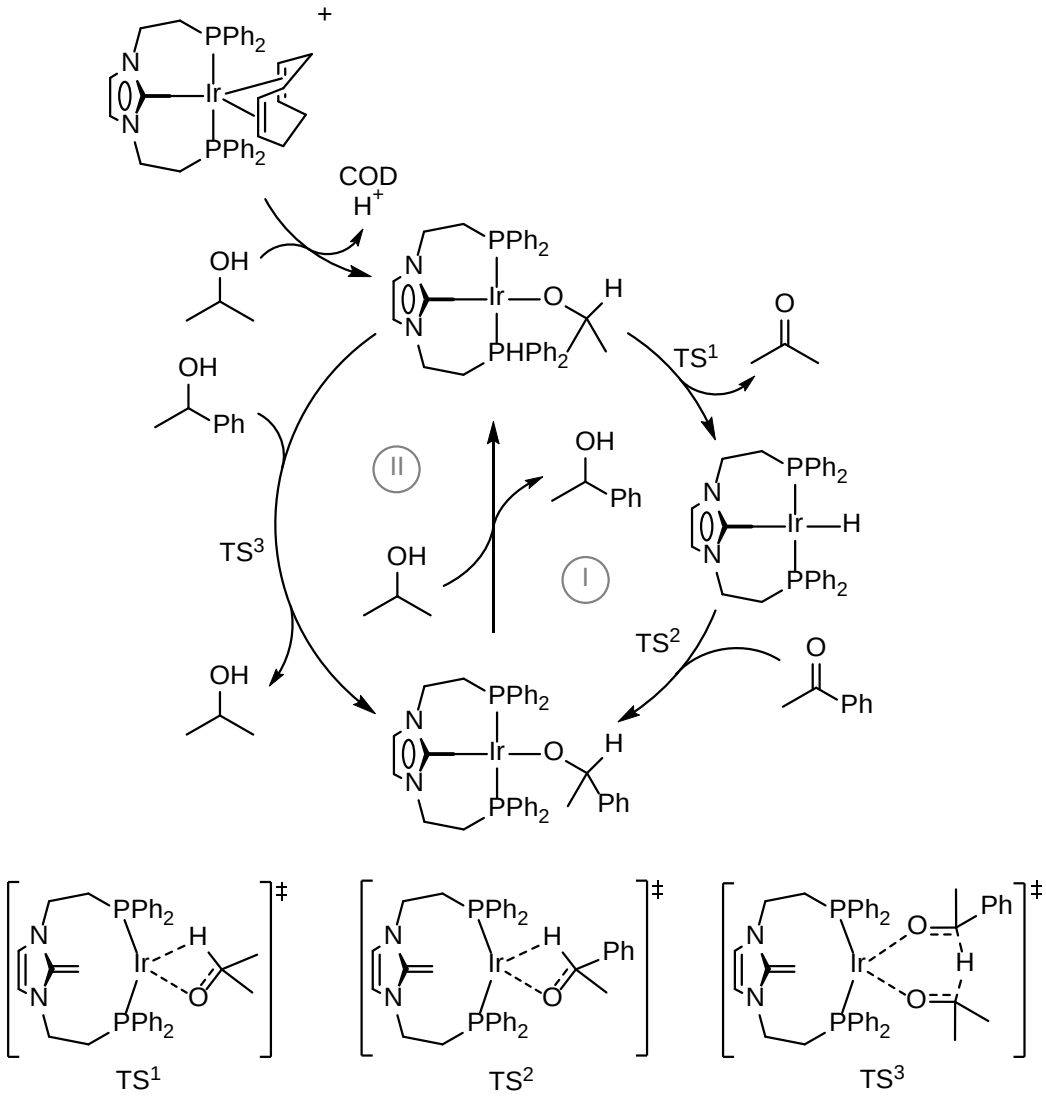

Scheme 78 Reaction paths and transition states for the TH of carbonyl compounds proposed by Iglesias and Oro [178]. Cycle I: monohydride route; cycle II: direct transfer

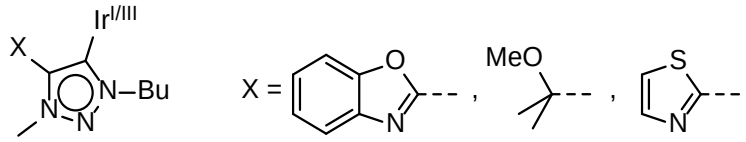

Scheme 79 Triazolylidene iridium complexes used as catalysts for the TH of carbonyl groups, imines and alkenes [155]

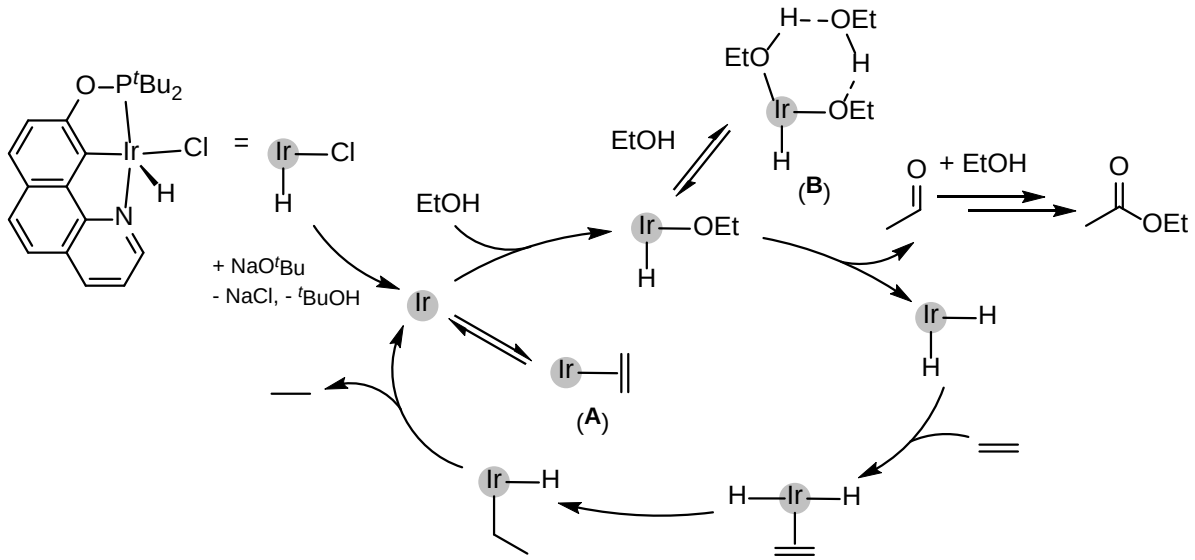

Scheme 80 Catalytic cycle for the TH of alkenes using ethanol as the hydrogen donor and an iridium *P*,*C*,*N* pincer catalyst, proposed by Huang [181]

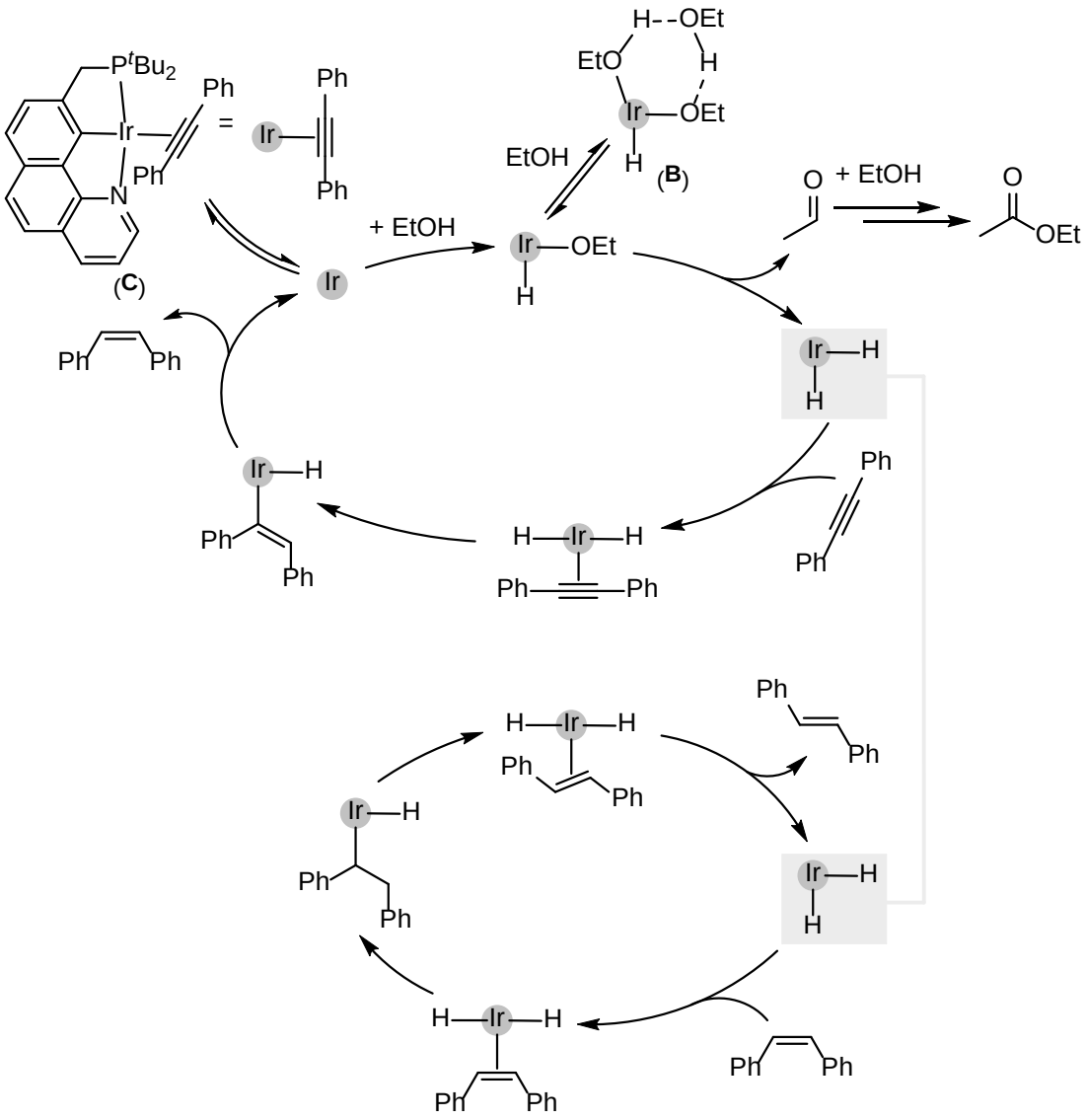

Scheme 81 Catalytic cycles, proposed by Huang [182], for the TH of alkynes to *E*-alkene (*top*) and *Z-E* isomerization (*bottom*) catalysed by an iridium *P,C,N* pincer complex using ethanol as the hydrogen donor

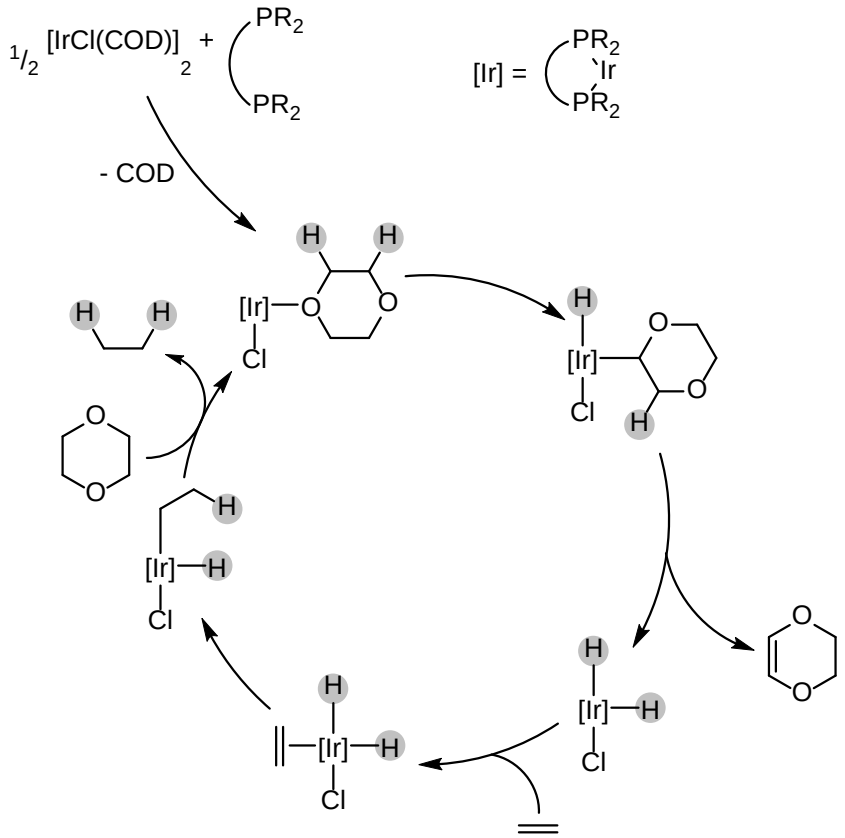

Scheme 82 Catalytic cycle for the TH of alkenes using 1,4-dioxane as the hydrogen donor with an in situ generated iridium(I) catalyst [194]

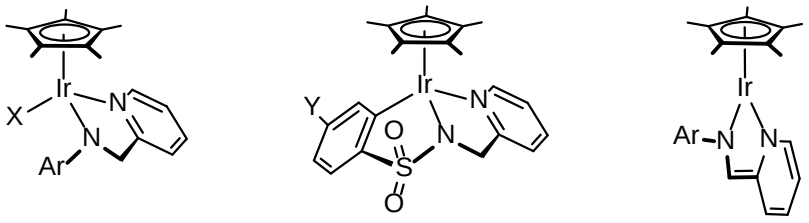

X = H, Cl; Ar = $SO_2(4\text{-}C_6H_4Y)$; Y = Me, F

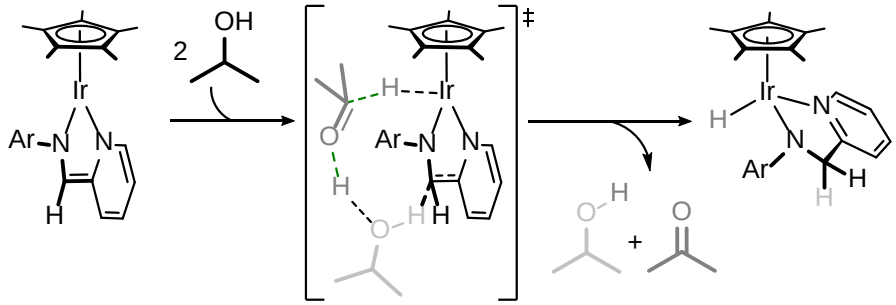

Scheme 83 Cp*Ir catalysts used by Williams [242] for the TH of carbonyl compounds using 2-propanol as the hydrogen donor (*top*) and outer sphere metal-ligand bifunctional reaction sequence (*bottom*)